NANOPARTICLES AND SURFACTANTS-STABILIZED FOAM AND EMULSION FOR GAS MOBILITY CONTROL IN PETROLEUM RESERVOIRS

A Dissertation

by

ZUHAIR ALI A AL YOUSEF

Submitted to the Office of Graduate and Professional Studies of
Texas A&M University
in partial fulfillment of the requirements for the degree of

DOCTOR OF PHILOSOPHY

Chair of Committee,	David S. Schechter
Committee Members,	Ibrahim Y. Akkutlu
	Hadi Nasrabadi
	James D. Batteas
Head of Department,	Daniel Hill

August 2017

Major Subject: Petroleum Engineering

Copyright 2017 Zuhair Ali A Al Yousef

ABSTRACT

This work proposes the use of nanoparticles (NPs) to stabilize foams/emulsions for gas mobility control and to improve the gas sweep efficiency. First, NPs were used alone to stabilize emulsion. Second, NPs and surfactants were used synergistically to improve the stability of foam.

Surface modified silica NPs with DCDMS, hidden chemical, and PEG were used to assess the ability of NPs to stabilize gas-liquid emulsions at reservoir conditions. Silica modified with DCDMS was able to increase the CO_2 viscosity 26-60 fold. Silica modified with hidden chemical was able to increase the CO_2 viscosity 25-53 fold and N_2 viscosity 22-54 fold. Finally, the presence of silica modified with PEG was able to increase the CO_2 viscosity 24-49 fold. All tested materials showed an inverse relationship between the emulsion quality and viscosity. In most cases, salinity was found to have a significant impact on emulsion strength. As salinity increased, the emulsion viscosity increased, too. The concentration of NPs showed similar behavior, with NPs concentration and viscosity being directly proportional. Shear rate was found to be a crucial parameter for emulsion stability and viscosity, with a threshold shear rate being necessary to stabilize emulsions. Also, increased pressure can improve emulsion stability to produce a more viscous emulsion.

The presence of NPs in all surfactant solutions enhanced foam stability and produced more viscous foams compared to surfactant alone. The presence of NPs with ENORDET A031 was able to increase the gas MRF up to 84.57 compared to 72.57 for surfactant. For the mixtures of silica NPs and nonionic surfactants, results showed that the concentration of surfactant and NPs is a crucial parameter for foam stability and that there is an optimum concentration for strong foam production. For N_2 foam, the mixture of surface modified silica

NPs and CNF surfactant resulted in a total recovery of 49.05% compared to 41.45% for surfactant alone. The total oil recovery for the same mixture with sc-CO_2 was 80.05% of the OOIP. This is around 4% higher than the surfactant case and 8.55% higher than sc-CO_2. In fractured rocks, oil recoveries during secondary production mechanisms for the mixture of surface modified silica NPs and CNF surfactant, the surfactant alone, and sc-CO_2 alone were 12.62, 8.41 and 7.21% of the OOIP, respectively.

DEDICATION

I dedicate this work to my father who is my first teacher after Allah. I also dedicate this work to my unforgettable mother; may Allah rest her soul in peace. Also, I dedicate this work to my loving family; wife, son, brothers and sisters who encouraged me to continue working hard. I would also like to express my appreciation to everyone who supported me and encouraged me to reach my goals.

ACKNOWLEDGEMENTS

I would like to thank everyone who helped and supported me in making this work possible.

First, I would like to thank my advisor, Dr. David S. Schechter, and my committee members, Dr. Ibrahim Y. Akkutlu, Dr. Hadi Nasrabadi and Dr. James D. Batteas, for all the guidance, help, and support throughout the research work.

I must thank my employer and sponsor company Saudi Aramco and its management for trust in me and giving me the opportunity to learn, expand my knowledge, and sharpen my skills.

I would like also to acknowledge my great friends for their help and support.

Also, I would like to thank all the faculty, students, and staff in the Texas A&M University Petroleum Engineering Department who helped and supported me during my study. Special thanks and appreciation to Mr. John Maldonado for his help and support with the laboratory needs.

Finally, I will always be proud to have been a student at Texas A&M University.

CONTRIBUTORS AND FUNDING SOURCES

Contributors

This work was supervised by a dissertation committee consisting of Professor David S. Schechter and Professor Ibrahim Y. Akkutlu and Professor Hadi Nasrabadi of the Department of Petroleum Engineering and Professor James D. Batteas of the Department of Chemistry.

Experimental work was completed by the student, in collaboration with Mohammed Almobarky, Rodolfo Marquez and John Maldonado of the Department of Petroleum Engineering.

All other work conducted for the dissertation was completed by the student independently.

Funding Sources

Graduate study was supported by a scholarship from Saudi Aramco.

NOMENCLATURE

A	Cross-sectional area
A_{GG}	Interaction potential between gases
A_{PG}	Interaction potential between particle and gas
A_{PP}	Interaction potential between particles
A_{PW}	Interaction potential between particle and liquid
A_{WW}	Interaction potential between liquids
API Gravity	American Petroleum Institute Gravity
α	Gas fraction
B	Bridging coefficient
BPR	Back pressure regulator
CMC	Critical micelle concentration
CNF	Complex nanofluid
CT	Computed tomography
d	Pipe diameter
D	Darcy
DCDMS	Dichlorodimethylsilane
ΔP	Drop in pressure
$\Delta P_{baseline}$	Baseline drop in pressure
DLS	Dynamic light scattering
DMS	Dimethylsilane
E	Energy of attachment

e	Entering coefficient
EOR	Enhanced Oil Recovery
HCB	Hydrophilic CO_2-philic balance
IFT	Interfacial tension
k	Permeability
L	Lamella number
l	Length of porous media
l*	Length of the capillary tube
MMP	Minimum miscibility pressure
MRF	Mobility reduction factor
$\mu_{apparent,\ porous}$	Apparent viscosity measured through porous media
$\mu_{emulsion}$	Emulsion viscosity
$\mu_{baseline}$	Baseline viscosity
NBU	North Burbank Unit
NPs	Nanoparticles, singular NP
OBP	Over burden pressure
OOIP	Original Oil in Place
p	Packing parameter
P_c^{max}	Maximum capillary pressure
PDI	Poly dispersity index
PEG	Polyethylene glycol
PPM	Part per million
PT	Pressure transducer

PV	Pore volume
q	Flow rate
r	Radius of capillary tube
R	Particle radius
Re	Reynold number
RF	Flow resistance factor
ρ_{CO_2}	CO_2 density
$\rho_{emulsion}$	Emulsion density
ρ_{liquid}	Liquid density
s	Surfactant
S	Spreading coefficient
SAG	Surfactant alternating gas
S_{wi}	Irreducible water saturation
sc	Supercritical
$\sigma_{a/o}$	Surface tension of gas and oil
$\sigma_{a/w}$	Surface tension of gas and water
$\sigma_{o/w}$	Surface tension of oil and water
TEM	Transmission electron microscope
θ	Contact angle
v	Fluid average velocity
WAG	Water alternating gas
XRD	X-Ray Diffraction

TABLE OF CONTENTS

Page

Page

LIST OF FIGURES

Page

Page

Page

Page

Page

Page

LIST OF TABLES

Page

Page

CHAPTER I

INTRODUCTION

1.1 General Introduction

There are so many challenges facing the oil industry, now and in the near future. There is a growing need for energy throughout the world. A significant amount of oil produced nowadays comes from mature oil fields and new discoveries have been declining steadily in recent decades (Manrique et al. 2010). The typical amount of oil produced following primary and secondary oil production mechanisms is in the range between 45 and 50% of the original oil in place (OOIP) (Sandrea and Sandrea 2007). Because of the huge amount of residual oil saturation remaining in the reservoirs following primary and secondary mechanisms (Hirasaki, Miller, and Puerto 2011), the oil produced is coming up short in meeting the ever increasing global energy demand (EIA 2011). The techniques for enhanced oil recovery (EOR) should be applied to solve the problems associated with the decline in oil production (Manrique et al. 2010). EOR is considered to be one of the most important areas of technology in the petroleum industry (Hite, Avasthi, and Bondor 2005). Gas injection is one of the most reported EOR techniques in the literature and applied in fields. It includes injection of hydrocarbon gases (Whorton and Kieschnick 1950) and non-hydrocarbon gases such as carbon dioxide and nitrogen. The biggest advantage of gas is that it can produce most of the oil in the zones swept by gas if the gas is miscible with the oil (Slobod and Koch 1953). For Example, CO_2 is widely used for EOR due to environmental and technical prospects (Alvarado and Manrique 2010). Environmentally, it is a good candidate because injecting CO_2 into petroleum reservoirs is one way to reduce greenhouse gases (DOE/NETL 2008). Technically, it can promote swelling,

reduce oil viscosity, vaporize, and extract portions of crude oil. Moreover, the easy solubility of CO_2 in oil makes it an ideal gas for EOR applications (Enick, Holder, and Morsi 1988, Christensen, Stenby, and Skauge 1998, Bayraktar and Kiran 2000). The successful results reported from CO_2 EOR projects in the world make the CO_2 injection method a leading EOR technique in the petroleum industry (Dong, Huang, and Srivastava 2000).

Despite the reported successes of gas injection, a major challenge facing this technique is poor volumetric sweep efficiency. Major factors that contribute to this problem are the low density and viscosity of injected gas relative to reservoir fluids, as well as reservoir heterogeneity such as high permeability and heavily fractured zones (Campbell and Orr 1985, Chakravarthy et al. 2004, Masalmeh et al. 2010). The high mobility of injected gas compared with the other fluids in reservoirs may lead to early breakthrough of gas, leaving most of the residual / trapped oil untouched and increasing the gas to oil ratio (GOR) which makes the overall technique inefficient.

Several methods have been tested to solve this issue. The most common approaches are: water alternating gas (WAG); generation of foams; and increasing gas viscosity by adding thickening agents (Dandge and Heller 1987, Heller 1994, Dalland and Hanssen 1997, Enick 1998, Chakravarthy et al. 2004, Hamilton 2004, Enick et al. 2012). The use of foam is one of the most promising techniques to overcome gas mobility challenges in petroleum reservoirs and improve the volumetric sweep efficiency (Kovscek and Radke 1994). Foam can reduce the gas mobility in petroleum reservoirs by increasing the gas apparent viscosity and reducing the gas relative permeability (Falls et al. 1988). However, there are many challenges associated with surfactant foam generation and stabilization at reservoir conditions. The harsh conditions such as reservoir temperature, high salinity, and surfactant adsorption to the rock may result in

weak foam generation and, therefore, poor sweep efficiency (Figdore 1982, Al-Hashim et al. 1988, Mannhardt, Schramm, and Novosad 1993, Grigg and Bai 2005). Moreover, the use of CO_2 in the foam generation processes is a major challenge. This is mainly because CO_2-philic tail is a poor solvent for surfactant tails. Consequently, instability of the foam can occur in the form of flocculation or coalescence of bubbles (Bartscherer, Minier, and Renon 1995, Eastoe et al. 2003).

Another innovative technique to stabilize gas-liquid foam/emulsion is the use of solid nanoparticles (NPs). The use of NPs can solve the issues associated with the application of surfactant to stabilize gas-liquid foams. Compared to surfactant molecules, NPs can strongly adsorb at the gas-brine interface and form stable CO_2 foams/emulsions. Also, NPs can withstand the harsh reservoir conditions and produce stable foam/emulsions. Moreover, these particles are solids in nature, compared to surfactants which are in liquid form, so they have less affinity to be adsorbed by reservoir rocks (Espinoza et al. 2010, Al Otaibi et al. 2013, Worthen, Bagaria, et al. 2013).

This work proposes the use of NPs to stabilize gas-liquid foams/emulsions at different conditions. This work uses surface modified NPs and also the synergistic effect of surfactants and NPs to stabilize gas-liquid foams/emulsions as alternatives to the use of surfactants to stabilize foams and control gas mobility in petroleum reservoirs. Throughout this work, the term “foam” is used to describe the final status as a result of mixing two or more materials in the presence of gas and liquid phases, while “emulsion” is used for liquid in liquid phases.

1.2 Literature Review

1.2.1 Gas Flooding Background

The use of the CO_2 as an EOR method first appeared in the 1930s and has had significant development as recently as the 1970s (Yongmao et al. 2004). Through use and additional development, CO_2 flooding has become a leading EOR technique for light and medium types of oil (Grigg and Schechter 1997). The United States produces a significant amount of its oil using EOR processes. As reported by *The Oil and Gas Journal* in 2010, 663,431 barrels per day of oil are produced from 193 EOR projects. Of these projects, there are 109 projects producing 272,109 barrels per day using CO_2 EOR processes. **Figure 1** shows the evolution of the CO_2 EOR projects and U.S. oil prices from 1980 to 2010.

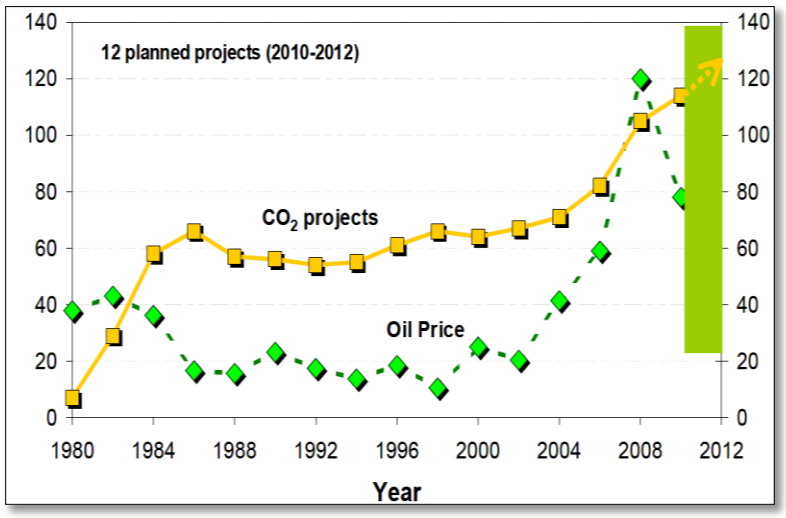

Figure 1: CO_2 EOR projects and oil prices in the U.S. (Reprinted from (Alvarado and Manrique 2010))

The major advantages of gas injection are: maintaining reservoir pressure at desired limits; displacing oil, both vertically and horizontally; and swelling of the oil for EOR. The successful results reported from CO_2 EOR projects around the world make the CO_2 injection method a leading EOR technique in the petroleum industry (Dong, Huang, and Srivastava 2000). However, there are several problems associated with the application of gas flooding that may result in making the overall project unstable and somewhat unfavorable. Gas flooding has very poor volumetric sweep efficiency and this is attributed to three main reasons: the gravity override, the gas fingering and the reservoir heterogeneity, which includes high permeability and heavily fractured zones (Campbell and Orr 1985, Chakravarthy et al. 2004, Masalmeh et al. 2010). The presence of heterogeneity (the variety of permeability, porosity, thickness, saturation, faults, fractures, rock facies, and rock characteristics) (Ahmed 2000) and the interaction of several forces inside the reservoir, namely viscous forces driven by adverse mobility ratios, capillary forces from interfacial forces between immiscible fluids, gravity forces driven by fluid density gradients, and dispersive forces caused by concentration gradients between fluids (Gharbi et al. 1997), might result in very poor volumetric sweep efficiency during gas injection processes. The injected gas, which has a very high mobility compared with oil and brine mobility, may lead to early breakthrough, which means fingering through the target zone while leaving most of the residual/trapped oil untouched, and increasing the gas to oil ratio, thus making the overall project uneconomic. Several methods have been tested to solve this issue. The most common approaches are: WAG, increasing the gas viscosity by adding thickening agents, and generation of foams (Dandge and Heller 1987, Heller 1994, Dalland and Hanssen 1997, Chakravarthy et al. 2004, Hamilton 2004, Enick et al. 2012).

1.2.2 Common Gas Mobility Techniques

Several methods have been proposed to solve the issues of high gas mobility during the gas injection process in petroleum reservoirs. Three major techniques will be described briefly in this section: WAG processes, CO_2 thickening agents, and foam generation.

1.2.2.1 Water – Alternating Gas WAG

Mainly, WAG is the reduction of CO_2 relative permeability in the reservoir via cyclic injection of gas and water. This method was the first attempt to diminish CO_2 mobility in the reservoir. Even though it reduces the CO_2 relative permeability and mobility, it has three main disadvantages: it might result in severe gravity segregation (i.e, water underlying and CO_2 overriding); water can act as a barrier preventing CO_2 from contacting oil; and it can prolong the project life because it requires the injection of water and gas in sequences. As a result, oil will be trapped/untouched and, hence, oil recovery will be reduced and the residual oil saturation will be high. These factors can make the overall project cost prohibitive (Christensen, Stenby, and Skauge 1998, Enick 1998, Chakravarthy et al. 2004, Manrique et al. 2010).

1.2.2.2 CO_2 Thickening Agents

In this method, a polymer or viscosifier agent is added to CO_2 in order to increase its viscosity by orders of magnitude. Thickening CO_2 by using a polymer as a direct thickener offers several distinct advantages compared to other methods. Because there is no water injection involved with the CO_2 thickening method, the water-blocking or shielding effect will be eliminated and the project life will be shorter relative to the WAG method. Another factor

that makes the CO_2 thickening method better than other methods is the stability of the CO_2 and polymer mixture under real reservoir conditions. The major obstacle to applying this method is that it requires a very high minimum solubility pressure, much higher than reservoir pressure, to solubilize the polymer in CO_2 and this might be impractical for field application. Even if there were a suitable material with a lower solubility pressure, it may not be suitable due to environmental concerns (Heller et al. 1985, Terry et al. 1987, Liave, Chung, and Burchfield 1990, Bae and Irani 1993, Gullapalli, Tsau, and Heller 1995, Rindfleisch, DiNoia, and McHugh 1996, Huang et al. 2000, Enick, Beckman, and Johnson 2010, Zhang, She, and Gu 2011).

1.2.2.3 Generation of Foam

There are lot of projects to test the ability of co-injection process gas-emulsifying agent (foam generation) or surfactant alternating gas (SAG) to reduce the gas relative permeability in petroleum reservoirs. The use of foam is one of the most promising techniques to overcome gas mobility challenges in petroleum reservoirs and improve the volumetric sweep efficiency (Kovscek and Radke 1994). The main principle of this method is to generate foam *in situ* to block the high permeable zones which result in the reduction of gas relative permeability and, therefore, gas mobility. Foam can reduce the gas mobility in petroleum reservoirs by increasing the gas apparent viscosity and reducing the gas relative permeability (Falls et al. 1988). Theoretically, this method seems to solve the problem of gas mobility and to enhance gas displacement processes.

Surfactants are the primary emulsifying agents used to generate foams to solve gas mobility issues. However, there are many challenges associated with foam generation and

stabilization at reservoir conditions. The harsh conditions, such as reservoir temperature, high salinity, and surfactant adsorption to the rock may result in weak foam generation and, therefore, poor sweep efficiency (Figdore 1982, Al-Hashim et al. 1988, Mannhardt, Schramm, and Novosad 1993, Grigg and Bai 2005). An innovative technique to stabilize gas-liquid foam/emulsion is the use of solid NPs. They provide an excellent alternative to the use of surfactants to stabilize foams and control gas mobility in petroleum reservoirs.

1.2.3 NPs- Stabilized Gas-Liquid Foam/Emulsion

In this section, the history and the applications of nanotechnology in different fields will be highlighted. Also, the applications of nanotechnology in gas and petroleum industry will be discussed briefly. Moreover, a literature review of the use of NPs to stabilize gas-liquid foam will be summarized.

1.2.3.1 History of Nanotechnology

The use of nanoscience and nanotechnology has grown rapidly in recent decades. This technology has become one of the most important innovations of science. The concept behind this technology started with a speech given by physicist Richard Feynman in 1959 in which he described a process by which future scientists would be able to control and manipulate items at atomic and molecular levels (Feynman 1960). In 1981, with the development of the scanning tunneling microscope (STM) that could image surfaces at the atomic level, Norio Taniguchi coined the term nanotechnology while working on ultraprecision machining. The term draws its name from the prefix “nano,” a billionth of any unit. As a practical matter, nanotechnology primarily uses tiny pieces of material with sizes between 1 and 100 nm. Nanomaterials may

have different forms of particles such as tubes, rods, or fibers (Schmidt and Malwitz 2003). This technology has found many uses and applications in different aspects of life. For example, it is used in medicine and health, in manufacturing, in the energy sector, in electronics and IT applications, and in environmental remediation (Liu 2006).

The most interesting aspect of nanotechnology is the unique features and characteristics of any material developed at a nanoscale. The physical, chemical, mechanical, and optical properties of materials developed at nanoscales are significantly different from other conventional (bulk) materials. Two principle factors differentiate nanomaterials from others, producing materials with unique and special features. These are quantum effects and their high relative surface area. These two factors play key roles in enhancing properties such as reactivity, strength, and electrical features (NNI 2017).

1.2.3.2 Nanotechnology in Gas and Petroleum Industry

Because of their unique properties, nanomaterials have been used in many fields of the gas and petroleum industry, ranging from exploration to refining processes. In exploration and field monitoring, nanosensors are injected into pore spaces to provide information about formation temperature, pressure, and saturation (Kanj, Funk, and Al-Yousif 2009, Ryoo et al. 2012, Yu et al. 2010). This may help in better managing oil fields and maximizing field productivity. Also, nanomaterials have been used in drilling and completion operations to solve technical and operational issues during these processes. For example, NPs can be used to: manage fluid loss control and wellbore stability issues; eliminate bit and stabilizer balling; reduce fractional resistance between the pipe and the borehole; assist in the removal of toxic gases; and increase the life of down hole tools (Amanullah and Al-Tahini 2009, Amanullah,

AlArfaj, and Al-abdullatif 2011, Hoelscher et al. 2012). Moreover, NPs show encouraging applications in the production field. For instance, they have been used in stimulation jobs, as scale inhibitors, and to produce gas hydrates (Huang and Crews 2008, Crews and 2008, Bhatia and Chacko 2011, Kumar et al. 2012). For EOR applications, NPs have been used to alter formation wettability and to improve oil recovery. Some kinds of bare and surface modified NPs have been reported to change the formation wettability or to reduce oil viscosity and, hence, EOR. For instance, silicon oxide (SiO_2) was reported to alter rock wettability, while aluminum oxide (Al_2O_3) reduces oil viscosity (McElfresh, Holcomb, and Ector 2012, Ogolo, Olafuyi, and Onyekonwu 2012, Hendraningrat, Li, and Torsaeter 2013, Hendraningrat, Li, and Torsater 2013, Li, Hendraningrat, and Torsaeter 2013). The use of NPs for EOR applications has also been applied to stabilize gas-liquid foam/emulsion. Several studies have been conducted reporting a potential of NPs to stabilize or improve gas-liquid foam/emulsion at different conditions. More details about these studies will be discussed in the next section. Two methods have been reported in the literature showing a potential of NPs to stabilize/improve gas-liquid foam/emulsion:

1- Using NPs alone
2- Mixing surfactant and NPs

1.2.3.3 Using Nanoparticles Alone

There are some drawbacks with CO_2 that makes it difficult to generate a stable emulsion with water and limits its applicability. CO_2 has low polarizability. This is attributed to the fact that CO_2 has a zero permanent dipole moment and also weak van der Waals forces. As a result, CO_2-philic tail is a poor solvent for both polar and high molecular weight solutes.

Consequently, instability of the emulsion can occur in the form of flocculation or coalescence (Bartscherer, Minier, and Renon 1995, Eastoe et al. 2003). Low molecular weight surfactants or polymers with low cohesive energy densities such as siloxanes, trisiloxanes, fluoroalkanes, fluoroethers, and fluoroacrylates were used as emulsifying agents to stabilize CO_2-water emulsions. However, the need for a stabilized CO_2-water emulsion to be applied at harsh conditions, such as high pressure, temperature, and high salinity environments, has encouraged researchers to find an alternative for surfactants to be used as an emulsifying agent.

Solid NPs have many advantages that make them attractive to researchers as an alternative to surfactant for stabilizing gas-liquid foam/emulsion. Compared to surfactant molecules, NPs can strongly adsorb at the gas-brine interface and form stable CO_2 foams/emulsions. Also, using NPs as a replacement for surfactant to stabilize foam/emulsion may offer a solution to the long-term instability and adsorption issues associated with surfactant foams. Moreover, they are showing excellent chemical stability and low retention on rock surfaces (Espinoza et al. 2010, Al Otaibi et al. 2013, Worthen, Bagaria, et al. 2013). Due to their sizes and chemical stability, NPs are capable of flowing through porous media (Caldelas et al. 2011). A wide variety of particles have been used to stabilize foams/emulsions, e.g., silica, iron oxide, hydroxides, metal sulfates, clays, and carbon. Silica NPs have been reported widely for EOR applications and this is attributed to four main reasons (Li, Hendraningrat, and Torsaeter 2013):

1- The excellent stability of colloid silica NPs, which is caused by the ability of surface forces to counterbalance the gravity force.
2- Silica NPs have great thermal, rheological and mechanical properties and these depend on size and shape of particles.
3- Silica NPs can be easily modified by using coating chemicals.

4- Silica NPs are considered to be environmentally friendly and can be used safely. This is mainly because these particles are made of silicon oxide (SiO_2).

NPs potentially have better CO_2 solvation capability, as studied by (Dickson, Binks, and Johnston 2004). Partially modified silica NPs using polyethylene glycol (PEG) and dichlorodimethylsilane (DCDMS) were successfully used to stabilize CO_2-water emulsions at harsh reservoir conditions (Espinoza et al. 2010, Al Otaibi et al. 2013, Worthen, Bagaria, et al. 2013). The hydrophilic CO_2-philic balance HCB (particle wetting) of the solid particles was found to have a significant effect on the emulsion stability and type. Depending on the degree of hydrophilicity, either CO_2 in water emulsion or water in CO_2 emulsion will be formed. This behavior can be explained in terms of the contact angles and the resulting energies of attachment for the different particles at the CO_2-water interface. As shown in **figure 2**, CO_2–water emulsion forms as a result of using hydrophilic particles. In such cases, the particles have a contact angle less than 90^o measured from the aqueous phase and the majority of particles like to be in the water phase. Consequently, the interface bends around the CO_2 phase. However, water-CO_2 emulsion forms as a result of using hydrophobic particles. In this case, the particles have a contact angle greater than 90^o measured from the aqueous phase and the majority of particles reside in the CO_2 phase. Accordingly, the interface bends around the water phase (Binks and Lumsdon 2000, Worthen, Bagaria, et al. 2013). **Table 1** summarizes the main results that have been reported for stabilizing CO_2-water foam/emulsion using NPs. More details about the mechanisms that NPs use to stabilize foam/emulsion will be discussed later in this chapter.

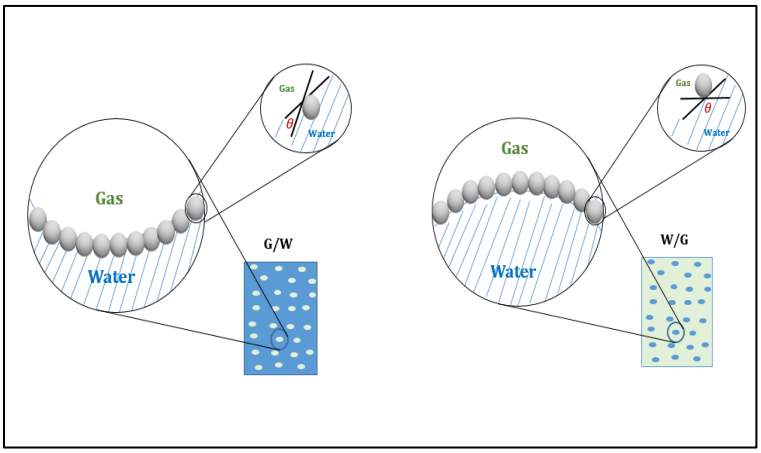

Figure 2: Emulsion type based on contact angle of spherical particles. (Modified from (Worthen, Bagaria, et al. 2013))

Table 1: Main results reported for foam/emulsion stabilized by NPs

Researcher	Material	Results
(Aroonsri et al. 2013)	▪ Silica coated with PEG ▪ Silica modified with a proprietary coating (EOR-5XS) and (EOR-12	▪ The HCB was reported to have a significant impact on foam stability. ▪ High salinity solutions can reduce the ability of foam to generate foam. ▪ Gas ratio is a crucial parameter on foam generation; ratios too high or too low have showed no foam. ▪ There must be a critical shear rate to start foam generation. This depends on experimental conditions.
(Dickson, Binks, and Johnston 2004)	▪ Amorphous fumed silica with different hydrophilicities, from 100 to 20% SiOH	▪ The concentration of NPs, CO_2 density, and shear rate are important parameters for foam stability. ▪ The HCB was reported to have a significant impact on foam stability and type. ▪ The foam stability and type were explained in terms of contact angle and resulting energy of attachment.
(Al Otaibi et al. 2013)	▪ Aerosil 972 ▪ Aerosil 974 ▪ Ludox TM-40	▪ NPs concentration and water/iso-octane ratio are important parameters on emulsion stability. ▪ The presence of NPs was able to increase the CO_2 viscosity 45 to 100 fold.
(Espinoza et al. 2010)	▪ Silica Coated with PEG (7 EG) ▪ Salt tolerant NPs	▪ There must be sufficient energy (shear rate) to bring the NPs to the CO_2/water interface. ▪ As salts were added to the mixture, high concentrations of NPs were required. ▪ Based on normalized mixture viscosity, neither the concentration nor the gas/liquid ratio have any effect on emulsion strength. ▪ The addition of NPs to the solutions increased flow resistance two to eighteen times.

Table 1: Continued

Researcher	Material	Results
(Worthen, Bagaria, et al. 2013)	▪ Silica coated with DCDMS (different hydrophilicity) ▪ Silica coated with PEG	▪ In the presence of NPs, the HCB is an important parameter in determining the emulsion's strength and stability. ▪ For silica coated with DCDMS, the highest emulsion stability was observed for 50% SiOH modification. ▪ The presence of NPs was able to increase the CO_2 viscosity 120 fold.
(Yu et al. 2014)	▪ Amorphous silica particles (super hydrophilic) ▪ HDK 30 ▪ Crystalline silica particles prepared in-house	▪ The ability of NPs to stabilize CO_2-water foam is independent of the structure of the NPs. ▪ The concentration of NPs was important to enhance the gas flow resistance factor. ▪ The gas to liquid ratio (GLR) is an important parameter on foam strength. ▪ The wettability of particles is a critical parameter for foam stability and strength. ▪ The shear rate has a significant effect on foam stability.

1.2.3.4 Mixing Surfactants and NPs

Another method proposed to enhance foam stability is using solid particles and surfactants. This can be achieved by surface-modification of solid NPs via physio-chemical interaction with surfactants or the synergistic effect of surfactants and NPs. The objective of the former method is to modify *in situ* the surface of NPs through physio-chemical interactions which has been reported to be cost-effective. These techniques have been reported to produce a more stable foam than using surfactant alone. (Zhang et al. 2008) used a mixture of laponite particles and nonionic surfactant, tetraethylene glycol monododecyl ether, and found an enhancement in foam stability under certain conditions. (Cui et al. 2010) improved foam stabilization using non-surface-active $CaCO_3$. (Worthen, Bryant, et al. 2013) produced a stable and viscous CO_2-in-water foam using non-modified silica NPs and caprylamidopropyl betaine (CAPB) surfactant where neither of these materials could stabilize foam individually. (Singh and Mohanty 2015) reported that a foam was produced by partial hydrophobization of alumina-coated silica NPs using a surface modifier. **Table 2** summarizes the major achievements that have been reported for stabilizing gas/liquid foam/emulsion using surfactant and NPs.

Table 2: Main results reported for foam stabilized by surfactants and NPs

Researcher	Material	Results
(Worthen, Bryant, et al. 2013)	▪ Silica NPs ▪ surfactant (caprylamidopropyl betaine)	▪ The mixture produced a stable and viscous CO_2-in-water foam when neither of these materials could stabilize foam individually at experimental conditions.
(Farhadi et al. 2016)	▪ Silica NPs ▪ Ethyl hexadecyl dimethylammonium bromide (cationic surfactant)	▪ Foam stability can be divided into two regions: Low adsorption where the stability occurs due to surfactant concentration, and then the presence of NPs. High adsorption where the stability is mainly controlled by both surfactant and NPs concentrations. ▪ The addition of NPs produced foam with smaller bubbles and high viscosity compared to that of surfactant. ▪ The increase in NPs concentration resulted in the generation of aggregates which caused the increase of solution viscosity, hence, slowing the rate of drainage.
(Singh et al. 2015)	▪ Fly ash powder ▪ Anionic surfactants ▪ Nonionic surfactants ▪ Cationic surfactants	▪ In presence of NPs, anionic and nonionic surfactants produced foam with smaller bubble size. ▪ In porous media, NPs and anionic surfactant produced a stable foam.
(Singh and Mohanty 2015)	▪ Alumina coated silica NPs ▪ Non-ionic surfactant Triton CG-110 ▪ Bioterge AS-40	▪ A foam was produced by partial hydrophobization of alumina-coated silica NPs using a surface modifier. ▪ The mixture of surfactants and NPs produced a more stable foam than the mixture of two surfactants.
(Singh and Mohanty 2014)	▪ Surface modified silica NPs (DP 9711) ▪ Bioterge AS-40	▪ Mixing NPs and surfactant resulted in a more stable foam compared to surfactant alone. ▪ Mixture enhances oil recovery

Table 2: Continued

Researcher	Material	Results
(Carn et al. 2009)	▪ Ludox HS-40 aqueous silica ▪ Trimethyl (tetradecyl) ▪ Ammonium bromide (CH3(CH2)13N(Br)	▪ The generation of aggregates or forming of corks as a result of mixing NPs and surfactant with opposite charges resulted in better foam stability.
(Xue et al. 2016)	▪ Silica NPs ▪ Laurylamidopropyl betaine (LAPB) surfactant ▪ Polyacrylamide (HPAM)	▪ The mixture of surfactant and NPs produced foams with small bubble sizes and high viscosity, 100 cp. ▪ NPs adsorbed at the gas-liquid interface, slowing down Ostwald ripening. ▪ The addition of polymer increases solution viscosity, hence, slowing the drainage rate.

1.2.4 Mechanisms of Foam Stabilized by Surfactant and NPs

Different mechanisms have been proposed explaining how solid NPs stabilized-foam/emulsion. Four main mechanisms are summarized in this section: particle attachment energy, particles arrangement during film drainage, maximum capillary pressure of coalescence and growing aggregates.

1.2.4.1 Particle Attachment Energy

(Binks and Lumsdon 2000) suggested that the major parameters affected detachment energy of spherical particle of radius (R) are contact angle (θ) and air-liquid interfacial tension σ_{aw}. The energy required to remove a particle from the interface (E) can be correlated with the contact angle that solid particle forms with the interface, resulting energy of attachment can be estimated as follow:

$$E = \pi R^2 \sigma_{aw} (1 \pm \cos\theta)^2 \quad (1)$$

As it is shown in **figure 3**, the highest energy can be achieved when the value in the parenthesis equal to unity and this can be resulted when $\theta \approx 90^o$. In this case, the energy required to remove the particles from the interface is sufficiently large because the particles are held equally by the two phases. Consequently, the formed emulsion will be very stable. However, if the particles are too hydrophilic or too hydrophobic, the energy required to remove the particle from interface is so small.

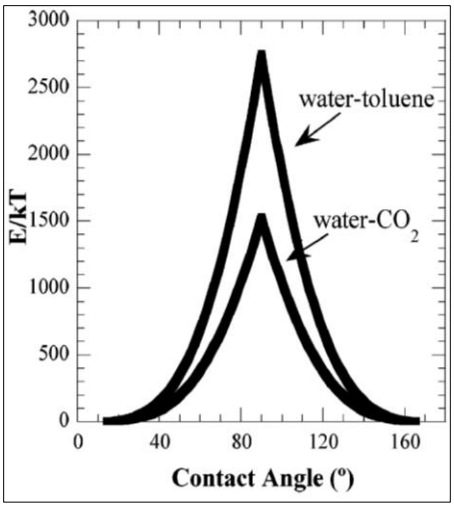

Figure 3: Energy of attachment of solid particles as a function of contact angles. (Reprinted from (Dickson, Binks, and Johnston 2004))

1.2.4.2 Particle Arrangement during Film Drainage

Three possible mechanisms of liquid film stabilization using solid NPs have been proposed by Horozov, 2008: a monolayer of bridging particles, a bilayer of close-packed particles and a network of particle aggregation, as shown in **figure 4**. In case where a dilute monolayer exists, the particles cannot withstand the hydrodynamic flow within the liquid film and move away from the center which create a vacancy that leads to film rupture. However, if close-packed monolayers particles formed, they can resist dragging by a stable bilayer or a bridging monolayer formed and therefore slow down the film thinning and prevent the film from breaking. The third mechanism, a network of particle aggregation, happens when the excess solid particles are flocculated inside the liquid film. This considers to be the most effective mechanism as the gas bubbles are kept separated, thus delaying the coalescence and drainage. Several studies suggested either a bridging monolayer or a bilayer of hexagonally close-packed particles are the main mechanisms to stabilized liquid film in generated foam (Horozov 2008).

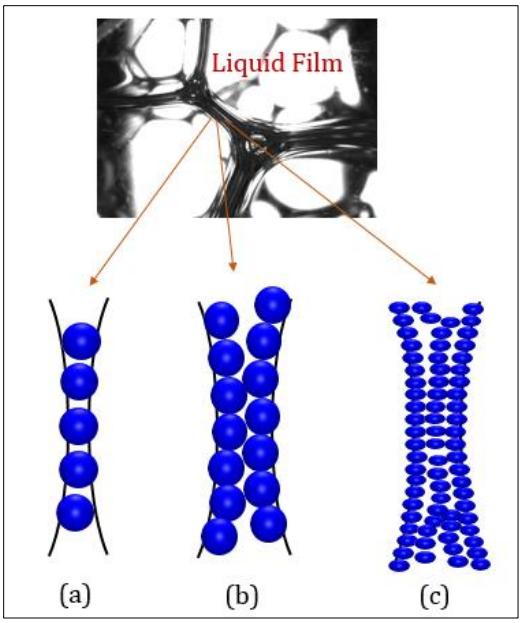

Figure 4: Three possible mechanisms of aqueous film stabilized by solid particles. (a) a monolayer of bridging particles; (b) a bilayer of closed-packed particles and (c) a network of particle aggregates (gel) inside the film. (Modified from (Horozov 2008))

1.2.4.3 Maximum Capillary Pressure of Coalescence

There is a maximum capillary pressure (P_{cmax}) at which the liquid film raptures (Denkov et al. 1992). As this value becomes high, the film can be more stable. In presence of NPs, the maximum capillary pressure of coalescence depends on packing parameter p (interface coverage and particle arrangement in the thin liquid film) , size of particles R, gas-liquid interfacial σ_{aw} and contact angle θ. (Kaptay 2006) presented below equation to describe the effect of NPs on the maximum capillary pressure of coalescence between bubbles.

$$P_c^{max} = \mathrm{p}\frac{2\sigma_{aw}}{R}\,cos\theta \qquad (2)$$

As the size of the particles gets smaller, the maximum capillary pressure increases. The hydrophobicity of the solid particles is a crucial parameter on the stability of aqueous film, as it affects the contact angle the solid particle makes with the aqueous phase. (Aveyard et al. 1994), as shown in **figure 5a**, found that when particles are hydrophobic (θ>90°), when

drainage occurs, aqueous film gets thinner and when the three phases (gas, liquid and solid) meet, holes form and film ruptures. In contrast, if the particles are hydrophilic ($\theta < 90^o$, **figure 5b**), the aqueous film starts thinning until it becomes flat. If the aqueous film thins further, capillary pressure will draw liquid toward the particle (as it is shown by the direction of the arrows) and stabilize the aqueous film by bridging mechanism.

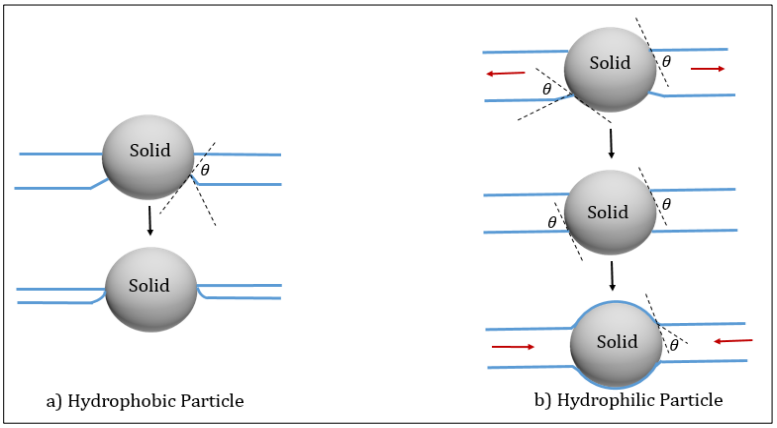

Figure 5: Particle bridging aqueous surfactant films. a) Contact angle of surfactant solution with solid particle, $\theta > 90^o$. b) Contact angle of surfactant solution with solid particle, $\theta < 90^o$. (Modified from (Aveyard et al. 1994))

1.2.4.4 Growing Aggregates

One of the methods proposed to stabilize the liquid film in foam generation process is the aggregate growing and cork formation (Carn et al. 2009), **figure 6**. Using silica NPs and cationic surfactant, the study found that the possibility of aggregates forming and cork formation at high concentration of silica particles (above 2 wt %) might increase the film viscosity, thus slowing down the drainage velocity and therefore improve the foam stability.

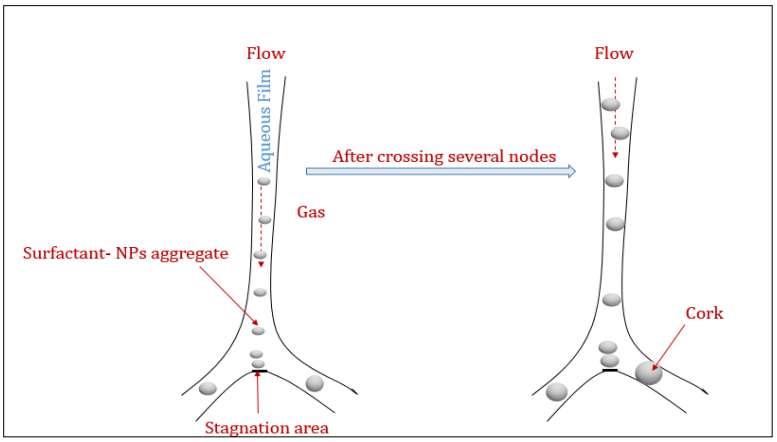

Figure 6: Growing aggregates and cork formation during film drainage. (Modified from (Carn et al. 2009))

1.3 Research Objectives

The main objectives of this study are to:

1- Evaluate the potential for commercially available silica NPs to stabilize CO_2-brine and N_2-brine foam/emulsion at harsh reservoir conditions: supercritical CO_2, high temperature, and high salinity.

2- Design applicable silica NPs with surface modifiers that can be used for stabilizing CO_2-brine or N_2-brine foam/emulsion at reservoir conditions.

3- Improve the stability of foam generated by surfactants by adding raw silica NPs or surface modified silica NPs.

4- Improve the understanding of the synergistic effect of surfactants and NPs on enhancing foam stability by assessing the role of NPs and evaluating the stability mechanisms.

5- Evaluate the potential of developed and selected materials to generate stable foams/emulsions and to reduce gas mobility in porous media.

6- Examine the ability of developed materials to reduce gas mobility and stabilize foam in presence of crude oil by testing the ability of the materials for EOR.

1.4 Research Milestones

Bare silica and surface modified silica NPs were used in this study to evaluate the potential of NPs to stabilize the gas-liquid foam/emulsion or to improve surfactant foam stability for gas mobility control and, thus, EOR. CO_2 and N_2 gases were used in this study to generate foams/emulsions. CO_2 was used mainly at the supercritical phase because it shows the highest performance for EOR. Also, it was used in some cases at the gaseous phase for the purpose of comparing the effect of pressure on foam/emulsion stability. Different surface modifiers of silica NPs (partially modified fumed silica with DCDMS, silica coated with PEG, and silica coated with a hidden chemical) at different conditions were used to evaluate their ability to stabilize the CO_2-brine or N_2-brine emulsions at harsh reservoir conditions: high salinity, high temperature, and in the presence of CO_2 at sc-CO_2. Also, new mixtures of bare silica NPs or surface modified silica NPs and anionic/nonionic surfactants were developed and used to improve foam stability for gas mobility control purposes.

We conducted our investigation of the ability of generated foam/emulsion to increase gas viscosity and, hence, to reduce gas mobility in five stages. **Figure 7** shows the stages and tests that will be conducted at each stage.

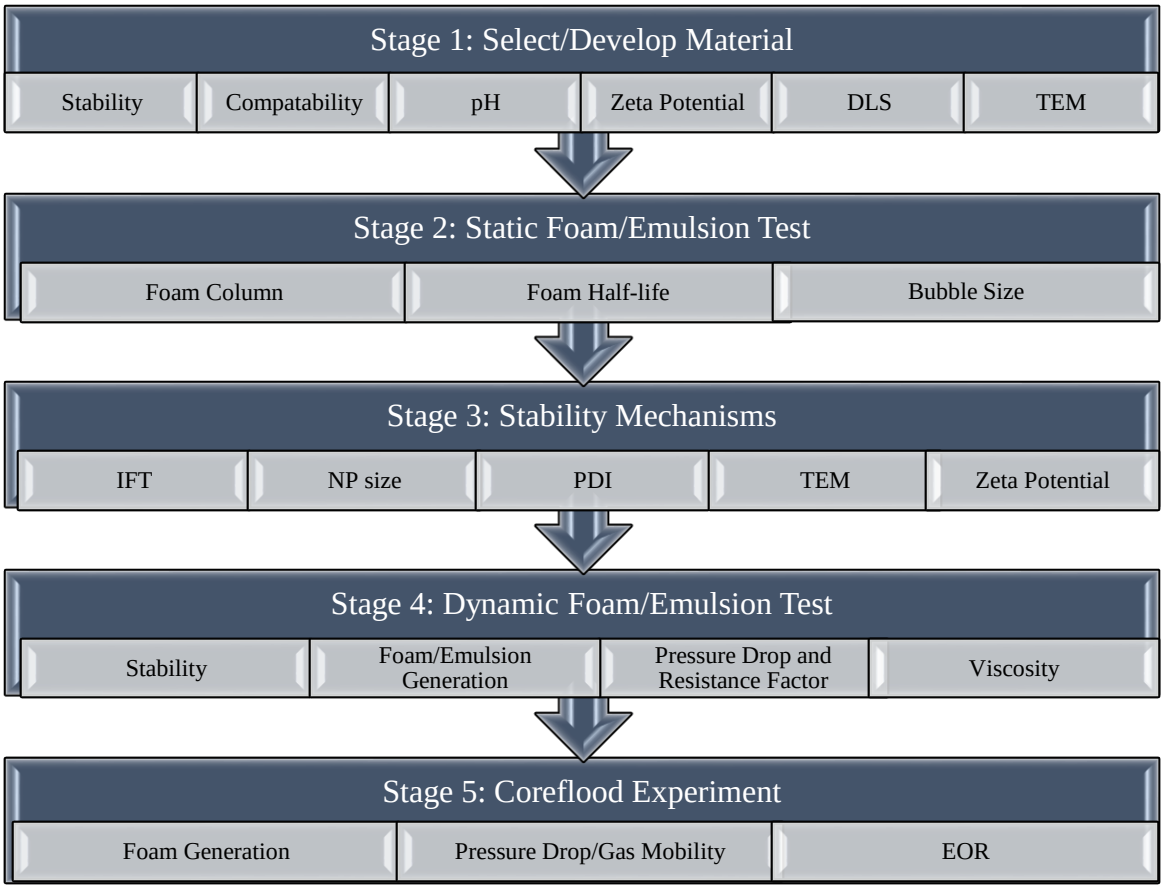

Figure 7: Research roadmap

1.4.1 Stage 1

This stage involved selecting and developing appropriate materials that can be used to meet the main goals of this study. Tests conducted at this stage include: compatibility and chemical stability of selected/developed materials, pH measurements, zeta potential measurements, and NPs characterization using dynamic light scattering (DLS) and transmission electron microscopy (TEM).

1.4.2 Stage 2

This stage consisted of conducting static foam/emulsion tests. Materials were tested for their ability to generate strong and stable foam/emulsion at ambient conditions. Foam column, foam half-life, and bubble size were measured to evaluate the static foam behavior. Also, different parameters such as salinity, concentration, and temperature were studied in this stage to assess their effects on foam/emulsion performance.

1.4.3 Stage 3

The objective of this stage was to understand foam stability mechanisms in the presence and absence of NPs. Interfacial tension (IFT) measurements of different systems (gas-water, gas-oil and oil-water), zeta potentials, DLS measurements, viscosity measurements and TEM results were interpreted to better understand the foam generation and stabilization mechanisms.

1.4.4 Stage 4

This stage involved testing the developed materials at various conditions such as different salinity concentrations, temperatures, and pressures to assess their ability to generate foam and reduce gas mobility in porous media. Viscosity of generated foam/emulsion, drop in pressure measurements, and mobility reduction factors (MRF) were calculated in these tests. In addition, a visual cell was used to capture generated foam/emulsion at reservoir conditions. Porous media were either in-house built (glass beads) or consolidated rock samples.

1.4.5 Stage 5

Coreflood experiments were conducted to evaluate the ability of selected material to generate and stabilize foam in the presence of crude oil, improve the gas sweep efficiency and EOR.

CHAPTER II

INSTRUMENTS, EXPERIMENTAL SETUP AND CHEMICALS

As discussed in the previous chapter, the objectives of this study require the measurement of many parameters. In this section, the instruments, setups, and software used to conduct this study will be described briefly. Also, all the chemicals and porous media used to run the tests will be listed.

2.1 Instruments

The main instruments used to conduct this study were*:* XA105DU Mettler Toledo balance, Anton Paar DMA 4100-M density meter**,** centrifuge, Nanobrook ZetaPALS analyzer, sonicator, DLS, Nikon Stereo Photomicroscope, Dataphysics OCA 15 Pro Contact Angle/IFT Device, Toshiba Aquillon RXL CT scanner, X-ray diffraction (XRD), and TEM. A brief description of each instrument is provided below.

2.1.1 XA105DU Mettler Toledo Balance

XA105DU Mettler Toledo balance is a highly accurate instrument for measuring weight. The design of this instrument makes it ideal for measuring small quantities of materials precisely. The maximum capacity at fine range is 41 g and the readability in this range is 0.01 mg. The instrument can read up to 5 decimals. It is also covered from all directions to minimize contamination during sample preparation. This instrument was used to accurately prepare solutions, surfactants, nanoparticles, and salt.

2.1.2 Anton Paar DMA 4100-M Density Meter

The Anton Paar density meter is considered one of the most precise instruments for measuring density. This machine has found wide application in the field. It has the ability to measure density at a range of different temperatures. In addition to its ability to display solution density, this instrument can also display density as an API value as well as the specific gravity. In this study, this instrument was used to measure solution densities and oil API gravity.

2.1.3 Centrifuge

The centrifuge used in this study was a Universal 320, manufactured by Hettich. This instrument can take up to 12 tubes with a maximum of 9000 RPM. The main use of this machine in this study was during the preparation of DCDMS coated silica NPs. It was used to separate solid particles from other chemicals added during sample preparation.

2.1.4 Nanobrook ZetaPALS Analyzer

The NanoBrookTM ZetaPALS is manufactured by Brookhaven Instruments Corporation and has the ability to measure several parameters including: zeta potential, solution conductance, and pH. To measure the zeta potential this instrument can employ one of two methods: electrophoretic light scattering (ELS), or phase analytical light scattering (PALS). This work uses NPs to stabilize foam/emulsion. Hence, it is necessary to study the stability of these particles by conducting zeta potential measurements at various conditions. Furthermore, the measurements of conductance and pH are required to assess the degree of stability and to understand the behavior of tested materials at desired experimental conditions.

2.1.5 Sonicator

The sonicator (Q55) used in this study is manufactured by QSONICA. It is particularly suited for sonicating small volumes. It has a power rating of 55 watts and a frequency of 20 kHz. This equipment was used during the preparation processes of some NPs to produce suspended and homogeneous solutions. **Figure 8** shows a photo of the Q55- Sonicator.

Figure 8: Q55- Sonicator

2.1.6 Dynamic Light Scattering

This instrument measures particle size using photon correlation spectroscopy (PCS) and measures the zeta potential using electrophoretic light scattering (ELS). This machine was used to measure NPs size and to determine the polydispersity index (PDI) of NPs in different solutions.

2.1.7 Nikon Stereo Photomicroscope

It was used to take images of foam/emulsion to determine bubble size.

2.1.8 Dataphysics OCA 15 Pro Contact Angle/IFT Device

The Dataphysics Optical Contact Angle 15 Pro is a high-precision device used to measure static and dynamic contact angles, surface/interfacial tension, surface free energy, liquid bridge analysis, and oscillation/relaxation. This device was used in this study to measure the contact angle that solid NPs make with air and water. It was also used to measure the interfacial tension values that different combination systems of air, water, and oil make at desired conditions. **Figure 9** shows a photo of OCA 15 Pro Contact Angle and IFT device.

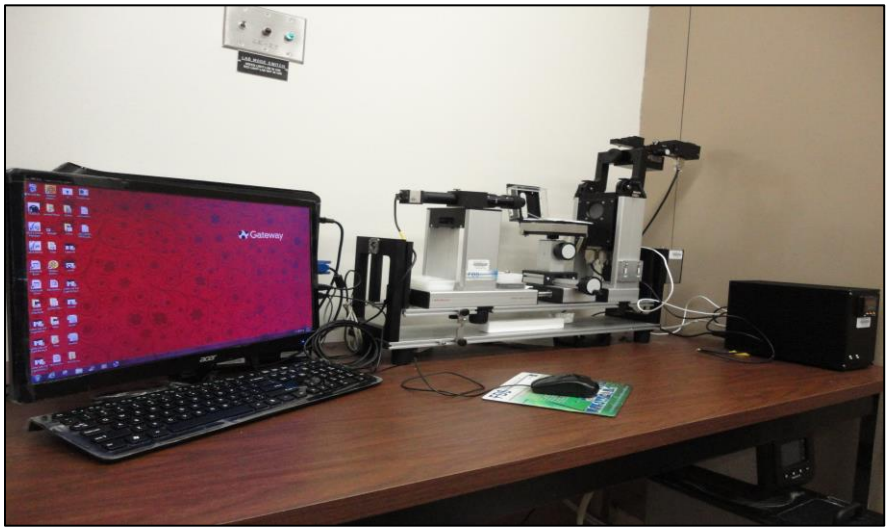

Figure 9: OCA 15 Pro Contact Angle and IFT device

2.1.9 Toshiba Aquillon RXL CT Scanner

The Toshiba Aquillon RXL CT Scanner is a sophisticated scanner with advanced features to enable users to capture high resolution images. This scanner has the ability to take

images with low contrast resolution of 2 mm at 0.3%. Also, the system has a 16-detector row CT system that can deliver precise images at a rate of 16 images per second. Moreover, the system is equipped with an advanced 3D visualization software package that makes image processing simple. The CT scanner was used in this study to identify the degree of homogeneity of rock samples. **Figure 10** shows a photo of Toshiba Aquillon RXL CT Scanner.

Figure 10: Toshiba Aquillon RXL CT Scanner

2.1.10 X-Ray Diffraction (XRD)

It is used to recognize crystalline compounds based on crystal structure. Based on the pattern of diffraction peaks and compared to standard peaks, crystalline compounds can be identified. XRD was used in this study to identify the major clay content of rock samples. This allowed for better assessment of the results from mobility tests to be discussed later.

2.1.11 Transmission Electron Microscope (TEM)

The features and limitations of this machine can be found in **table 3**. The main use of this apparatus was to visualize the NPs in the presence and absence of surfactants. The objective was to better understand the stabilization mechanisms of foam and the behavior of NPs as a result of mixing NPs and surfactants. **Figure 11** shows a photo of the FEI Tecnai G2 F20 ST FE-TEM.

Table 3: Features and limitations of FEI Tecnai G2 F20 ST FE-TEM

Feature	Limit
Point resolution	0.24 nm
Information limit	0.15 nm
Magnification range	21.5 x -1050 kx in TEM mode
Camera length range	30-4600 mm in TEM mode

2.2 Experimental Setup

To meet the objectives of this study, three setups were designed to perform experiments under desired conditions. All three use essentially the same equipment with only small changes in the configuration or in the porous media used to meet the specifications of each test. The three main systems are: viscosity measurement, mobility test, and coreflood. Each setup and its objectives are briefly described below.

2.2.1 Viscosity Measurement Setup

A schematic of the setup used for conducting viscosity measurements is shown in **figure 11**. It consists mainly of an injection system, porous media, a visualization system, a capillary tube, a production system and a heating system. It also has a data acquisition system connected to a computer to record important parameters.

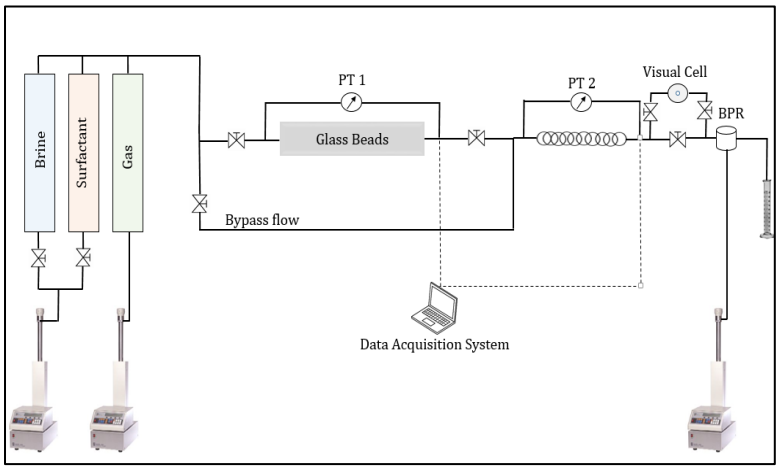

Figure 11: Schematic of viscosity measurement setup

2.2.1.1 Injection System

The injection system consists mainly of two units: the injection pumps and the accumulators. The injection pumps are used to pump fluids stored in the accumulators to the porous media or to the bypass line. The pumps used are D-Series Pumps from Teledyne ISCO and can operate under two schemes: constant flow rate or constant pressure. The flow rate can be as low as 0.001 ml/min, and these pumps can hold pressure up to 3750 psi. The capacity of the pump is 507 ml. These pumps, as shown in **figure 11**, are connected directly to the accumulators. They are manufactured by Core Laboratory and have a total capacity of 1000 ml. Moreover, they can handle pressure up to 10,000 psi. These accumulators store the fluids to be injected. The fluids injected are: brine, surfactant solution, NPs solution, oil, and gases (N_2 or CO_2). The accumulators are connected to a bypass line, the purpose of which is to ensure the injection of the correct fluids before they contact the main system, the porous media.

2.2.1.2 Porous Media

The porous media used in this study were either glass beads or consolidated rocks. The objective of using glass beads as a porous medium is to generate a homogenous clean porous medium to eliminate more complex fluid/rock interactions. An example of these interactions is the adsorption of injected fluids to the rock system. **Figure 12** shows a sample of the glass beads used to build the homogeneous porous media.

Figure 12: Glass beads

Glass beads were purchased from Potters Industries LLC. Two sizes were used in this study, 120-180 μm and 150-210 μm. More details about the specifications and compositions of these beads can be found in **table 4** and **table 5**, respectively. The purpose of using the porous media is to act as a foam/emulsion generator. The porous media is connected to a transducer (PT1) so the drop in pressure can be measured.

Table 4: Properties of glass beads

Feature	Value	Unit
Specific gravity	2.5	-
Refractive index	1.51	-
Hardness	6	Moh
Young's modulus	10 x 106	psi
Softening point	704	^{o}C

Table 5: Composition of glass beads

Composition	Amount (%)
SiO_2	72.50
Na_2O	13.70
CaO	9.80
MgO	3.30
Al_2O_3	0.40
FeO/Fe_2O_3	0.20
K_2O	0.10

2.2.1.3 Visualization System

A visual cell designed and manufactured by Core Laboratory was used in this study. This cell can handle pressure up to 10,000 psi. The purpose of the visual cell is to confirm the generation of the foam/emulsion at experimental conditions. It is connected directly after the foam capillary tube where the final foam/emulsion is generated. **Figure 13** shows a photo of the visual cell.

Figure 13: Visual cell

2.2.1.4 Capillary Tube

The capillary tube is basically an empty, thin line used to measure the viscosity of generated foam/emulsion. Two capillary tubes were used in this study. One has a length of 111.81 in, the other has a length of 40 in, and both have the same diameter, 0.0225 in. The small diameter of the line was selected in order to measure the viscosity at relatively low flow rates. The Hagen–Poiseuille equation was used to calculate the viscosity of generated emulsion based on the flow rate, the pressure drop as measured using a transducer (PT2), capillary tube length, and diameter. Full details about these measurements will be reported in the next chapter.

2.2.1.5 Production System

The production system consists mainly of two parts: the backpressure regulator (BPR) and a graduated cylinder. The BPR is designed and manufactured by Core Laboratory and can handle up to 10,000 psi. The purpose of the BPR is to provide the desired pressure for experiments. It is connected directly to a D-Series pump from Teledyne ISCO which provides the source fluid required to apply the desired pressure on the BPR. This pump has the same properties as those mentioned for the injection system discussed above. The graduated cylinder is used to collect liquids.

2.2.1.6 Heating System

The heating system is basically an oven combined all the equipment described above. It is manufactured by Memmert Company and can operate at high temperature; it reaches up to 125^{o}C. A photo of the whole setup with the oven can be seen in **figure 14**.

Figure 14: Experimental setup

2.2.1.7 Data Acquisition System

The data acquisition system consists of transducers, a data acquisition box, and a laptop. The transducers are manufactured by Validyne Engineering and have low and high ranges based on the experimental requirements. The purpose of the transducer is to measure the change in voltage across two points. As shown in **figure 12**, the two locations set to measure the change in voltage are across the porous media and across the capillary tube. The measured voltages are then converted to pressure via a correlation that was developed based on the range and type of transducer. These data are then transferred from the transducer box to the computer via the data acquisition box using software especially developed for that purpose.

2.2.2 Mobility Test Setup

A schematic of the setup used to conduct mobility tests can be shown in **figure 15**. The setup consists of: an injection system, porous media, visualization system, production system,

heating system, and data acquisition system. The major differences between this setup and the viscosity measurement setup are the porous media and the lack of a capillary tube. The porous media here consists of consolidated rocks instead of glass beads. The rocks used are either Boise, or Bentheimer sandstone. All rocks used in this study were purchased from Kocurek Industries. The core holder is made of aluminum and can hold a rock with maximum length of 12 in and a diameter of 1 in. The core sample is surrounded by a rubber Hassler sleeve in which an ISCO-pump is used to apply the overburden pressure on the core sample.

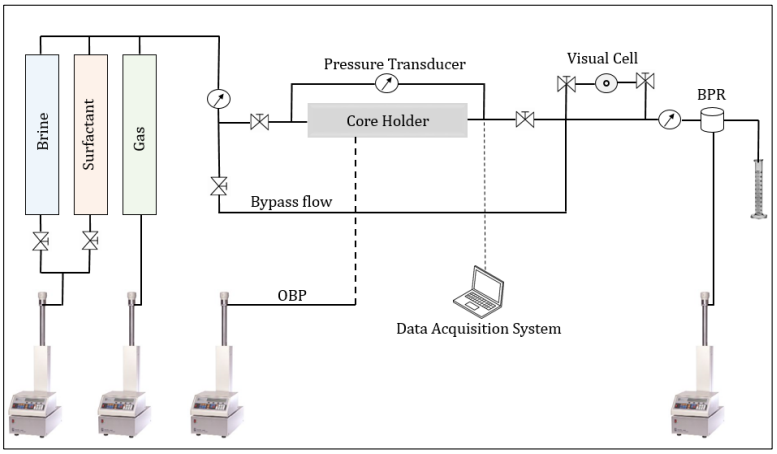

Figure 15: Schematic of mobility test setup

2.2.3 Coreflood Setup

A schematic of the setup used for conducting coreflood experiments is shown in **figure 16**. The major difference between this setup and the mobility test setup is the visualization system. The visual cell adds more dead volume which could affect the precise measurement of oil recovery. Therefore, it was removed for this setup.

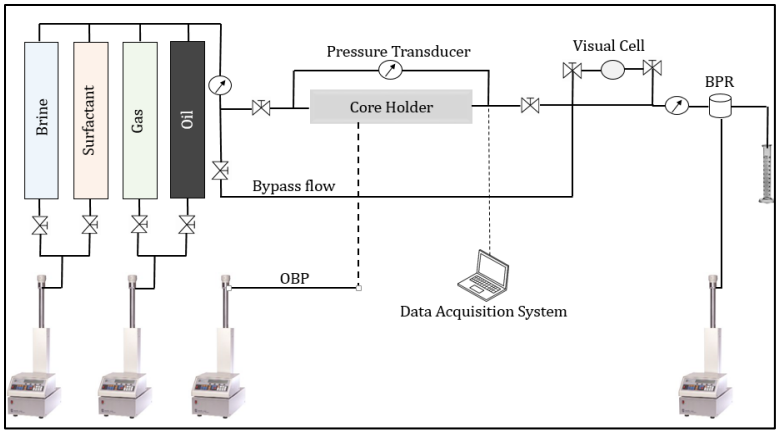

Figure 16: Schematic of coreflood setup

2.3 Chemicals

This section briefly describes the chemicals used to achieve foam/emulsion stabilization using NPs and surfactants. Other ancillary chemicals needed to perform the tests will be discussed as well.

2.3.1 Surfactant

Different commercially available surfactants were used, both individually and also mixed with NPs. The properties of CNF (complex nanofluid), NEODOL 91-8, NEODOL 25-7, NEODOL 25-9, and ENORDET A031surfactants are described below.

2.3.1.1 CNF

This is a newly developed surfactant with many desirable properties that have made it one of the top surfactants recommended for foam and conformance control applications in petroleum reservoirs. It is a complicated mixture of solvent, co-solvent foamer, and surfactants. The biggest advantages of this product are the low adsorption its surfactants exhibit in sandstone formations and its high stability in the presence of crude oil. Also, it is very compatible with acidic solutions and other additives. **Table 6** lists the properties of this surfactant.

Table 6: Properties of CNF

Properties	Value
Form	Liquid
Chemical Family	Complex Nanofluid
Odor	Citrus
pH	7.73
Density	1.07 g/ml
Charge	Anionic
Flash point	>93.3ºC

2.3.1.2 NEODOL 91-8

The main properties of this surfactant can be found in **table 7**.

Table 7: Properties of NEODOL 91-8

Properties	Value
Chemical Family	Alcohol Exthoxylate
Company	Shell Chemical LP
Appearance	Slightly viscous liquid
Carbon chain length	9-11
Ethylene Oxide	< 6.00 PPM
Odor	Mild
Specific gravity	1.008 at 25ºC
Charge	Nonionic
Flash point	159ºC

2.3.1.3 NEODOL 25-7

The main properties of this surfactant can be found in **table 8**.

Table 8: Properties of NEODOL 25-7

Properties	Value
Chemical Family	Alcohol Exthoxylate
Company	Shell Chemical LP
Carbon chain length	12-15
Ethylene Oxide	< 6.00 PPM
pH	6.8
Appearance	Hazy to semi-solid liquid
Odor	Mild
Specific gravity	0.965 at 122^{o}C
Charge	Nonionic
Flash point	186.1^{o}C
Water solubility	100.0 g/l complete

2.3.1.4 NEODOL 25-9

The main properties of this surfactant can be found in **table 9**.

Table 9: Properties of NEODOL 25-9

Properties	Value
Chemical Family	Alcohol Exthoxylate
Company	Shell Chemical LP
Carbon chain length	12-15
Ethylene Oxide	6.00 PPM
pH	6.8
Appearance	White. Waxy solid at ambient temperature
Odor	Mild
Specific gravity	0.992 at 40ºC
Charge	Nonionic
Cloud point	78ºC
Flash point	190ºC
Water solubility	Miscible

2.3.1.5 ENORDET A031

The main properties of this surfactant can be found in **table 10**.

Table 10: Properties of ENORDET A031

Properties	Value
Chemical Family	Olefin Sulphonate Sodium Salt Water
Company	Shell Chemical LP
pH	12-13
Appearance	Amber liquid
Odor	Mild
Charge	Anionic
Flash point	>100ºC

2.3.2 Nanoparticles

Different types of silica NPs were used. Bare silica and surface modified silica NPs with different modifiers were tested for the purpose of stabilizing CO_2-brine foam/emulsion and improving the stability of foam generated by surfactants. Bare silica, silica modified with DCDMS, silica modified with hidden chemical, and silica modified with PEG will be described briefly here.

2.3.2.1 Silica NPs

Bare silica NPs (SiO_2) of size 20 nm, were purchased from NYACOL NANO TECHNOLOGIES, Inc. and have been used to improve the stability of foam generated by surfactants. **Table 11** summarizes the properties of silica NPs.

Table 11: Properties of silica NPs

Properties	Value
Commercial name	NexSil 20
Typical particle size	20 nm
Typical surface area	135 m2/g
Wt% silica as SiO2	40%
pH	8.9 at 25°C
Specific gravity	1.3
Charge	Negative

2.3.2.2 Silica Modified with DCDMS

Two different sizes of coated fumed silica were received from WACKER. Thesefumed silica are surface modified with DCDMS. These materials were received as powder. They were used mainly to stabilize CO_2-brine emulsion at harsh reservoir conditions. The chemical structure of silica coated with DMS is shown in **figure 17**. The main properties of silica modified with DCDMS are listed in **table 12**.

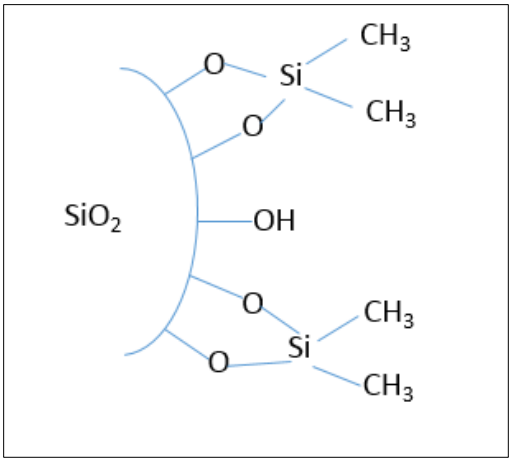

Figure 17: Chemical structure of silica coated with DMS

Table 12: Properties of silica modified with DCDMS

Properties	Value	Value
Commercial name	H 15	H 30
BET surface area of hydrophobic silica	120 m2/g	250 m2/g
pH	4.3 in 4% dispersion	4.3 in 4% dispersion

2.3.2.3 Silica Modified with Hidden Chemical

Silica NPs modified with a hidden chemical was purchased from NYACOL NANO TECHNOLOGIES, Inc. It was received as dispersed particles in water with a total solid concentration of 30.5 wt%. The average particle size of these particles was measured using DLS and found to be 30 nm +/- 1. This material was used in this study to stabilize CO_2-brine and N_2-brine foam/emulsion and also to improve the stability and strength of foam generated by surfactants. This is the only information available about this material.

2.3.2.4 Silica Modified with PEG

A silica coated with PEG was designed based on a request sent from our laboratory to a vendor to evaluate the potential of such chemical in stabilizing the CO_2-brine emulsion at harsh reservoir conditions. The size of the silica NPs was 10 nm. The sample was received as dispersed particles in deionized water with a concentration of 5 g in 125 ml. The chemical structure of PEG is shown in **figure 18**.

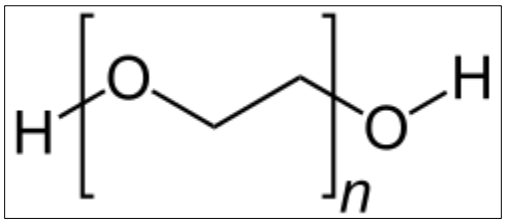

Figure 18: Chemical structure of PEG

2.3.3 Complementary Chemicals

In this section the properties of additional chemicals, such as water, salts, gases and oil, required for foam generation bulk tests, mobility tests and coreflood experiments will be described.

2.3.3.1 Deionized Water

Many of the tests in this study, such as the measurement of zeta potential, require the precision preparation of pure reagents. For this reason, deionized water, ASTM type II, obtained from LabChem was used to prepare all solutions.

2.3.3.2 Salts

Two salts were used to prepare solutions in this study: sodium chloride (NaCl) and calcium chloride ($CaCl_2$). Sodium chloride (99%) was obtained from Cole-Parmer, and calcium chloride (99-105 %) was obtained from Fisher Chemical.

2.3.3.3 Crude Oil

The crude oil used in this study is North Burbank Unit (NBU) oil. It has a viscosity of 8.1 cp at 23^{o}C and 3.2 cp at 50^{o}C, and an API gravity of 33.77 at 15.56^{o}C. The oil was used to test the stability of foam in the presence of crude oil and it was also used to conduct coreflood experiments.

2.3.3.4 Gases

Nitrogen (N_2) and carbon dioxide (CO_2), industrial grade, were used to generate foams/emulsions. N_2 was used in the gaseous phase. However, CO_2 was used in gaseous and supercritical phases. The uses of these gases at different phases will be discussed in the next chapter.

2.3.3.5 Toluene

Toluene is an aromatic hydrocarbon that is widely used as an industrial feedstock and as a solvent. Because of its ability to act as a solvent for a wide variety of chemicals, toluene was used in this study to clean the setups after finishing experiments.

CHAPTER III

EXPERIMENTAL PREPARATIONS AND PROCEDURES

This chapter will cover the experimental preparations and procedures used to conduct the tests required to meet the goals of the study. The experimental preparations include: solution preparation, porous media formation, and rock sample characterization. The section on experimental procedures will discuss the conditions and procedures used for: bulk tests, IFT measurements, DLS measurements, zeta potential measurements, TEM visualization, viscosity measurements, mobility tests, and coreflood experiments.

3.1 Experimental Preparations

As stated above, this section will cover solution preparation, porous media formation, and rock sample characterization.

3.1.1 Solution Preparation

Solution preparation varies from one test to another and from one material to another. Also, the tools used to prepare samples change depending on the solution. Preparations of solutions containing only NPs in the absence of surfactant were made by adding NPs to deionized water in stepwise fashion to avoid the formation of aggregates. Mixing was usually performed using a sonicator, primarily because NPs require high energy to produce stable and homogeneous solutions.

Samples containing NPs and surfactant were prepared a bit differently. The original surfactant and silica NP samples were first diluted separately in deionized water and stirred

overnight to ensure homogeneity. NPs, but not the mixture, were sonicated. These became stocks used to prepare the surfactant and NP mixtures for the static and dynamic tests. NPs were added to surfactants in stepwise fashion to minimize aggregation of NPs during the mixing process. To avoid the generation of foam during this step, samples were stirred at moderate revolutions per minute. This procedure was followed for all tested samples containing surfactant and NPs.

3.1.2 Porous Media Formation

As mentioned previously, glass beads were used as porous media. In-house porous medium was prepared to conduct the viscosity measurements for solutions containing only NPs. Two sizes of the same glass beads were used to build clean and homogenous porous media with high permeability. The main parameters and properties of porous media are summarized in **table 13**. The procedure of preparing the porous media is as follows:

1- An empty stainless tube with a diameter of 0.18 in and a length of 12 in was cleaned and dried.
2- The bottom side of the tube was closed.
3- About half of the tube was filled with DI water.
4- Glass beads were added gently until the beads were seen at the top of the tube.
5- The top part was closed and the tube was exposed to vibration using ultrasonic bath.
6- Filters were connected to both sides to allow flow through the porous medium while preventing the loss of glass beads.
7- High pressure was applied to the tube to ensure tight packing of the glass beads inside the tube.

8- The drop in pressure was calculated across the tube at different flow rates, low and high, to ensure the permeability remained constant.

Table 13: Properties of porous media

Properties	Glass beads 1	Glass beads 2
Glass beads size	120-180 μm	150-210 μm
Length	12 in	12 in
Diameter	0.18 in	0.18 in
Pore volume	1.5 ml	1.7 ml
Porosity	30%	34%
Permeability	17.21 Darcy	23.74 Darcy

3.1.3 Rock Sample Characterization

Two types of rocks were used in this work: Boise and Bentheimer sandstone. The diameter of all rocks were 1 in. All mobility and coreflood tests were conducted using rocks with 12 in length. Interpreting the results of these experiments depends critically on understanding the content and homogeneity of the rocks used. This is because the construction and homogeneity of rocks can affect fluid flow in porous media. Furthermore, foam is significantly influenced by rock properties and heterogeneity. In this study, a CT scanner was used to evaluate the heterogeneity of the rocks. Finally, identifying the rock composition can help assess rock-fluid interactions, which can strongly affect foam generation and strength. XRD was used to identify the rocks' composition. In the following sections, the results of both studies, CT scanner and XRD, for all rocks mentioned above are briefly discussed.

3.1.3.1 Boise Sandstone

Based on the CT scanner results, (**figure 19)** the Boise sandstone can be classified as a homogenous rock. The change in the average CT number is not significant, around 50. Higher fluctuation of rock CT number indicates the presence of heterogeneity, which is not the case for the Boise sandstone. The XRD results (**figure 20**) shows that Boise sandstone contains mostly quartz (45%) and feldspar (27%). It also shows a peak of clay, namely illite (13%). The presence of clays is one of the primary factors affecting foam generation and strength in porous media. This is attributed to the high adsorption of surfactants caused by the clay minerals.

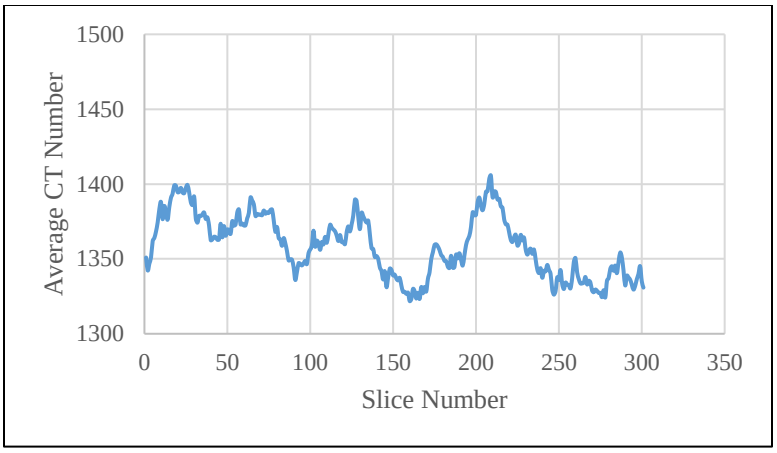

Figure 19: Average CT number for Boise sandstone

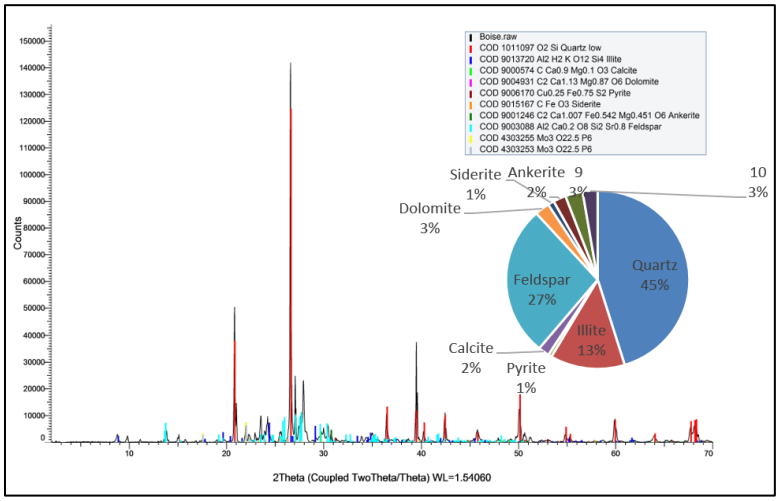

Figure 20: XRD result of Boise sandstone

3.1.3.2 Bentheimer Sandstone

Based on the CT scanner results (**figure 21**) the Bentheimer sandstone can be classified as a homogenous rock. The change in the average CT number is very small, mostly less than 20. The XRD result (**figure 22)**, shows that Bentheimer sandstone contains only quartz (100%). Due to the absence of the clay minerals, the rock could be classified as a clean rock. Based on these analyses, anionic surfactants should not have any adsorption issues with such type of rocks.

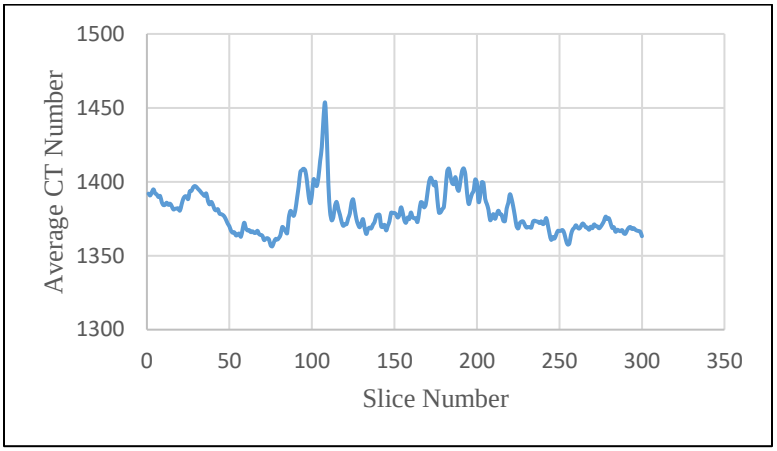

Figure 21: Average CT number for Bentheimer sandstone

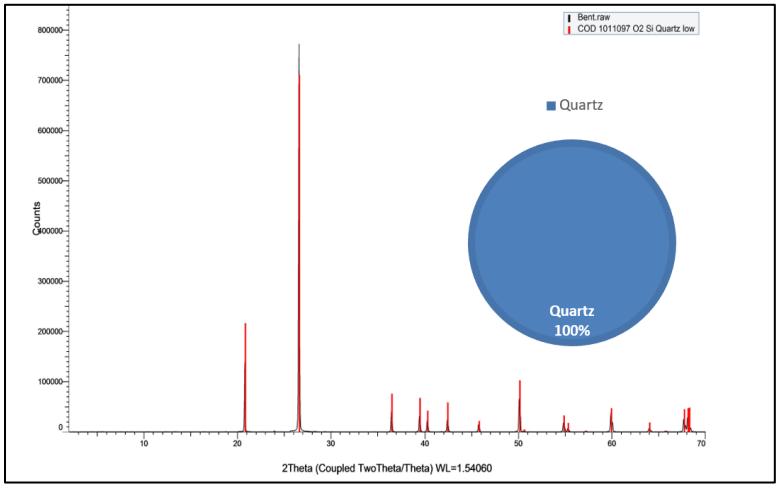

Figure 22: XRD result of Bentheimer sandstone

3.2 Experimental Procedures

This section covers the specific procedures used to evaluate the potential of NPs to stabilize CO_2-brine emulsion or to improve the stability of foam generated primarily by surfactants. The tests or measurements covered in the following sections are: bulk tests, IFT measurements, DLS measurements, zeta potential measurements, TEM visualization, viscosity measurements, mobility tests, and coreflood experiments.

3.2.1 Bulk Tests

- Objectives

  The main goals of these tests were to:

- Study visually the chemical stability of tested materials at various conditions.
- Evaluate the potential of tested materials to generate and stabilize foams/emulsions.
- Assess the strength of each material to generate strong foam/emulsion.

- Type of tests conducted

  Bulk tests consisted primarily of measuring foam half-life and bubble sizes.

3.2.1.1 Foam Half-Life Measurements

The foam half-life tests were conducted by preparing solutions in glass tubes. The solutions were then shaken at least 5 times and photos of foam columns were captured over time. These images were then evaluated using ImageJ software to measure foam half-life. Longer foam half-lives indicate increased stabilization of foam/emulsion. In addition to half-

life measurements, solutions were monitored over long periods of time to ensure their chemical stability, which was assessed by observing any precipitate formation or color changes.

3.2.1.2 Bubble Size Measurements

As in the previous test, the solutions that were already shaken were used to study the change in bubble size over time. A Nikon Stereo Photomicroscope was used to capture the foam bubbles. Bubble size is an indication of the ability of materials to stabilize foam/emulsion; smaller bubbles indicate better stability. This type of test was conducted at ambient conditions.

3.2.2 IFT Measurements

- Objectives

The main goals of these tests were to:

- Define the critical micelle concentration (cmc) of the surfactants.
- Study the change of cmc as a result of adding NPs to surfactants.
- Study the effect of NPs in reducing the air-water interfacial tension when added to surfactant.
- Study the foam stability in the presence of crude oil.

- Types of tests conducted

The major parameters needed to understand foam generation and stability in the presence of surfactant as a foaming agent in bulk are the IFT values of three fluids: water, oil, and gas. In the absence of oil, $\sigma_{w/g}$ is the parameter controlling foam

generation but not stability. Therefore, to meet the objectives specified for IFT measurements, two types of measurements were conducted: air-water IFT measurements and foam stability in the presence of crude oil.

3.2.2.1 Air- Water IFT Measurements

Air-water ($\sigma_{w/g}$) IFT measurements were conducted to study the effect of surfactant and the mixture of surfactant and NPs in reducing the air-water IFT value. Samples at different surfactant concentrations and mixtures of surfactant and NPs were prepared and air-water IFT values were measured. The main outcomes from these measurements are: the cmc of surfactant in the presence and absence of NPs, and the ability to generate foam. The air-water IFT values reflect the foamability.

3.2.2.2 Foam Stability in The Presence of Crude Oil

As one of the purposes of generating foam is to reduce gas mobility and therefore improve the sweep efficiency to enhance oil recovery, it is important to consider the oil when conducting a foam study. Four parameters were used to evaluate the foam generation process in presence of crude oil: spreading (S), entering (E), bridging (B), and lamella number (L). Equations 3 through 6 represent these four parameters. OCA20 goniometer device was used to measure the IFT values of the three systems mentioned above needed in these equations. These values can then be interpreted to understand the foam generation and stabilization processes qualitatively. (Harkins 1941) developed an equation to estimate the spreading coefficient and reached the conclusion that a negative value of spreading coefficient (S) will lead to a stable foam in the presence of oil. This means that the water-oil interfacial tension ($\sigma_{w/o}$) and the oil-

gas interfacial tension ($\sigma_{o/g}$) values should be relatively high to satisfy this condition. (Robinson and Woods 1948) developed a method of selecting foam inhibitors based on IFT values and reported that a negative value of entering, rupture coefficient (e) produces a stable foam in the presence of crude oil. In this case, the oil-gas interfacial tension ($\sigma_{o/g}$) value should be relatively high to attain this condition. Another parameter had been developed by (Denkov 2004). He found that oil could act as an active antifoaming agent if the bridging (B) value is positive. This can happen if the $\sigma_{o/g}$ is relatively small. Also, lamella number (L) can be used to assess the presence of oil in foam stability. (Schramm and Novosad 1990) developed the concept of lamella number. It was categorized into three ranges (L<1, 1<L<5.5, and L>5.5) to explain if the oil becomes emulsified and imbibed into the thin film (lamella) to destroy it. For L<<1, the oil cannot be emulsified to smaller droplet sizes and, therefore, cannot get into the thin film. For 1 <L< 5.5, oil can be emulsified to smaller droplets and can, thus, penetrate the thin film and reside within the larger plateau borders. The worst case is when L>5.5. In this case, the oil can emulsify to smaller droplets where they can easily access the entire thin film and destroy the foam.

$$S = \sigma_{w/g} - \sigma_{w/o} - \sigma_{o/g} \quad (3)$$

$$e = \sigma_{w/g} + \sigma_{w/o} - \sigma_{o/g} \quad (4)$$

$$B = {\sigma_{w/g}}^2 + {\sigma_{w/o}}^2 - {\sigma_{o/g}}^2 \quad (5)$$

$$L = 0.15 \ \frac{\sigma_{w/g}}{\sigma_{w/o}} \quad (6)$$

Where;

$\sigma_{w/g}$: interfacial tension of water and gas

$\sigma_{w/o}$: interfacial tension of water and oil

$\sigma_{o/g}$: interfacial tension of oil and gas

3.2.3 DLS Measurements

- Objectives

The main objectives of this type of test were to:

- Determine the sizes of NPs.
- Study the changes of NP's size as a result of mixing NPs and surfactant.
- Study the changes of NP's size when added to saline water (brine).
- Understand the mechanisms of foam stability when NPs used to improve the foam/emulsion stability.

- Types of tests conducted

DLS was used to conduct two main types of measurements, NPs size and PDI. Samples were prepared with NPs suspended only in DI water, mixed either with surfactants or with salts. These two parameters were used to study the effect of each additive in NP's behavior and, hence, to draw conclusions about the role of NPs in foam stability, whether positive or negative as will be explained later when discussing the results of this study.

3.2.4 Zeta Potential Measurements

- Objectives

The major objectives of measuring zeta potential were to:

- Evaluate the stability of solutions.
- Understand the surface interactions of NP-NP or NP-surfactant systems.

- Type of tests conducted

This instrument was used primarily to measure the zeta potential for different solutions. The zeta potential of NPs alone or mixtures of NPs and surfactants were measured to assess the chemical stability and surface interactions of these species in solution. Also, this instrument was used to measure the pH, which could also be used to evaluate the stability and chemical changes that might happen in solution.

3.2.5 TEM Visualization

- Objectives

The major objectives of using TEM were to:

- Visualize the NPs to measure their sizes for comparison with the results obtained from DLS.
- Study the behavior of NPs as a result of mixing particles with surfactants.
- Combine the results with those obtained from DLS and zeta potential measurements to draw a conclusion about the role of NPs in improving foam stability.

- Types of tests conducted

For TEM analysis, 2–5 µl of a sample were adsorbed onto a fresh glow-discharged carbon-coated Formvar grid, washed briefly in water, and negatively stained with a 2% (w/v) aqueous solution of uranyl acetate. Specimens were observed using a JEOL 1200 EX TEM operated at an acceleration voltage of 100 kV. Electron micrographs were recorded at calibrated magnifications using a 3k slow-scan CCD camera (model 15C, SIA). Image analysis was carried using the ImageJ software package.

3.2.6 Viscosity Measurements

- Objectives

The major objective of conducting viscosity measurements was to assess the ability of NPs to increase the gas apparent viscosity by producing foams/emulsions.

- Types of tests conducted

Mainly, there were two systems used to measure the viscosity: glass beads and capillary tube systems.

3.2.6.1 Glass Beads

In glass beads the apparent viscosity ($\mu_{apparent,porous}$) of fluids can be calculated using Darcy's law:

$$\mu_{apparent,porous} = \frac{k\ A\ \Delta P}{l\ q} \tag{7}$$

Where:

k is the permeability of the porous media (glass beads) (m^2)

A is the cross sectional area of the porous media (m^2)

ΔP is the pressure drop across the porous media (Pa)

l is the length of the porous media (m)

q is the total injection flow rate (m^3/s)

3.2.6.2 Capillary Tube

In a capillary tube the fluid viscosity can be calculated using the Hagen–Poiseuille equation:

$$\mu_{apparent} = \frac{\pi \, \Delta P r^4}{8 \, l^* \, q} \tag{8}$$

Where:

r is the radius of the capillary tube (m)

ΔP is the pressure drop across the capillary tube (Pa)

l^* is the length of the capillary tube (m)

q is the total injection flow rate (m^3/s)

In general, the ratio of apparent viscosity of injected fluid to a baseline viscosity ($\mu_{baseline}$) can be used to estimate the gas flow resistance factor (RF).

$$RF = \frac{\mu_{apparent,porous/apparent}}{\mu_{baseline}} = \frac{\Delta P}{\Delta P_{baseline}} \tag{9}$$

The Hagen–Poiseuille equation assumes a laminar flow regime so it is necessary to ensure that the flow regime of the generated emulsion satisfies this condition. Calculating the Reynolds number determines the type of flow regime as R_e less than 2300 represents laminar flow. The R_e can be calculated as follows:

$$R_e = \frac{v.d.\rho_{emulsion}}{\mu_{apparent}} \quad (10)$$

Where:

v is the fluid average velocity (m/s)

d is the pipe diameter (m)

$\rho_{emulsion}$ is the emulsion density (g/cm^3)

The density of the emulsion can be estimated from the density of the liquid and the density of the gas phase as follows:

$$\rho_{emulsion} = \alpha.\rho_{CO_2} + (1-\alpha).\rho_{liquid} \quad (11)$$

Where:

α is the fraction of gas relative to the total injected fluid

ρ_{CO_2} is CO_2 density at experimental conditions (g/cm^3)

ρ_{liquid} is the liquid density at experimental conditions (g/cm^3)

The protocol for viscosity measurements was as follows:

1- The system was first fully saturated with brine.

2- The experimental pressure and temperature were then set.

3- One pore volume of tested solution was injected into the porous media.

4- The gas and liquid solution were then co-injected into the porous media.

5- The pressure drop across the porous media and capillary tube was then measured.

3.2.7 Foamability and Mobility Test

- Objectives

The major objectives of conducting foamability and mobility tests were to:

- Evaluate the ability of tested materials to produce foam in porous media (rocks).
- Compare the foam strength and stability of tested materials.
- Estimate the gas mobility reduction factor (MRF).

- Type of tests conducted

The foam/emulsion generation was conducted by a co-injection of gas and liquid into porous media. The effect of different parameters, namely chemical concentration, salinity, quality (gas flow rate/total flow rate), pressure, and temperature, were studied to assess foam generation and stability of selected materials. The comparison was made based on the MRF, similar to RF, as follows:

$$MRF = \frac{\Delta P}{\Delta P_{baseline}} \quad (12)$$

ΔP in this case is the pressure drop across the rock sample.

The experimental procedure of foamability and mobility tests was as follows:

1- Incubate the sample in an oven overnight to ensure that the sample is dry.
2- Cover the sample with lead foil, to prevent gas diffusion from the sample to the confining fluid Apply an over burden pressure (OBP) on the rock sample (Mazumder, Karnik, and Wolf 2006).
3- Use a vacuum pump to remove air from the core sample.
4- Inject a known volume of brine into the core sample and measure porosity.

5- Inject at least 5 PV of brine to ensure the sample is 100% saturated with brine.

6- Set the experimental pressure and temperature.

7- Measure the rock permeability.

8- Inject 1 PV of surfactant/mixture into the core sample to minimize the adsorption that might occur during the foam generation and recovery processes.

9- Start co-injection of the gas and liquid solution.

10- Measure the pressure drop across the rock sample.

3.2.8 Coreflood Experiments

- Objectives

The main objectives of conducting coreflood experiments were to:

- Evaluate the ability of tested materials to produce foam in the presence of crude oil.
- Evaluate the ability of tested materials to improve the sweep efficiency and to enhance the oil recovery (EOR)

- Types of tests conducted

Coreflood experiments were similar to foamability and mobility tests except that coreflood experiments were conducted in the presence of crude oil. The experimental procedure of coreflood tests (non-fractured rocks) was as follows:

1- Incubate the sample in an oven overnight to ensure that the sample is dry.

2- Cover the sample with lead foil, to prevent gas diffusion from the sample to the confining fluid Apply an over burden pressure (OBP) on the rock sample.

3- Use a vacuum pump to remove air from the core sample.

4- Inject a known volume of brine into the core sample and measure porosity.
5- Inject at least 5 PV of brine to ensure the sample is 100% saturated with brine.
6- Set the experimental pressure and temperature.
7- Measure the rock permeability.
8- Inject oil into the rock until it reaches the initial water saturation (S_{wi}) where no more water produced.
9- Measure the volume of water produced to calculate the S_{wi}.
10- Start water flooding and collect the oil produced.
11- Inject 1 PV of surfactant/mixture into the core sample to minimize the adsorption that might occur during the foam generation and recovery processes.
12- Start co-injection of the gas and liquid solution.
13- Measure the pressure drop across the rock sample and collect the oil produced.

Fractures were created through the horizontal axis by cutting the rocks from the center. The experimental procedure of coreflood tests (fractured rocks) was as follows:

1- Incubate the sample in an oven overnight to ensure that the sample is dry.
2- Cover the sample with lead foil, to prevent gas diffusion from the sample to the confining fluid Apply an over burden pressure (OBP) on the rock sample.
3- Use a vacuum pump to remove air from the core sample.
4- Inject a known volume of oil into the core sample and measure porosity.
5- Inject at least 5 PV of oil to ensure the sample is 100% saturated with oil.
6- Set the experimental pressure and temperature.
7- Measure the rock permeability.

8- Start water flooding and collect the oil produced.

9- Inject 1 PV of surfactant/mixture into the core sample to minimize the adsorption that might occur during the foam generation and recovery processes.

10- Start co-injection of the gas and liquid solution.

11- Measure the pressure drop across the rock sample and collect the oil produced.

CHAPTER IV

EXPERIMENTAL RESULTS AND DISCUSSION

This chapter will present and discuss the results of all measurements and tests in this study. The chapter is divided into two separate sections:

1- NPs-stabilized gas-liquid foam/emulsion

2- NPs and surfactants stabilized gas-liquid foam

Each section covers all the results for each experiment individually. This means, for example, that results of the bulk tests, zeta potential measurements, DLS measurements, TEM visualizations, viscosity measurements, mobility tests, and coreflood experiments for a given material will be presented and discussed together before discussing these results for the next material. Note that not every study uses exactly the same measurements. For example, not every tested material required TEM visualization. Finally, it is important to mention that the coreflood experiments were conducted for the best material that gave the highest foam stability and strength.

4.1 NPs-Stabilized Gas-Liquid Foam/Emulsion

In this section, the results of three tested materials will be presented and discussed. These materials are: fumed silica modified with DCDMS, silica modified with hidden chemical, and silica modified with PEG.

4.1.1 Fumed Silica Modified with DCDMS

This section discusses the results of silica coated with DCDMS. Even though this material has been reported previously in the literature as a CO_2-water emulsion stabilizer, this study examines the impact of several parameters on the strength of generated emulsions and compares the results of this material with other materials that will be presented later. These parameters include quality, shear rates, NP's size, and solution salinity. These parameters were evaluated based on viscosity measurements taken from a capillary tube and calculated from the Hagen–Poiseuille equation. The viscosity measurements conducted with glass beads 1 and capillary tubes will be presented only for the purpose of showing the effect of shear rates on emulsion strength.

4.1.1.1 Materials

Fumed silica partially modified with DCDMS was prepared with 1wt% concentration and two different sizes. Most of the tests were conducted using H30 (250 m^2/g) NPs. H15 (120 m^2/g) was only used to compare the effect of size on foam stability and strength. All of the properties of this material have already been listed in **table 12**.

4.1.1.2 Experimental Procedure and Conditions

The porous media used for this study consisted of glass beads 1. The viscosity measurement setup, depicted in figure 11, was used to conduct the tests. The experimental parameters and conditions used to conduct this study are shown in **table 14**. The salts used were NaCl and $CaCl_2$. The shear rates were different for the porous media (glass beads 1) and the capillary tube. At the same flow rate, the shear rate in capillary tubes is higher than that for the glass beads 1. The objectives of this design were to test the effect of different shear rates in porous media separately and, at the same time, to evaluate the emulsion strength in capillary tubes at much higher shear rates. Therefore, many shear rates were tested. This means that the emulsion generated at the glass beads 1 is not related to that at the capillary tube.

Table 14: Experimental parameters and conditions for silica modified with DCDMS

Parameter	Range	Unit
Pressure	1800	Psi
Temperature	50	^{o}C
Gas	Sc-CO_2	-
Quality	50-70-90	%
Salinity	1-3-8 NaCl 1 NaCl + 0.5 $CaCl_2$	wt% wt%
Shear rates (Glass beads 1)	655-980-1310	s^{-1}
Shear rates (Capillary tube)	910- 1365- 1820	s^{-1}
NPs surface area	120 -250	m^2/g

4.1.1.3 Results and Discussion

4.1.1.3.1 Effect of Quality

The effect of quality on emulsion strength was conducted for three qualities: 50, 70, and 90%. The results show that quality is a crucial parameter on emulsion strength. Emulsion viscosity increases as quality decreases, with the strongest emulsion achieved at 50% quality. The effect of quality was tested in porous media by recording pressure for each of the three qualities. **Figures 23**, **24**, and **25** show the pressure drop across porous media for the three qualities under the same conditions. The highest steady state pressure drop, 3 psi, was reported for 50% quality while the lowest, 2.25 psi, was reported for 90% quality. At 70%, the pressure drop, 2.40 psi, is very close to that of 90% quality. Taken together, these data indicate that 50%

quality is the best in term of emulsion strength since it produced the highest resistance to gas flow.

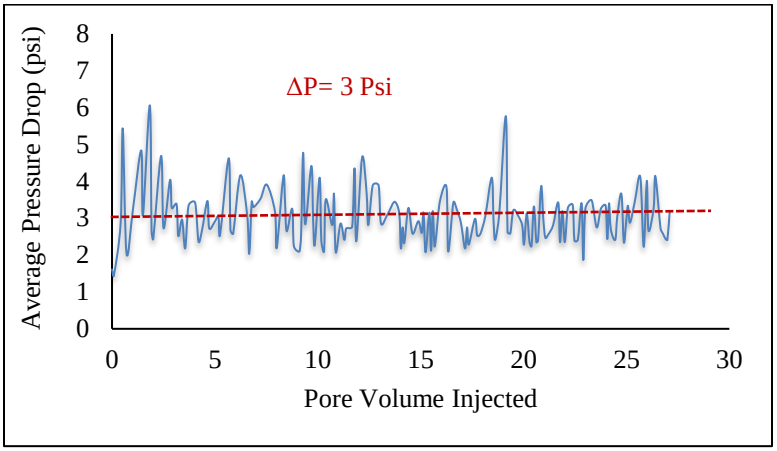

Figure 23: Pressure drop across glass beads 1 at 50% quality

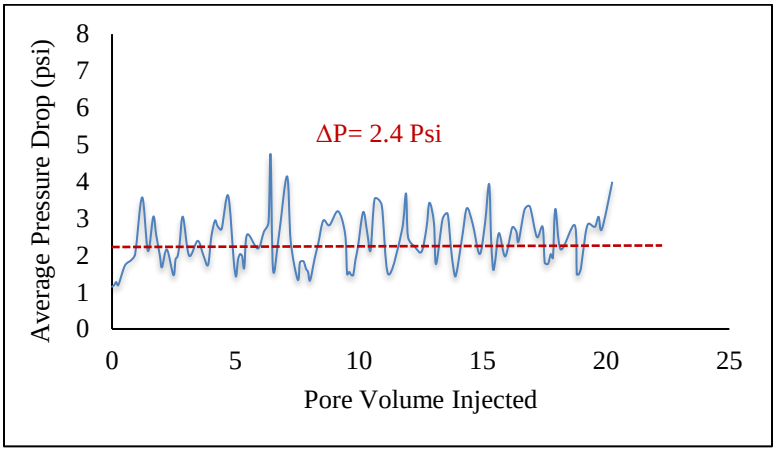

Figure 24: Pressure drop across glass beads 1 at 70% quality

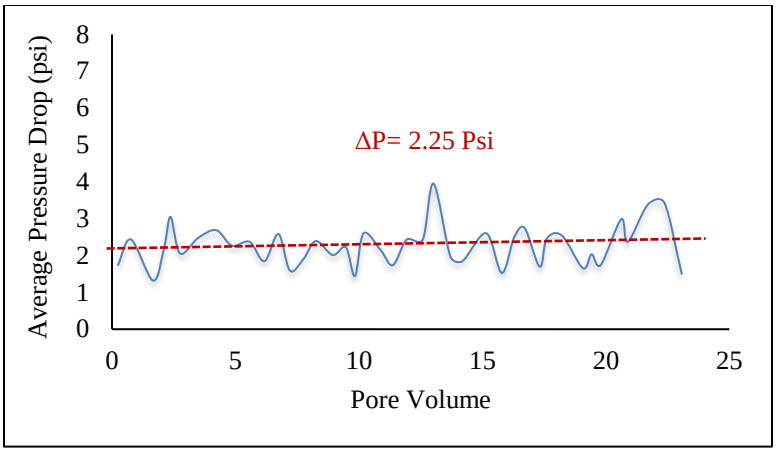

Figure 25: Pressure drop across glass beads 1 at 90% quality

Viscosity measurements at different qualities were conducted at several conditions (e.g. different shear rates) and the conclusion was almost the same. The 50% quality produced the highest viscosity followed by the 70% quality. The lowest quality, 50%, had a high volume of liquid containing NPs compared to the other tested qualities. Thus, the probability that a large number of particles will be adsorbed at the CO_2-water interface is high. This means the gas to liquid ratio (GLR) is an important parameter on emulsion strength. **Figures 26** and **27** show the viscosity values at different qualities and at two shear rates: 1365, and 1820 s^{-1}, respectively.

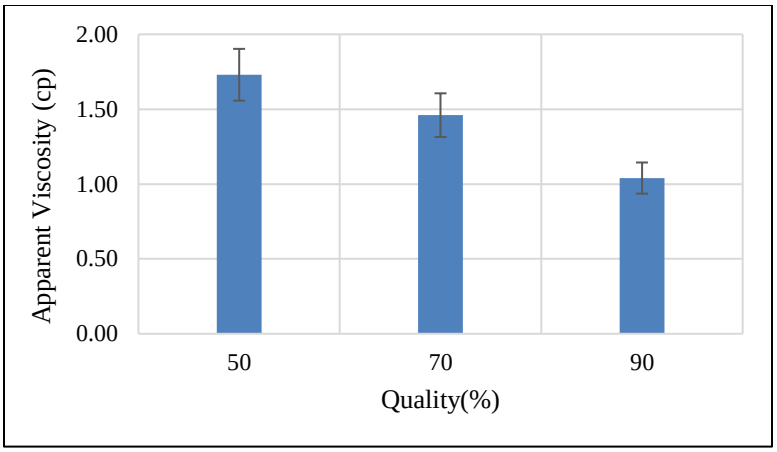

Figure 26: Effect of quality on viscosity measurement at 1365 s^{-1}

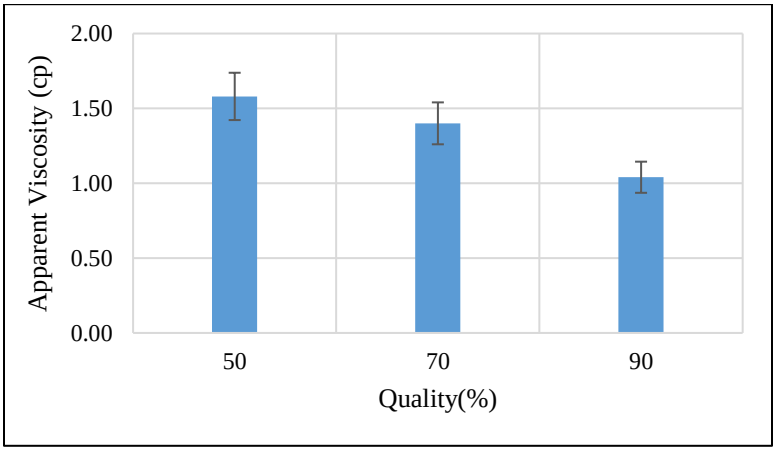

Figure 27: Effect of quality on viscosity measurement at 1820 s^{-1}

4.1.1.3.2 Effect of Salinity

The effect of salinity on the ability of silica modified with DMS to stabilize CO_2-brine emulsion at reservoir conditions was assessed. This study was done at 10,000, 30,000, and 80,000 ppm NaCl, corresponding to 1, 3, and 8 wt%, respectively. Also, 10,000 ppm of NaCl and 5,000 ppm of $CaCl_2$ were used to assess the effect of divalent ions on emulsion strength. The results showed that salinity has no significant effect on emulsion strength. Almost the same viscosity values were reported for the cases where only NaCl was used. To ensure

consistency, the effect of salinity (**figures 28** and **29**) was determined at two shear rates: 1365, and 1820 s^{-1}.

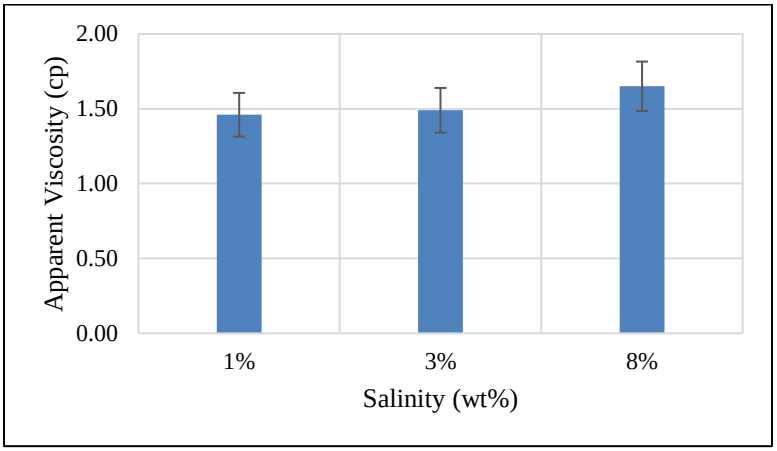

Figure 28: Effect of salinity on viscosity measurement at 1365 s^{-1}

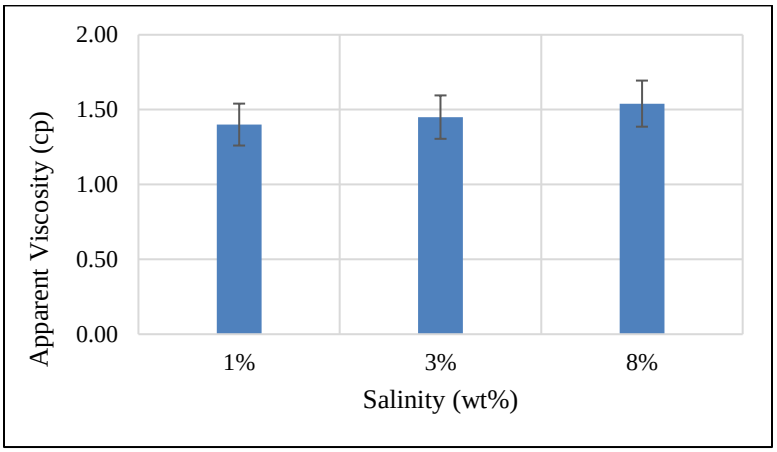

Figure 29: Effect of salinity on viscosity measurement at 1820 s^{-1}

Three qualities: 50, 70 and 90%, and three shear rates: 910, 1365 and 1820 s^{-1}, were used to evaluate the effect of the addition of $CaCl_2$ and NaCl on emulsion viscosity. The addition of $CaCl_2$ had different effects on the emulsion strength and this was found to be related

to the quality of the injected fluids. At 50 and 70% qualities, the addition of $CaCl_2$ produced emulsions with lower viscosity than those without $CaCl_2$ (**figures 30** and **31**). This behavior was most obvious at 910 s^{-1} shear rate. At 90% quality, however, the addition of $CaCl_2$ produced emulsions with a bit higher viscosity than those with only NaCl (**figure 32**). However, the changes were not significant.

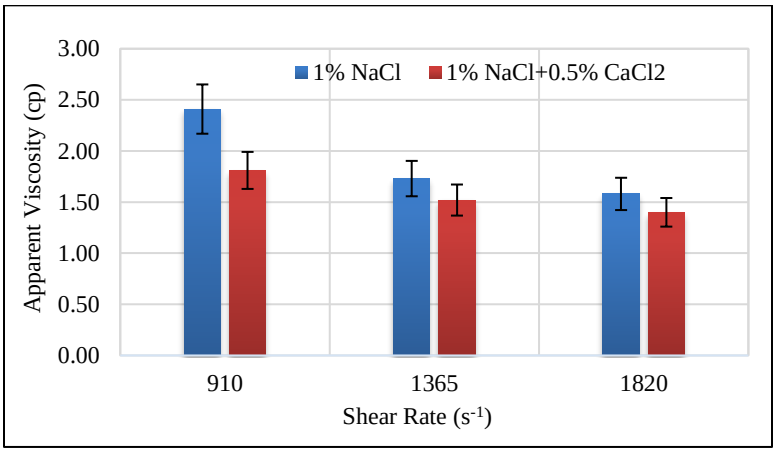

Figure 30: Effect of adding $CaCl_2$ on viscosity measurement at 50% quality

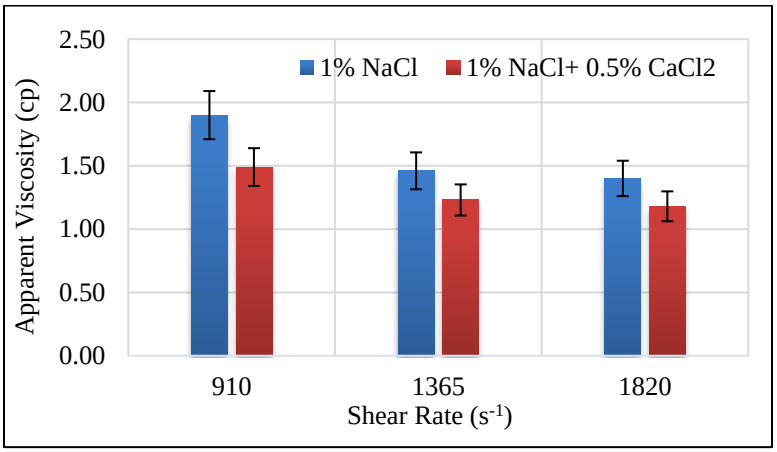

Figure 31: Effect of adding $CaCl_2$ on viscosity measurement at 70% quality

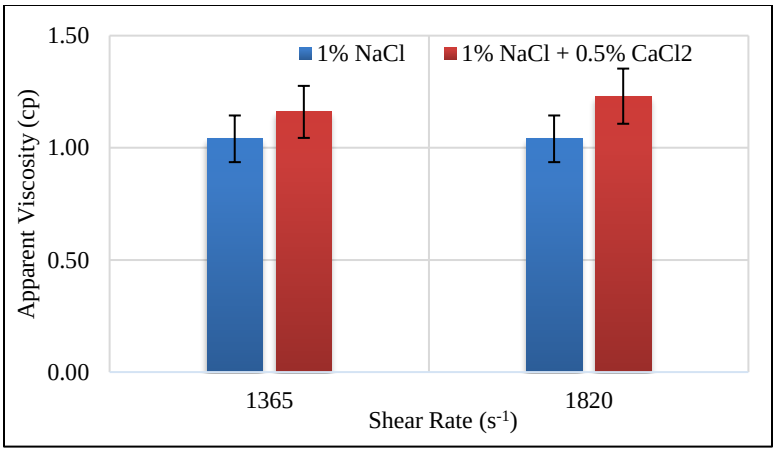

Figure 32: Effect of adding $CaCl_2$ on viscosity measurement at 90% quality

4.1.1.3.3 Effect of Shear Rate

The role of shear rate on emulsion stability and strength was examined by measuring the viscosity in porous media (glass beads 1) and the capillary tube. Six shear rates, at different salinities and qualities, were tested. In glass beads at 655 s^{-1} shear rate, no emulsion was generated at any conditions that have been tested. At higher shear rates, 980 and 1310 s^{-1}, emulsions were generated and this was confirmed using the visual cell and the calculated viscosity values. The pressure drop across the glass beads was recorded at three shear rates: 655, 980 and 1310 s^{-1} (**figure 33**). Under the same conditions, using the steady state pressure drop and Darcy equation (7), the measured viscosity of the three shear rates were found to be: 1, 1.30 and 1.1, respectively.

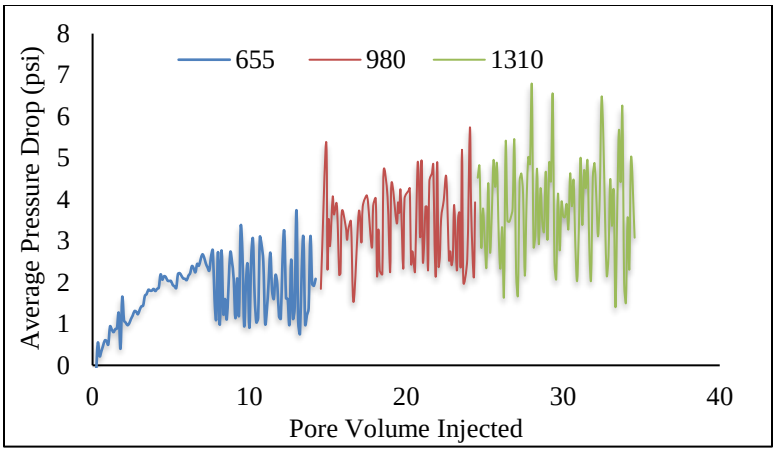

Figure 33: Pressure drop across the glass beads 1 at different shear rates

Further measurements were conducted using capillary tubes. Three shear rates, 910, 1365 and 1820 s^{-1}, were examined. As the shear rate increases, the emulsion viscosity decreases. This behavior was most obvious for the change from 910 to 1365 s^{-1} shear rates. The change from 1365 to 1820 s^{-1} shear rates showed no significant impact on emulsion viscosity. To confirm these results, these experiments were repeated using different conditions. **Figure 34** shows the viscosity measurements at 3wt% salinity and 70% quality while **figure 35** presents the viscosity values at 8 wt% salinity and 70% quality.

In general, emulsions are classified as non-Newtonian fluids whose viscosity is shear rate dependent. Based on the shear rates, emulsions can have a shear thickening or a shear thinning behavior. The results of the emulsions reported here exhibit shear thinning since their viscosity values decrease as shear rates increase.

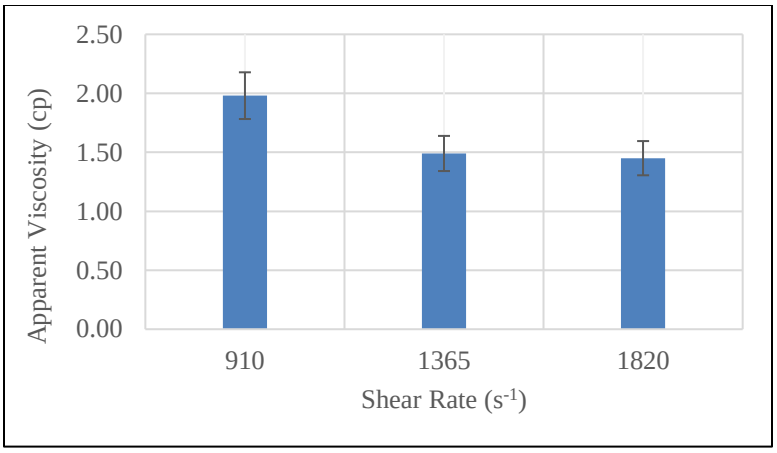

Figure 34: Effect of shear rates on viscosity at 3wt% salinity and 70% quality

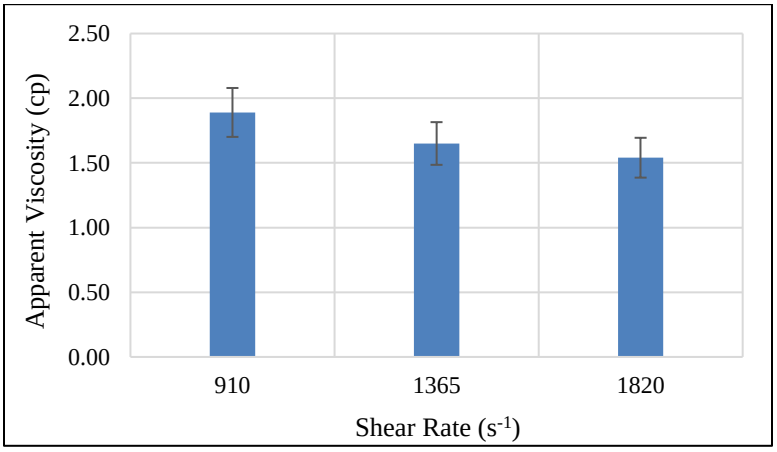

Figure 35: Effect of shear rates on viscosity at 8 wt% salinity and 70% quality

4.1.1.3.4 Effect of NP Size

To examine the effect of NP's size, two sizes were selected. H15 and H30 particles were used to conduct the comparison. The results showed that the change of NPs size has no significant effect on emulsion viscosity. Repeatability of the test was conducted at different shear rates and quality and no significant changes were observed. As shown in **figure 36**, there might be small changes, specifically at 910 and 1365 s^{-1} shear rates and 50% quality, but generally there is no obvious trend apparent from these data. Similarly, **figure 37** shows the

viscosity values for the two sizes at different shear rates and 70% quality. Again, no clear trend is apparent.

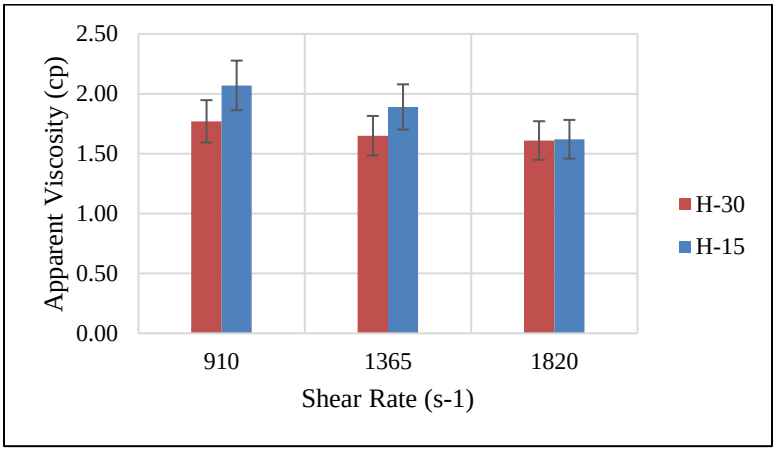

Figure 36: Effect of NPs size on viscosity values at 50% quality

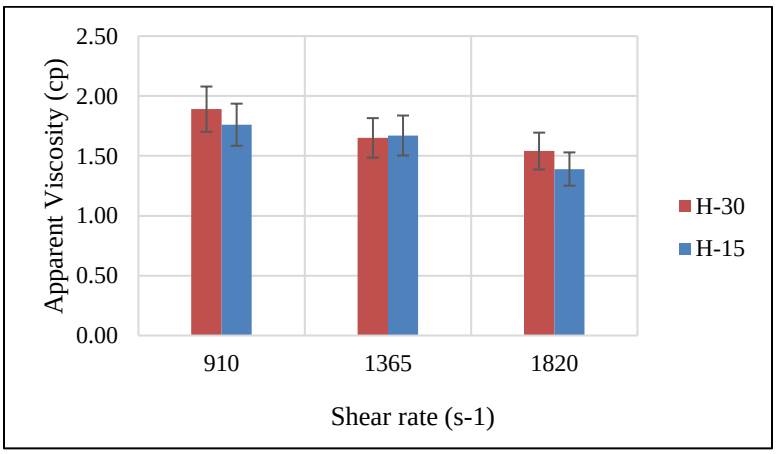

Figure 37: Effect of NPs size on viscosity values at 70% quality

4.1.1.4 Mechanism of Emulsion Stabilization

The main mechanism to explain the CO_2-brine emulsion stabilization here is the energy of attachment. The energy required to remove a particle from the interface (E) is correlated with the contact angle that solid particle forms with the interface. The resulting energy of attachment can be estimated using equation (1). Changing the contact angle can strongly affect the HCB. As discussed previously, the HCB of solid particles was found to have a significant effect on the emulsion stability and type. Based on the degree of hydrophobicity, either CO_2 in water emulsion or water in CO_2 emulsion will be formed. The equivalent HCB (Worthen, Bagaria, et al. 2013) for NPs with uniform surface (P) is defined as:

$$\frac{1}{HCB} = \frac{A_{PG} - A_{PP} - A_{GG}}{A_{PW} - A_{PP} - A_{WW}} \quad (13)$$

Where, A is the interaction potential between two phases, G (gas) and W (water). The partially modified silica with DCDMS makes particles less hydrophilic, so A_{PP} and A_{PW} decrease. Additionally, the methylsilyl ligands attached to the silica particle have low cohesive energy and, therefore, are easily solvated by CO_2, thus increasing A_{PG}. As a result, the presence of silica partially modified with DCDMS at the CO_2-water interface can affect the contact angle the particle makes with the water phase and, therefore, control the HCB. This can be done if there is sufficient energy to enable the particle to be adsorbed at the interface. Because these particles require high energy (high shear rate) to be adsorbed at the interface, sufficient energy is required to remove these particles from the interface. As a result, the generated emulsion becomes very strong and stable (Binks and Lumsdon 2000, Worthen, Bagaria, et al. 2013).

4.1.1.5 Summary

The results of all experiments conducted in this section are summarized in **table 15**. Based on these results, the presence of NPs stabilized the CO_2–brine emulsion and produced emulsions with higher viscosities than CO_2 alone. The strength and viscosity of the emulsions depends strongly on the experimental conditions including the quality, the shear rate, and, to some extent, the salinity. Quality had an inverse relationship with emulsion viscosity. Furthermore, as the shear rate increased, the emulsion viscosity decreased. This behavior was most obvious for the change from 910 to 1365 s^{-1} shear rate. The change from 1365 to 1820 s^{-1} shear rate showed almost no changes in emulsion viscosity. The salinity in some cases was found to be shear rate and fluid quality dependent. NP's size, generally speaking, had no influence on emulsion viscosity. Based on viscosity measurements, silica modified with DCDMS was able to increase the CO_2 viscosity 26-60 fold.

Table 15: Summary of silica modified with DCDMS results

Test #	Material	NP Concentration	Salinity	Quality	Shear rate	ρ(emulsion)	Re	μ(emulsion)	RF
		wt%	wt%	%	s^{-1}	kg/m^3		cp	
1	H-30	1	1% NaCl	50	910	762	12	2.41	60
2	H-30	1	1% NaCl	50	1365	762	25	1.73	43
3	H-30	1	1% NaCl	50	1820	762	36	1.58	40
4	H-30	1	1% NaCl	70	910	672	13	1.90	48
5	H-30	1	1% NaCl	70	1365	672	26	1.46	37
6	H-30	1	1% NaCl	70	1820	672	36	1.40	35
7	H-30	1	1% NaCl	90	1365	582	31	1.04	26
8	H-30	1	1% NaCl	90	1820	582	42	1.04	26
9	H-30	1	3% NaCl	50	910	762	14	2.09	52
10	H-30	1	3% NaCl	50	1365	762	35	1.22	31
11	H-30	1	3% NaCl	50	1820	762	39	1.45	36
12	H-30	1	3% NaCl	70	910	672	13	1.98	50
13	H-30	1	3% NaCl	70	1365	672	25	1.49	37
14	H-30	1	3% NaCl	70	1820	672	34	1.45	36
15	H-30	1	3% NaCl	90	1365	582	33	0.99	25
16	H-30	1	3% NaCl	90	1820	582	41	1.05	26
17	H-30	1	8% NaCl	50	910	762	16	1.77	44
18	H-30	1	8% NaCl	50	1365	762	26	1.65	41
19	H-30	1	8% NaCl	50	1820	762	35	1.61	40
20	H-30	1	8% NaCl	70	910	672	13	1.89	47
21	H-30	1	8% NaCl	70	1365	672	23	1.65	41
22	H-30	1	8% NaCl	70	1820	672	32	1.54	39
23	H-30	1	8% NaCl	90	1365	582	27	1.20	30
24	H-30	1	8% NaCl	90	1820	582	31	1.41	35
25	H-30	1	1% Nacl + 0.5% $CaCl_2$	50	1365	762	28	1.52	38
26	H-30	1	1% Nacl + 0.5% $CaCl_2$	50	1820	762	40	1.40	35
27	H-30	1	1% Nacl + 0.5% $CaCl_2$	70	910	672	17	1.49	37
28	H-30	1	1% Nacl + 0.5% $CaCl_2$	70	1365	672	30	1.23	31
29	H-30	1	1% Nacl + 0.5% $CaCl_2$	70	1820	672	42	1.18	30
30	H-30	1	1% Nacl + 0.5% $CaCl_2$	90	1365	582	28	1.16	29
31	H-30	1	1% Nacl + 0.5% $CaCl_2$	90	1820	582	35	1.23	31
32	H-15	1	8% NaCl	50	910	762	14	2.07	52
33	H-15	1	8% NaCl	50	1365	762	22	1.89	47
34	H-15	1	8% NaCl	50	1820	762	35	1.62	41
35	H-15	1	8% NaCl	70	910	672	14	1.76	44
36	H-15	1	8% NaCl	70	1365	672	22	1.67	42
37	H-15	1	8% NaCl	70	1820	672	36	1.39	35
38	H-15	1	8% NaCl	90	1365	582	30	1.08	27
39	H-15	1	8% NaCl	90	1820	582	41	1.06	27

4.1.2 Silica Modified with Hidden Chemical

This section discusses the results of silica modified with hidden chemical. This study covered the impact of several parameters on emulsion viscosity in order to compare the results of this material with the other materials discussed in this report. These parameters include quality, salinity, shear rates, NP's concentration, pressure, and type of gas used. These parameters were evaluated based on viscosity measurements conducted using capillary tubes and calculated from the Hagen–Poiseuille equation.

4.1.2.1 Materials

The surface modified silica NPs used in this section was prepared at two different concentrations, 1 and 2 wt%. Most of the experiments were conducted using 1 wt% NPs. However, 2 wt% was used to evaluate the effect of NP's concentration on emulsion viscosity. DLS was used to measure the size of particles which was found to be 30 ±1 nm. Two gases were used, CO_2 and N_2.

4.1.2.2 Experimental Procedure and Conditions

The porous media used for this study consisted of glass beads 2. The viscosity measurements setup, in figure 11, was used to conduct the tests. The experimental parameters and conditions used to conduct this study are shown in **table 16**. The salt used was NaCl. The shear rates were different for the porous media (glass beads 2) and the capillary tube. At the same flow rate, the shear rate in capillary tube is higher than that at the glass beads 2. The objectives of this design were to test the effect of different shear rates in porous media separately and, at the same time, to evaluate the emulsion strength in capillary tubes at much

higher shear rates. This means that emulsion generated at the glass beads 2 is not related to that at the capillary tube. The tests were conducted using CO_2 and N_2 and at different pressures. The two tested pressures for CO_2 were 800 and 1800 psi. This enabled testing emulsion stability at gaseous and supercritical phases, respectively.

Table 16: Experimental conditions for silica modified with hidden chemical

Parameter	Range	Unit
Pressure	800-1800	Psi
Temperature	50	^oC
Gas	$CO_2 – N_2$	-
NP concentration	1-2	wt%
Quality	50-70-90	%
Salinity	1-3-8 % NaCl	wt%
Shear rates (Capillary tube)	1365- 2090- 2730	s^{-1}

4.1.2.3 Results and Discussion

4.1.2.3.1 Effect of Quality

The effect of quality on emulsion strength was studied at three qualities: 50, 70, and 90%. Quality was found to be a crucial parameter for emulsion strength. The results showed that emulsion viscosity increases as quality decreases, which indicates that the strongest emulsion is produced at 50% quality. The viscosity measurements at different qualities were also taken at different salinities and the conclusion was the same. In general, the 70% and 90% qualities showed similar results in all tested cases. **Figure 38** shows the viscosity values at different qualities and at 3 and 8 wt% salinity. As mentioned above when discussing the effect of quality on emulsion strength, the lower quality, 50%, had the highest volume of liquid containing NPs in the three tested qualities. Thus, the probability that a large number of particles will be adsorbed at the CO_2-brine interface is high. This leads to the production of emulsions with high viscosity as the liquid fraction in the total injection fluid increases. This means as stated previously, the GLR is an important parameter on emulsion viscosity.

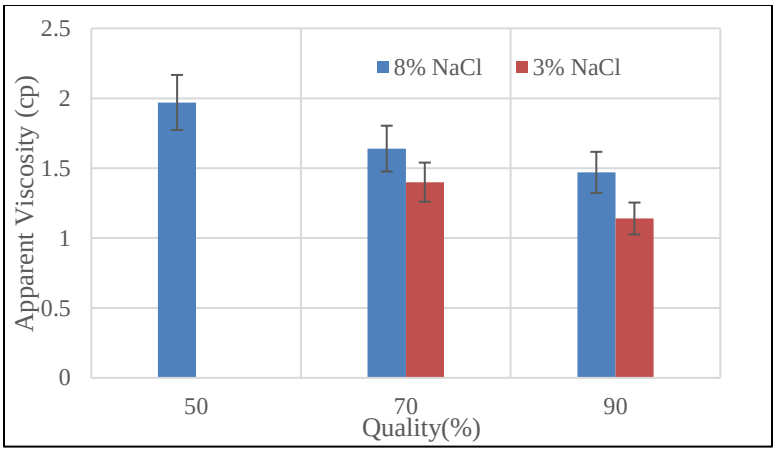

Figure 38: Effect of quality on viscosity measurement at 3 and 8wt% NaCl

4.1.2.3.2 Effect of Salinity

The effect of salinity was studied to assess the ability of surface modified silica NPs to stabilize CO_2-brine emulsions at reservoir conditions. Solutions at 1, 3 and 8 wt% salinity were used to examine the effect of salinity on emulsion behavior. The results showed that salinity has a significant impact on emulsion strength and viscosity. As the salinity increases, the emulsion becomes more viscous. This means that solutions with 8 wt% salinity resulted in the highest viscosity values and the ones with 1 wt% produced the lowest viscosity. An increase in salinity makes the particles less hydrophilic, thus, increasing the affinity of the particles to be adsorbed by CO_2 at the interface and, hence, enhancing CO_2-brine emulsion stability. To test the consistency of these results, the effect of salinity (**figure 39**) was conducted at two different qualities, 70 and 90%.

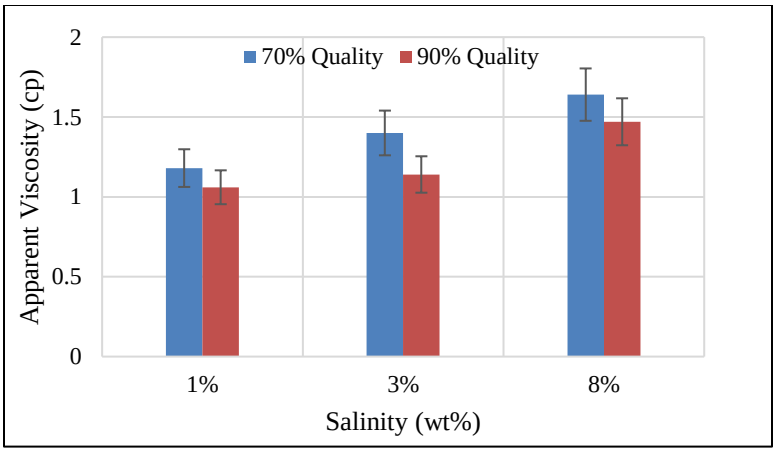

Figure 39: Effect of salinity on viscosity measurements at 70 and 90% quality

4.1.2.3.3 Effect of Shear Rate

The role of shear rate in emulsion stability and strength was examined by measuring viscosity using the capillary tubes. Three shear rates, 1365, 2090 and 2730 s^{-1}, at different salinities and qualities were tested. For this range of shear rates, the results showed no significant effect of shear rates on emulsion viscosity. However, at lower shear rates the NPs were not able to stabilize the emulsion. This means that the shear rate needs to exceed a threshold to stabilize the emulsion. Repeating these tests at different salinities and qualities produced no significant changes. **Figures 40**, **41**, and **42** report the viscosity values at different shear rates and at: 50% quality and 8% salinity; 70% quality and 1% salinity; and 90% quality and 3% salinity, respectively.

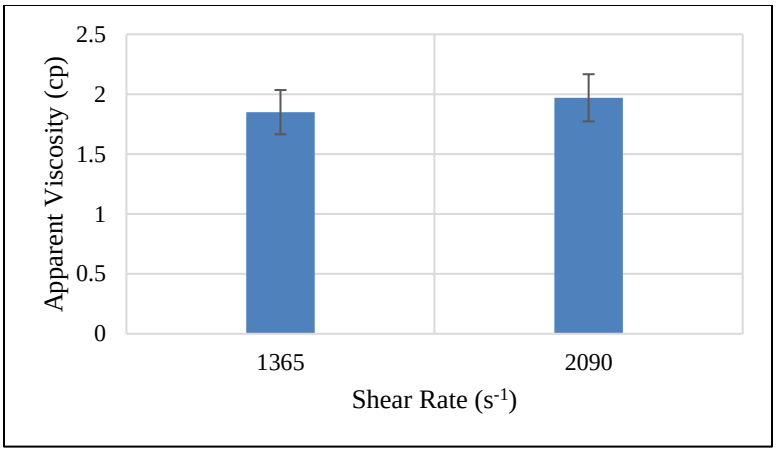

Figure 40: Effect of shear rates on viscosity at 8 wt% salinity and 50% quality

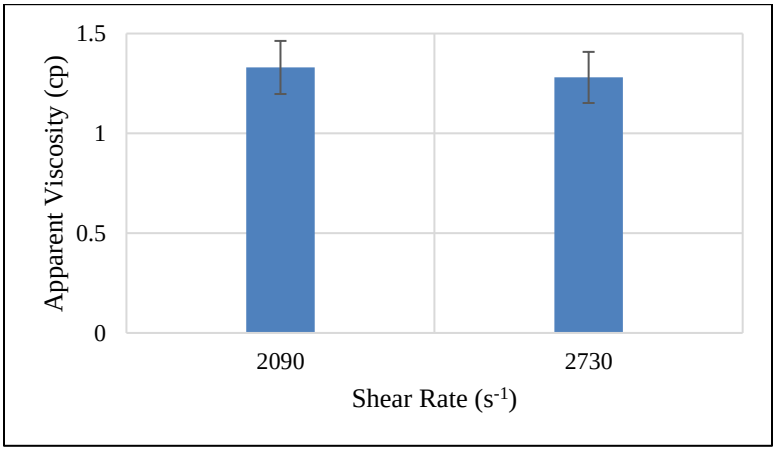

Figure 41: Effect of shear rates on viscosity at 1 wt% salinity and 70% quality

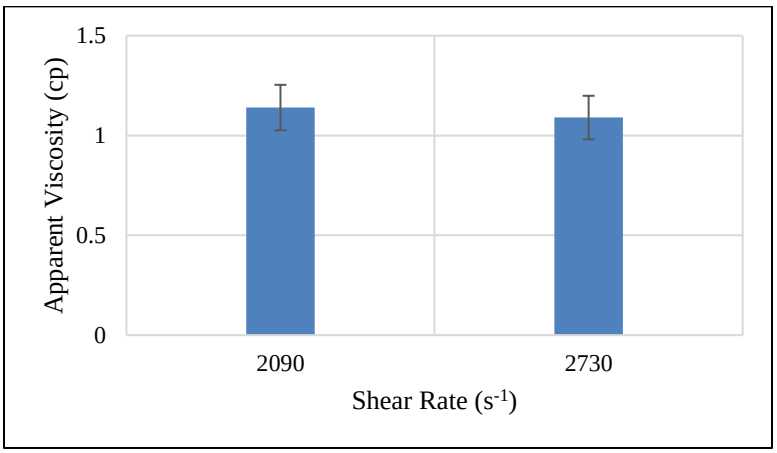

Figure 42: Effect of shear rates on viscosity at 3 wt% salinity and 90% quality

4.1.2.3.4 Effect of NP Concentration

The effect of NP concentration on emulsion strength was conducted at 1 and 2% NPs. The NP concentration was found to have a proportional relationship with emulsion viscosity. **Figure 43** shows the viscosity measured at 1 and 2 wt% NPs. This finding was expected since the presence of more particles at the interface can increase the chances that these particles will be adsorbed by the CO_2 and brine and, hence, improve the stability of generated emulsion. Even though the changes here are not significant, higher concentration of NPs might produce stronger emulsions.

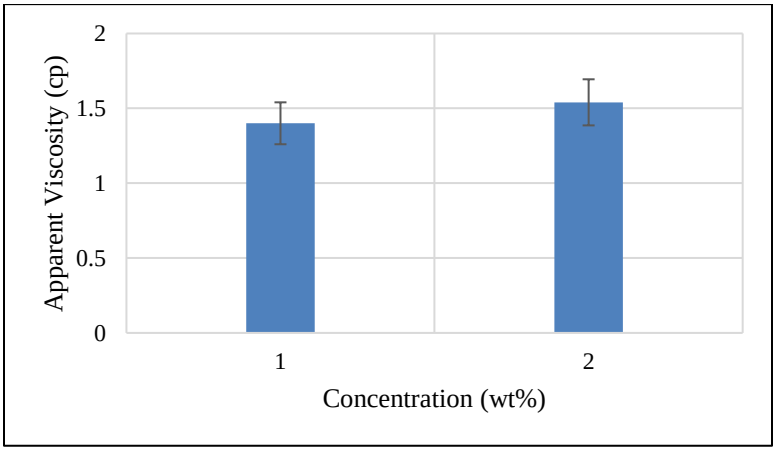

Figure 43: Effect of NP concentration on viscosity measurement

4.1.2.3.5 Effect of Pressure

Two pressures, 800 and 1800 psi, were selected to study the effect of pressure on emulsion stability and strength. At 800 psi, CO_2 is at gaseous phase, whereas at 1800 psi it is at supercritical phase. To ensure the consistency of the results, the effect of pressure was conducted at two different qualities, 70 and 90% (**figures 44** and **45**). As pressure increased from 800 to 1800 psi, emulsion viscosity increased. This is attributed to the greater density of

CO_2 at 1800 psi. The difference in density between two species reduces IFT. Thus, higher densities (smaller difference in density) should facilitate the emulsion generation process, creating emulsions with higher viscosity. **Figure 46** shows the density of CO_2 at different pressures. Note that this is consistent with the results reported in **figure 38** supporting the earlier finding related to the effect of quality on emulsion viscosity. The emulsion viscosities at 70% quality are higher than those reported at 90% quality.

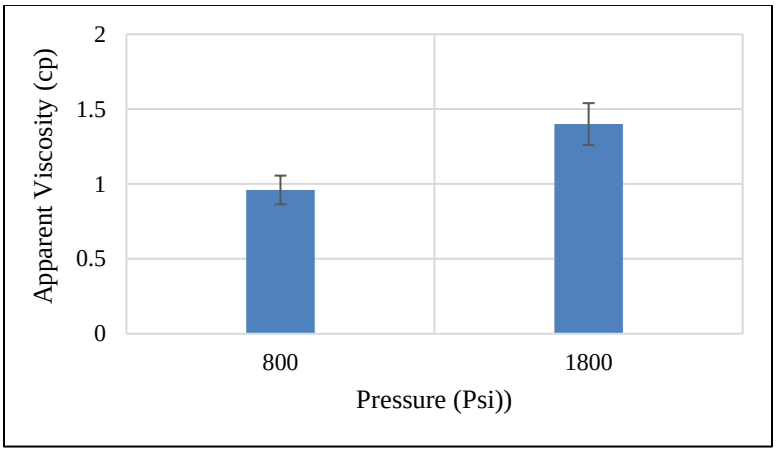

Figure 44: Effect of CO_2 pressure on viscosity measurements at 70% quality

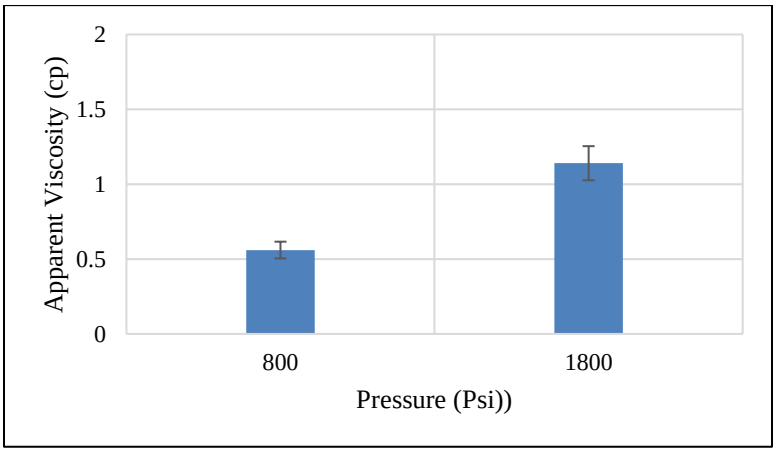

Figure 45: Effect of CO_2 pressure on viscosity measurements at 90% quality

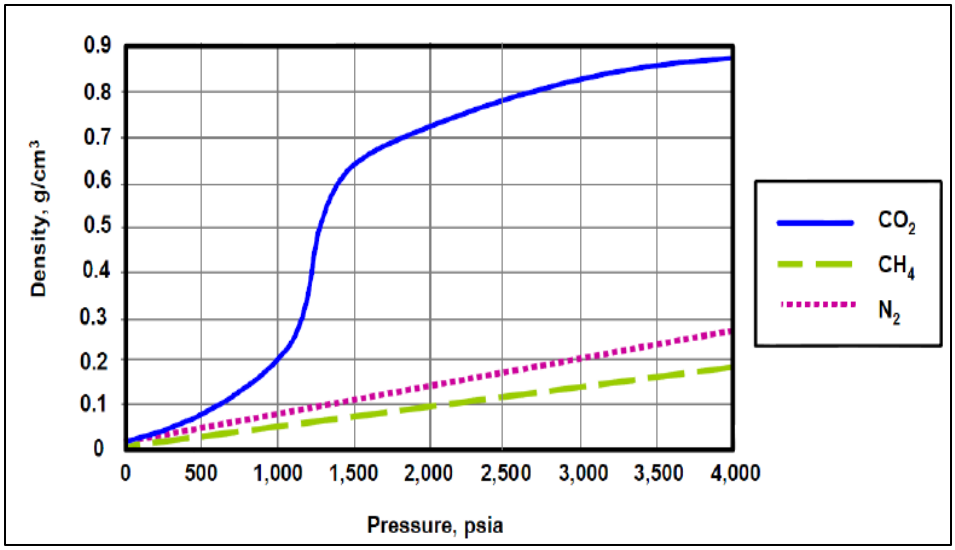

Figure 46: Density of CO_2, N_2, and CH_4 at 105°F. (Reprinted from (Bank, Riestenberg, and Koperna 2007))

4.1.2.3.6 Effect of Gas Type

One of the major reasons to use NPs as a foam/emulsion stabilizing agent is because of the drawbacks of CO_2 that make it difficult to generate a stable emulsion with water when surfactant is used as the emulsifying agent. As mentioned previously, CO_2 has low polarizability. This is attributed to the fact that CO_2 has a zero permanent dipole moment and weak van der Waals forces. As a result, a CO_2-philic tail is a poor solvent for both polar and high molecular weight solutes. For these reasons, it is important to report the potential of the proposed material to stabilize CO_2-brine emulsion and to compare it to that of N_2. The tests were conducted at 800 psi and 50°C, and at two different qualities, 70 and 90%. Both gases produced almost the same emulsion, although the viscosity was about 10% higher when CO_2 was used. This small difference in emulsion viscosity can be explained by the ability of CO_2 to reduce the IFT relative to N_2 under the same conditions. Because CO_2 at the experimental pressure and temperature has a higher density than N_2, its effect on IFT reduction is more pronounced. These results support the finding that using surface modified silica NPs has the

potential to stabilize gas-liquid emulsions at harsh reservoir conditions, even when CO_2 is used. **Figure 47** shows the results of the viscosity measurements for CO_2 and N_2 at 70 and 90% quality. As mentioned above, the lower quality resulted in higher viscosity. The effect of gas type at different qualities showed the same trend.

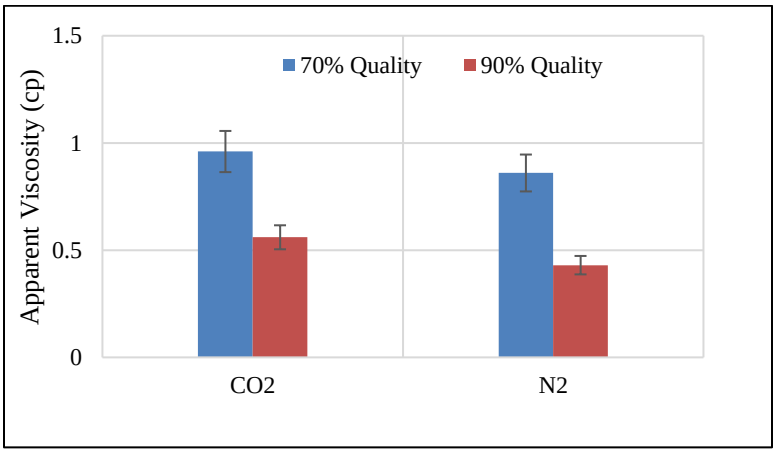

Figure 47: Effect of type of gas on emulsion viscosity at 70 and 90% quality

4.1.2.4 Mechanism of Emulsion Stabilization

The main mechanism to explain the CO_2- water and N_2-water emulsions stabilization here is the energy of attachment. The resulting energy of attachment can be estimated using equation (1). Changing the contact angle can strongly affect the HCB. Also, the surface modified silica NP cannot reduce the gas-liquid IFT (very close to air-water IFT~73.33 mN/m), so the resultant energy of attachment is the only mechanism can be used here to explain the emulsion stability. However, it is mandatory to apply sufficient energy (high shear rate) to enable the particle to be adsorbed at the interface. The emulsion/foam generated using this modified silica NPs was weaker than that produced with DCDMS. The foam had coarse bubbles and the half-life was only few minutes.

4.1.2.5 Summary

The results of all tests conducted for this material are summarized in **table 17**. Based on these results, the presence of NPs in solution stabilized the CO_2–brine and N_2-brine emulsions and produced emulsions with higher viscosities than CO_2 or N_2 alone. The strength and viscosity of the emulsions depend strongly on the experimental conditions: quality, salinity, NP concentration, pressure, and type of gas used to conduct the experiments. The quality had an inverse relationship with emulsion viscosity. Furthermore, the results showed that, as the solution salinity and NP concentration increased, the emulsion viscosity increased, too. Similarly, higher pressure produced more viscous emulsions. The results also showed that both gases, CO_2 and N_2, produced nearly the same viscosity, although CO_2 created emulsions with slightly higher viscosity. Based on viscosity measurements, modified silica was able to increase the CO_2 viscosity 25-53 fold and N_2 viscosity 22-54 fold.

Table 17: Summary of surface modified silica results

Test #	Gas	Pressure	Concentration	Salinity	Quality	Shear rate	μ(emulsion)	Re	RF
		psi	wt%	wt%	%	s^{-1}	cp		
1	CO_2	1800	1	8	50	1365	1.85	23	44
2	CO_2	1800	1	8	50	2090	1.97	33	47
3	CO_2	1800	1	1	70	2090	1.18	49	28
4	CO_2	1800	1	3	70	2090	1.4	41	33
5	CO_2	1800	1	8	70	2090	1.64	35	39
6	CO_2	1800	1	1	70	2730	1.28	58	30
7	CO_2	1800	1	1	90	2090	1.06	47	25
8	CO_2	1800	1	3	90	2090	1.14	44	27
9	CO_2	1800	1	8	90	2090	1.47	34	35
10	CO_2	1800	1	1	90	1365	1.24	26	30
11	CO_2	1800	1	3	90	2730	1.09	59	26
12	CO_2	1800	2	3	50	2090	1.77	37	42
13	CO_2	1800	2	3	70	2090	1.54	37	37
14	CO_2	800	1	3	70	2090	0.96	34	53
15	CO_2	800	1	3	90	2090	0.56	32	31
16	N_2	800	1	3	50	2090	1.07	42	54
17	N_2	800	1	3	70	2090	0.86	33	43
18	N_2	800	1	3	90	2090	0.43	30	22

4.1.3 Silica Modified with PEG

This section will discuss the results of silica modified with PEG. This study examines the role of several parameters on emulsion viscosity and compares the results of this material to materials discussed previously. These parameters include salinity, shear rates, NP concentration, and pressure. These parameters were evaluated based on viscosity measured using capillary tubes and calculated using the Hagen–Poiseuille equation.

4.1.3.1 Materials

The modified silica with PEG, 10 nm, was prepared at 1 and 1.5 wt%. Most of the studies were conducted using 1 wt% NPs. However, 1.5 wt% was prepared to evaluate the effect of NP concentration on emulsion viscosity.

4.1.3.2 Experimental Procedure and Conditions

The porous media used for this study consisted of glass beads 1. The viscosity measurement setup, in figure 11, was used to conduct the tests. The experimental parameters and conditions used to conduct this study are shown in **table 18**. The salt used was NaCl. These tests were conducted using sc-CO_2 and at different pressures. The two selected pressures for CO_2 were 1800 psi and 2500 psi. This enabled testing emulsion stability at CO_2 supercritical phase.

Table 18: Experimental parameters and conditions for silica modified with PEG

Parameter	Range	Unit
Pressure	1800-2500	Psi
Temperature	50	^{o}C
Gas	CO_2	-
NP concentration	1-1.5	wt%
Quality	90	%
Salinity	1-3 % NaCl	wt%
Shear rates (Capillary tube)	1365- 1820	s^{-1}

4.1.3.3 Results and Discussion

4.1.3.3.1 Effect of Salinity

The effect of salinity was studied to assess the ability of silica modified with PEG to stabilize CO_2-brine emulsion at moderate salinities, 1 and 3 wt%. The results showed that salinity had a significant impact on emulsion strength and viscosity. As the salinity increased, the emulsion viscosity increased, too. The increase in salinity makes the particles less hydrophilic, thus, increasing the affinity of the particle to be adsorbed by CO_2 at the interface and, hence, enhancing CO_2-water emulsion stability. To ensure consistency, the effect of salinity (**figures 48**and **49**) was studied at two different shear rates, 1365, and 1820 s^{-1}. All tested conditions showed the same behavior; an increase in salinity produced more viscous emulsions.

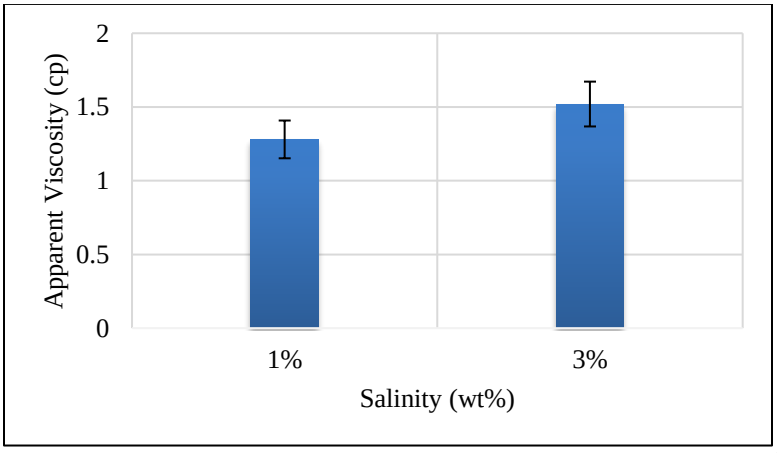

Figure 48: Effect of salinity on emulsion viscosity at 1365 s^{-1}

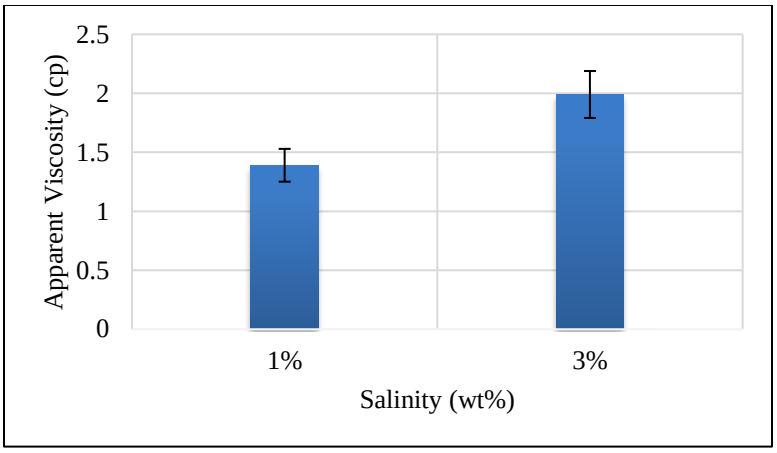

Figure 49: Effect of salinity on emulsion viscosity at 1820 s^{-1}

4.1.3.3.2 Effect of Shear Rate

The impact of shear rate on emulsion stability and viscosity was examined by measuring the viscosity through a capillary tube using the Hagen–Poiseuille equation. Two shear rates, 1365 and 1820 s^{-1}, at different salinities and pressure, were tested to study the effect of shear rate on emulsion stability. The highest viscosity was reported at 1820 s^{-1} shear rate. Under the same conditions, the lowest viscosity values were reported at 1365 s^{-1} shear rate. **Figure 50** shows the viscosity measurements at 1 and 3 wt% salinity and 90% quality. The results at 2500 psi (**figure 51)** showed the same behavior. This means the high energy (high shear rate) required to bring the particles at the interface will help generate stronger emulsions.

As mentioned, emulsions are classified as non-Newtonian fluids whose viscosity is shear rate dependent. Based on the shear rates, emulsions can have a shear thickening or a shear thinning behavior. The results of the emulsions reported here exhibit shear thickening since their viscosity values increase as shear rates increase.

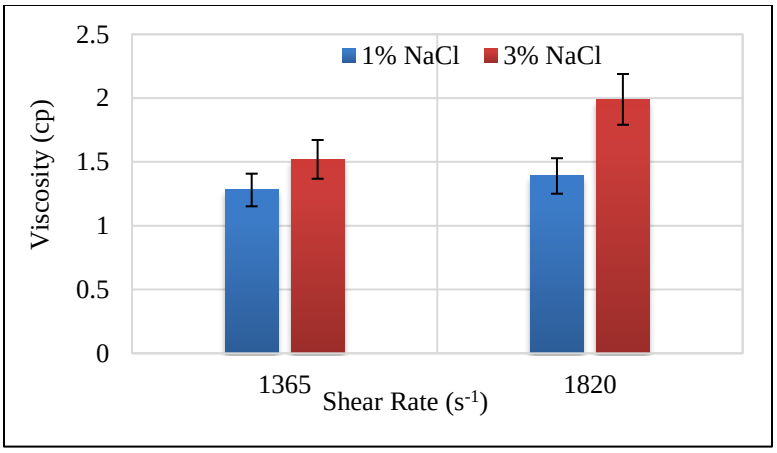

Figure 50: Effect of shear rates on viscosity measurements at 1 and 3 wt% salinity

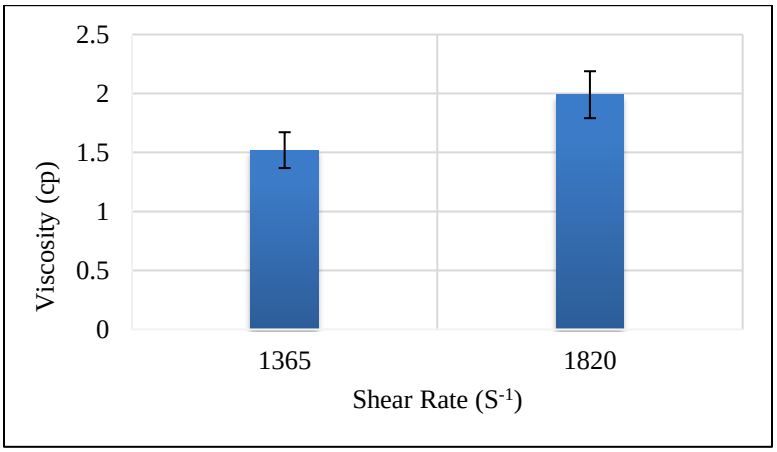

Figure 51: Effect of shear rates on viscosity measurements at 2500 psi

4.1.3.3.3 Effect of NP Concentration

The effect of NP concentration on emulsion viscosity was conducted at 1 and 1.5 wt%. The results showed a proportional relationship between NP concentration and emulsion viscosity. **Figure 52** presents the viscosity measured at 1 and 1.5 wt% NPs. This finding was expected since the presence of more particles in solutions increases the chances of those particles being adsorbed by the CO_2 and brine, thus improving the stability of the generated emulsion. This behavior was also reported for previous materials with noticeable results here.

The change of NP concentration from 1 to 1.5 wt% resulted in about 0.7 cp increase in emulsion viscosity.

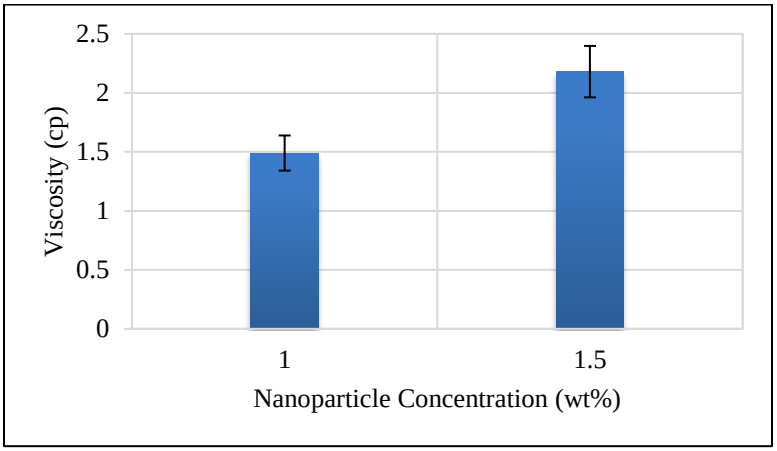

Figure 52: Effect of NP concentration on viscosity measurement for silica with PEG

4.1.3.3.4 Effect of Pressure

The role of pressure on emulsion viscosity and stability was conducted at 1800 and 2500 psi. As mentioned earlier, these two pressures are at the supercritical phase of CO_2. The effect of pressure (**figure 53**) was evaluated at two different shear rates, 1365 and 1820 s^{-1}, to ensure the results reported are consistent. As the pressure increased, the emulsion viscosity increased, too. This is attributed to the ability of denser CO_2, at 2500 psi, to further reduces the IFT compared with that at 1800 psi. This facilitates and enhances the emulsion generation process and, thus, produces more viscous emulsion. The change of CO_2 density with pressure was already reported in figure 48.

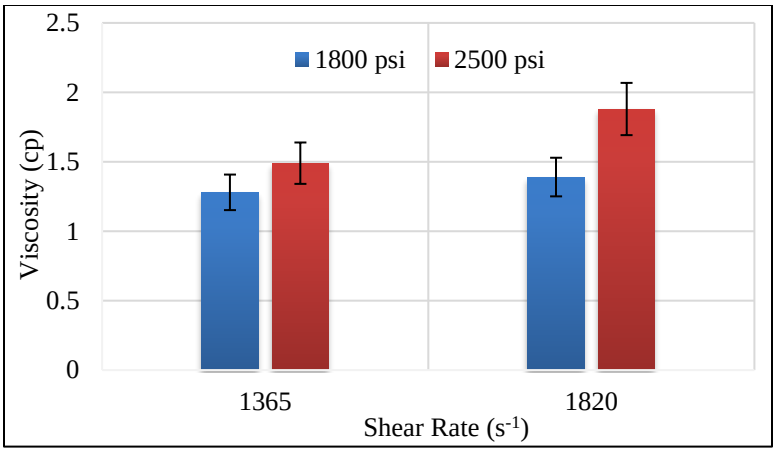

Figure 53: Effect of CO_2 pressure on viscosity measurement

4.1.3.4 Mechanism of Emulsion Stabilization

The same mechanism reported for the previous materials, silica modified with DCDMS and hidden chemical, is applied here. The energy required to remove a particle from the interface (E) is correlated with the contact angle that solid particle forms with the interface. The resulting energy of attachment can be estimated using equation (1). Changing the contact angle can strongly affect the HCB. Also, the surface modified silica cannot reduce the gas-liquid IFT, thus, the resultant energy of attachment will be relatively high. However, it requires applying sufficient energy to enable the particle to be adsorbed at the interface. Because these particles require high energy (high shear rate) to be adsorbed at the interface, sufficient energy is required to remove these particles from the interface. As a result, the generated emulsion becomes very strong and stable.

4.1.3.5 Summary

The results of all tests conducted for this material are summarized in **table 19**. Based on these results, the presence of NPs in solution stabilized the CO_2–brine emulsion and produced emulsions with higher viscosities than CO_2 alone. The stability and viscosity of the emulsions depends strongly on the experimental conditions, salinity, shear rate, NP concentration, and pressure. The results showed that as the solution salinity and NP concentration increased, the emulsion viscosity increased, too. The results of the emulsions reported here exhibit shear thickening behavior since their viscosity values increase as shear rates increase. Finally, more viscous emulsions were reported at 2500 psi than at 1800 psi. Based on viscosity measurements, modified silica with PEG was able to increase the CO_2 viscosity 24-49 fold.

Table 19: Summary of silica modified with PEG results

Test #	Gas	Pressure	Concentration	Salinity	Quality	Shear rate	μ(emulsion)	ρemulsion	Re	RF
		psi	wt%	wt%	%	s^{-1}	cp	kg/m^3		
1	CO_2	1800	1	1	90.00	1365	1.28	582	25	31
2	CO_2	1800	1	1	90.00	1820	1.39	582	31	34
3	CO_2	1800	1	3	90.00	1365	1.52	582	21	37
4	CO_2	1800	1	3	90.00	1820	1.99	582	22	49
5	CO_2	2500	1	1	90.00	1365	1.49	763	29	24
6	CO_2	2500	1	1	90.00	1820	1.88	763	30	30
7	CO_2	2500	1.5	1	90.00	1365	2.18	763	19	35

4.1.4 Summary of NP-Stabilized Gas-Liquid Foam/Emulsion Results

To facilitate comparisons, the results of the three materials tested in this part are summarized in **table 20**. The table reports whether a parameter tested was significant or does not have any influence on emulsion stability and viscosity. Also, the summary shows the magnitude of change each material achieved compared to the viscosity of CO_2 or N_2 at the same conditions.

Table 20: Summary of NP-stabilized gas-liquid emulsion results

Parameter	Silica modified with DCDMS	Silica modified with hidden chemical	Silica modified with PEG
Quality	Significant	Significant	-
Salinity	Not significant	Significant	Significant
Shear rate	Significant	Not significant	Significant
NP concentration	-	Significant	Significant
NP size	Not significant	-	-
Pressure	-	Significant	Significant
Type of gas	-	Significant	-
Viscosity magnitude rise	25-60	22-54	24-49

4.2 NP and Surfactant-Stabilized Gas-Liquid Foam

In this section, the results of five tested mixtures will be discussed. These mixtures consist of silica NPs and three nonionic surfactants, surface modified silica NPs and CNF surfactant (two cases, N_2 foam and CO_2 foam), and surface modified silica NPs and ENORDET A031.

4.2.1 Silica NPs and Nonionic Surfactants

This section will cover the results of the mixtures of silica NPs and three nonionic surfactants. The addition of NPs to surfactant has the potential to enhance the stability and strength of foam. The combination of NPs and surfactant may offer a novel technique for generating stronger foams for gas mobility control. This study evaluates the potential of silica NPs to enhance the foam stability of three nonionic surfactants.

4.2.1.1 Materials

This study used three nonionic surfactants: nonionic 1, nonionic 2, and nonionic 3. **Table 21** lists their properties. The silica NPs used were NexSilTM 20, received in aqueous form from Nyacol Chemicals. Using Dynamic Light Scattering (DLS), the size of the particles was found to be 22 ± 1 nm. Deionized water (DI) (ASTM Type II, Lab Chem) was used to prepare the solutions. Nitrogen gas (industrial grade) was used to conduct dynamic foam experiments. The cores used in this study were Boise sandstone from Kocurek Industries. **Table 22** summarizes the properties of these cores.

Table 21: Properties of surfactants

Surfactant Name	Commercial Name	Carbon Chain Length	pH	Water Solubility 100 g/l
Nonionic 1	NEODOL 91-8	9-11	6.80	Complete
Nonionic 2	NEODOL 25-7	12-15	6.80	Complete
Nonionic 3	NEODOL 25-9	12-15	6.80	Miscible

Table 22: Properties of Boise sandstone samples

Sample #	Length (inch)	Diameter (inch)	Porosity (%)	Pore Volume (ml)	Permeability (Darcy)
1	12	1	29.06	44.88	3.49
2	12	1	29.76	45.96	3.47
3	12	1	27.39	42.31	4.09
4	12	1	28.64	44.24	2.89

4.2.1.2 Experimental Procedure and Conditions

The effects of NPs concentration on surfactant foam stability enhancement were assessed using static and dynamic foam tests. Static foams for the three nonionic surfactants and for the mixtures of the same surfactants and silica NPs were generated in glass tubes. The two major outputs from these tests are foam half-lives and bubble size of the generated foam. Generated foam columns were captured and the foam half-lives were measured using Image-J software. Bubble sizes were captured using a Nikon Stereo Photomicroscope and Image-J software was used to measure the average and distribution of bubble sizes. Dynamic foam tests were conducted, using mobility setup shown in figure 15, in rock samples to assess the ability of surfactant and NP mixtures to stabilize gas-liquid foam in porous media. IFT measurements, Zeta potential analysis, DLS, and TEM were used to understand the surfactant foam stabilization enhancement mechanisms in the presence of NPs.

To prepare the samples, the original surfactant and silica NP samples were first diluted separately in deionized water and stirred overnight to ensure homogeneity. These became

stocks used to prepare the surfactant and NP mixtures for the static and dynamic tests. Surfactants were added to NPs in stepwise fashion to minimize aggregation of NPs during the mixing process. To avoid the generation of foam during this step, samples were stirred at moderate revolutions per minute. This procedure was followed for all tested samples.

4.2.1.2.1 CMC Measurements

The IFT value is a crucial parameter in determining the ability of surface-active agents (surfactants) to generate foams. At low concentrations, far away from its cmc, a surfactant shows a slight change in the surface tension value. However, near the cmc or a little higher, a surfactant shows the highest performance in terms of reducing the surface tension value. For these reasons, it is important to measure the cmc of the surfactant and the impact of NPs on the IFT values since these reflect the ability of surfactant to generate foams. The cmc of nonionic 1 and the cmc as a result of mixing the surfactant with 0.025, 0.25 and 0.50 wt% NPs were measured using the OCA 15 Pro Contact Angle and IFT device. The cmc values for nonionic 2 and nonionic 3 will be reported as provided by the manufacturer.

4.2.1.2.2 Foam Static Tests

Foam half-life tests were performed to ensure that surfactants and the mixtures of surfactants and NPs could generate stable foams. It was also necessary to assess the chemical stability of the solutions, to ensure that mixing surfactants and NPs resulted in no precipitation. These tests served as an introductory step to evaluate the ability of NPs to improve the stability of foam generated by surfactants and also to evaluate the importance of NPs concentration in foam stability. These tests were conducted in 9 ml glass tubes, which were filled with 4 ml of prepared solutions and then shaken at least five times to generate foams. The samples used in

these tests were prepared with 0.10 wt% of the three nonionic surfactants and mixtures of the three surfactants and 0.25, 0.50, 0.75, and 1 wt% solid NPs. Images of foam columns at different times were captured and uploaded to Image-J software to measure foam length.

As a complement to the foam half-life tests, the same samples prepared as described above were used to study foam texture. The objective of this test was to evaluate the strength of the foams by comparing bubble size at different NPs concentration. The foam texture, which can be defined as bubble size or number of lamellae per unit volume, is a crucial parameter for determining the strength of the generated foam. The smaller the bubble size, the stronger the foam generated and, hence, the ability of the foam to reduce gas mobility, which, as described in the introduction is the purpose of generating foams (Falls et al. 1988, Kovscek and Radke 1994).

4.2.1.2.3 Foam Dynamic Tests

These tests were performed to assess the ability of surfactant and NP mixtures to generate foam in porous media and to measure the strength of any foam generated. The dynamic tests were conducted based on the results of the static tests. To test foam strength and stability, the pressure drop across rock samples was measured. Higher pressure drops indicate more viscous foam and, hence, more resistance to gas flow in porous media. Boise sandstone rock samples 1 through 4 were used to perform these tests. Core samples were put in oven overnight to ensure they were dry. To remove any gases trapped inside pore spaces, the core samples were then set in a core holder and a vacuum was applied. Then at least five pore volumes (PV) of water were injected at 5 ft/day to ensure the samples were 100% saturated with water. The back pressure regulator (BPR) was set to 150 psi. Next, the samples were pre-

flushed with surfactant or a mixture of surfactant and NPs at 5 ft/day for 1 PV. Finally, the co-injection of gas and surfactant/mixture was conducted at 70% quality (the gas fractional flow in the co-injection process) and the drop in pressure was recorded for each case. Tests were conducted using 0.30 and 1 wt% of nonionic 1 surfactant and a mixture of 0.30 and 1wt% of the same surfactant and 0.50 wt% of NPs.

4.2.1.3 Results and Discussion

4.2.1.3.1 CMC Measurements

The cmc for nonionic 1 and mixtures of nonionic 1 and 0.025, 0.25 and 0.50 wt% NPs were measured. The presence of NP in nonionic 1 surfactant had a significant impact on cmc measurements. As the NP concentration increased, the cmc value decreased. The reported values for nonionic 1 surfactant and mixtures of the surfactant and 0.025, 0.25 and 0.50 wt% NPs were 0.038, 0.0375, 0.03, and 0.028 mN/m, respectively. This means that the presence of NPs in surfactant solution can expedite the processes of micelle generation. Based on IFT measurements, it is not necessary for NPs to reduce the IFT values. The results reported the ability of NPs in surfactant solution to form micelles faster. **Figure 54** shows the cmc values of the surfactant and 0.025 and 0.25 wt% NPs.

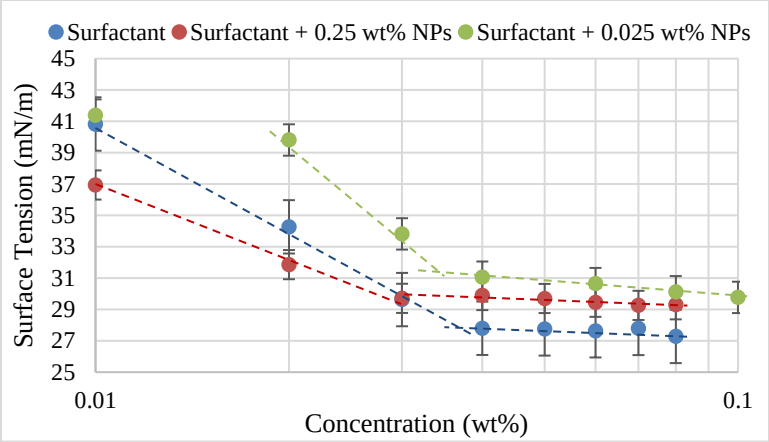

Figure 54: CMC of nonionic 1 surfactant and mixtures of the surfactant and NP

4.2.1.3.2 Foam Half-Life

As discussed above, foam half-life tests were conducted using the three nonionic surfactants. **Figure 55** shows foam behavior with time for nonionic 1 surfactant and a mixture of the same surfactant with 0.25, 0.50, 0.75, and 1 wt% NPs. The concentration of NPs is crucial to foam strength and stability and, based on these results, there are optimum concentrations at which stronger foam can be produced. Neither the low concentration of NPs, 0.25 wt%, nor the high concentration, 1 wt%, were able to improve the foam stability of nonionic 1 surfactant. Indeed, at both low and high concentrations of NPs, foams almost behaved the same as foams created without NPs. Optimum behaviors were observed at 0.50 and 0.75 wt% NPs.

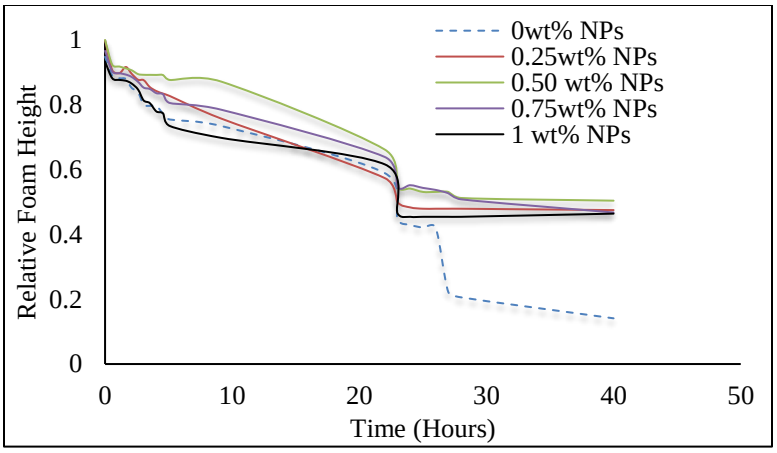

Figure 55: Foam life for 0.10 wt% nonionic1 and mixture of surfactant and NPs

Figure 56 shows that, based on relative foam height measurements, nonionic 3 surfactant produced more stable foams at moderate concentrations, (0.25, 0.50 and 0.75 wt% NPs). The best performance for this surfactant was achieved with 0.25 wt% NPs while the worst was with 1 wt% NPs. In this test, the surfactant behavior is the worst among all other tested cases, the decay of the foam column was faster compared with other cases that had NPs.

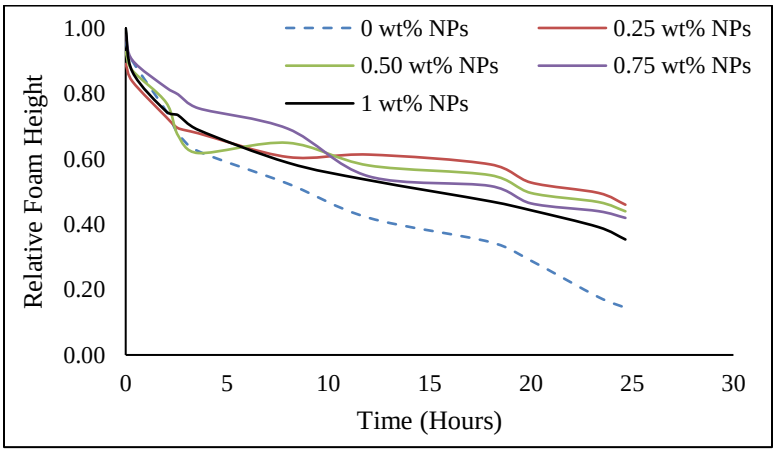

Figure 56: Foam life for 0.10 wt% nonionic 3 and mixture of surfactant and NPs

The foam half-lives for the five cases of nonionic 1 surfactant are shown in **figure 57**. The longest foam half-lives were reported at 0.50 and 0.75 wt% NPs, 28 and 29 hours, respectively. However, the foam half-lives of the other cases, 0.25 and 1 wt%, are similar to that of surfactant alone, 23 hours.

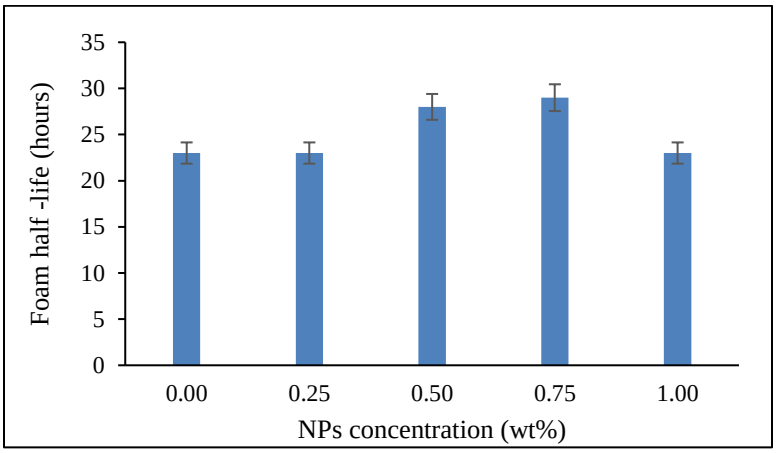

Figure 57: Foam half-lives of 0.10 wt% nonionic 1 and mixture of surfactant and NPs

The results of the nonionic 2 surfactant also emphasized the importance of NP concentration. As shown in **figure 58**, the highest foam half-lives with this surfactant were achieved at 0.25 and 0.50 wt% NPs, 20 hours. At 0.75 wt% NPs, the results were very close to the previous cases. However, the shortest foam half-life was reported with 1 wt% of NPs, 15 hours, which is worse than using surfactant alone. Therefore, it is not recommended to use high concentrations of NPs to achieve the best stability.

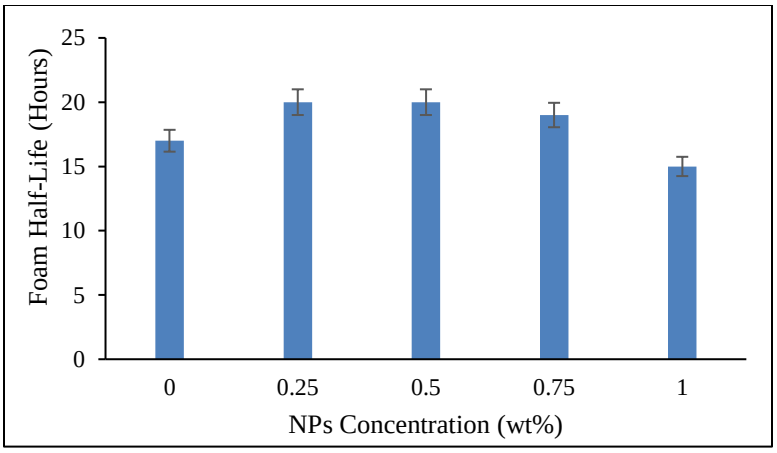

Figure 58: Foam half-lives of 0.10 wt% nonionic 2 and mixture of surfactant and NPs

The results of nonionic 3 surfactant were similar to those of nonionic 1 and nonionic 2. As shown in **figure 59**, the strongest foam was reported for 0.25 wt% of NPs, 23 hours. The next strongest was reported for 0.50 and 0.75 wt% of NPs, 20 and19 hours, respectively. Even though 1 wt% NPs concentration showed the lowest stability among the other cases where NPs were added, its stability was better than that of surfactant by itself.

These results suggested that the addition of NPs, at certain concentrations, might help to slow the drainage of thin aqueous film (lamellae) and, therefore, to produce a more stable foam. However, it is important to note that even though NPs enhanced foam stability, based on the initial foam columns, they were not able to improve foamability (i.e. the ability to generate foam). This was also confirmed using IFT measurements of 0.10 wt% nonionic 1 surfactant and mixtures of the surfactant and 0.25 and 0.50 wt% NPs. The IFT values were slightly higher for the samples with NPs, which confirms the inability of the mixtures to further reduce the gas-liquid IFT and, hence, the inability to generate more foams. The IFT values for surfactant and mixtures with 0.25 and 0.50 wt% NPs as shown in **figure 60** were 27.28, 29.3 and 28.77, respectively.

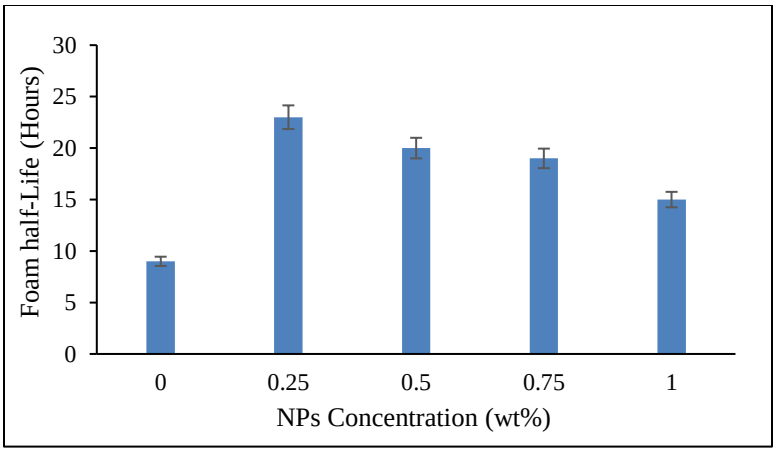

Figure 59: Foam half-lives of 0.10 wt% nonionic 3 and mixture of surfactant and NPs

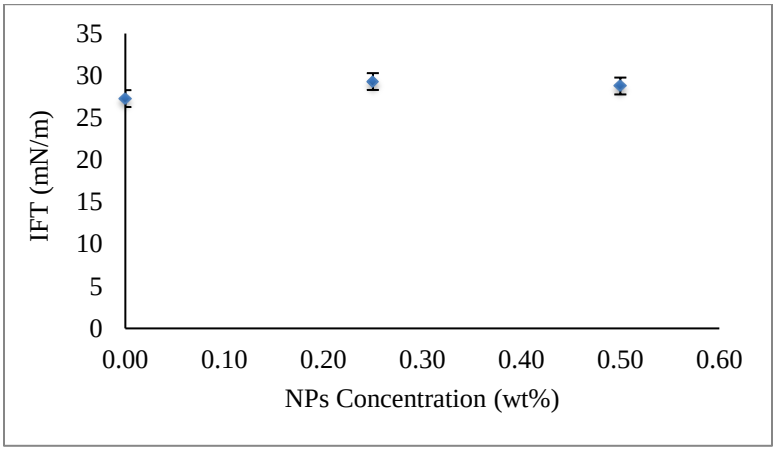

Figure 60: IFT values for 0.10 wt% nonionic1 surfactant and mixtures of 0.10 wt% surfactant and 0.25 wt% and 0.50 wt% NPs

4.2.1.3.3 Foam Texture

Bubbles for the three nonionic surfactants were captured and measured at two different times. The initial bubbles and the bubbles after a few minutes of shaking were captured and analyzed. Comparisons were made for each surfactant in the absence and presence of NPs. **Figure 61** clearly shows differences in bubble sizes for nonionic 1 surfactant with and without NPs.

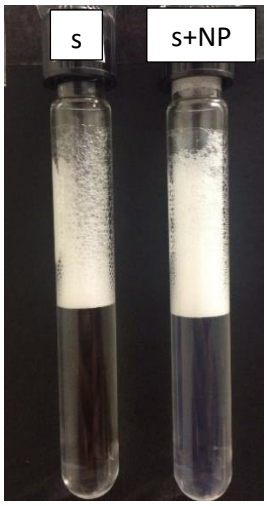

Figure 61: Foam bubbles after 10 miutes of initial shaking for nonionic 1 surfactant (s) and surfactant and silica NPs (s+NPs)

At certain concentrations, the presence of NPs produced smaller bubbles compared to surfactant alone. These results were confirmed in measurements of bubble size using a Nikon Stereo Photomicroscope. **Figures 62a** through **62c** show initial bubble size captured few seconds after shaking for 0.10 wt% nonionic 3 surfactant and mixtures of nonionic 3 and 0.25 and 0.50 wt% NPs. The initial bubble sizes in all tests were nearly the same; the presence of NPs did not change the initial behavior of this surfactant.

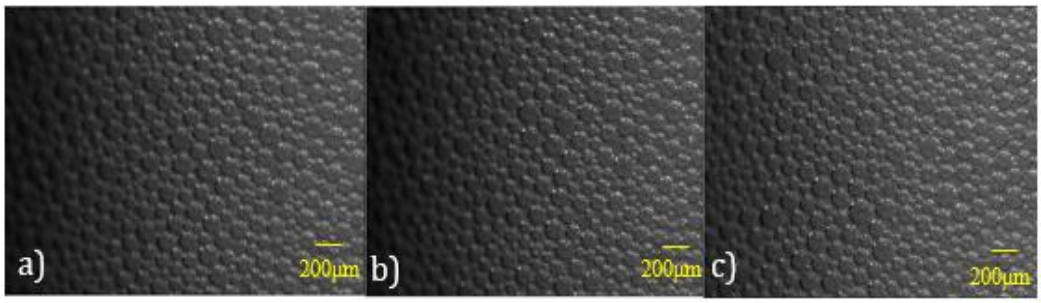

Figure 62: Initial foam bubbles. a) 0.10 wt% nonionic 3 surfactant, b) 0.10 wt% nonionic surfactant 3 + 0.25 wt% NPs, and c) 0.10 wt% nonionic surfactant 3 + 0.50 wt% NPs

However, as shown in **figures 63a** through **63c**, twenty five minutes later the behavior of the foams was completely different. As indicated by the smaller bubble sizes, the presence of NPs improved foam stability and slowed the rate of drainage of thin aqueous film. As mentioned above, the concentration of NPs is a crucial parameter to enhance foam stability and strength. In some cases, lower concentrations produced better enhancement, as those with nonionic 3 presented in **figure 63**, while in others moderate concentrations, as those with nonionic 1 surfactant, performed better. More details about the bubble size distribution for nonionic 3 are shown in **figure 64**. The figure shows that the bubble size has a non-uniform distribution and the range of bubble size is between 218-602 μm.

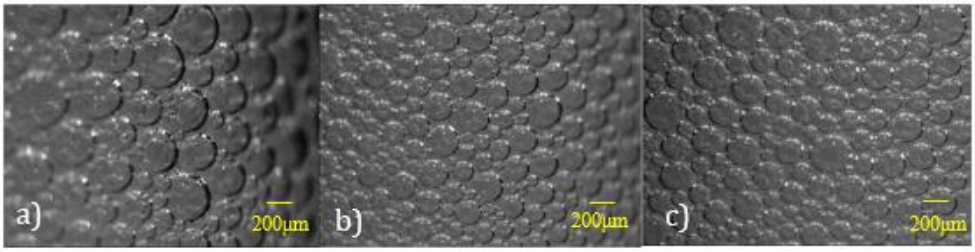

Figure 63: Foam bubbles after 25 miutes of shaking. a) 0.10 wt% nonionic 3 surfactant, b) 0.10 wt% nonionic surfactant 3 + 0.25 wt% NPs, and c) 0.10 wt% nonionic surfactant 3 + 0.50 wt% NPs

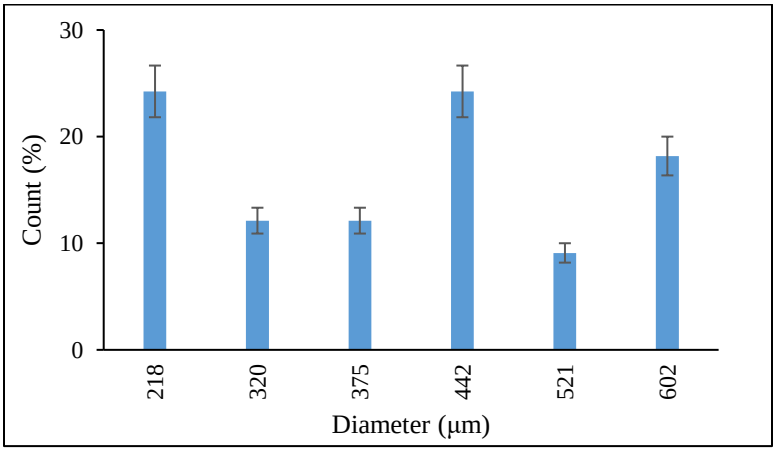

Figure 64: Bubble size distribution for surfactant 3 after 25 minutes of shaking

The bubble size distribution is much smaller for the cases where NPs were added compared to the surfactant alone. For surfactant 3 and 0.25 wt% NPs, the range of bubble size is much smaller than that reported for surfactant case. As shown in **figure 65**, the range of bubble size is between 126-373 μm with high count toward the smaller bubbles. Based on the shape of data distribution, the bubble size distribution is positively skewed.

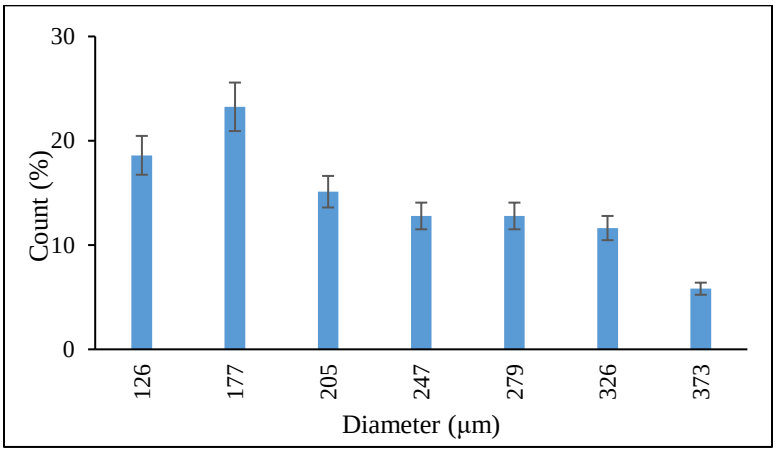

Figure 65: Bubble size distribution for surfactant 3 and 0.25 wt% NPs after 25 minutes of shaking

For surfactant 3 and 0.50 wt% NPs, the range of bubble size is much smaller than that reported for surfactant case but a little larger than the case with 0.25 wt% NPs. As shown in **figure 66**, the range of bubble size is between 158-494 μm with high count of bubble size towards the medium bubbles. Based on the shape of data distribution, the bubble size distribution is positively skewed.

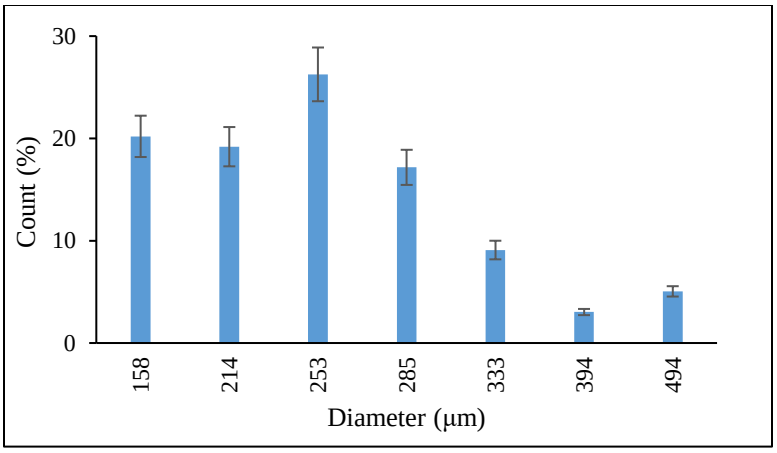

Figure 66: Bubble size distribution for surfactant 3 and 0.50 wt% NPs after 25 minutes of shaking

The average bubble sizes and the range of bubble sizes for the three surfactants and the NP mixtures are summarized in **table 23**. NP mixtures produced smaller bubble sizes, as it is reported from the average and range of bubble sizes, compared to surfactants alone and this can be affected strongly by the concentration of NPs. For the concentrations of NPs used in this analysis, as the concentration of NPs decrease bubbles get smaller, except for the case of nonionic 1, in which 0.50 wt% NPs showed smaller bubbles than 0.25 wt% NPs.

These results showed that the presence of NPs was able to improve foam stability and produced foams with smaller bubbles. Moreover, the concentration of NPs can play a major role in foam enhancement and strength.

Table 23: Average and range of bubble size after 25 minutes of shaking

Material	Average Diameter (μm)	Range of Bubble Size (μm)
Nonionic 1	452	289-725
Nonionic 1+ 0.25 wt% NPs	306	174-567
Nonionic 1+ 0.50 wt% NPs	250	130-550
Nonionic 2	298	170-662
Nonionic 2+ 0.25 wt% NPs	233	128-438
Nonionic 2+ 0.50 wt% NPs	246	131-497
Nonionic 3	401	218-602
Nonionic 3+ 0.25 wt% NPs	222	126-373
Nonionic 3+ 0.50 wt% NPs	256	158-494

4.2.1.3.4 Foam Dynamic Tests

Reporting foam behavior in porous media is important. Static foam tests may help anticipate foam strength and stability, but foam behavior and generation processes are totally different in porous media. The foamability and stability tests were conducted using rocks 1 and 2 and solutions prepared with 0.30 wt% of nonionic 1 surfactant and a mixture of 0.30 wt% surfactant and 0.50 wt% NPs. Rocks 3 and 4 were used to run the experiments using 1 wt% of nonionic 1 surfactant and a mixture of 1 wt% surfactant and 0.50 wt% NPs. Here, the comparison was based on the pressure drop across the rock samples for all cases. Stronger foam will produce a higher pressure drop due to the resistance to flow created by the changes to injected solutions' apparent viscosity and the reduction of solutions' relative permeability.

Figure 67 shows the results of these tests. Foam generation was very slow for surfactant alone. This might be attributed to adsorption of the surfactant to the rock sample as this is expected to be significant. In general, nonionic surfactants lose significant amounts of injected volume during surfactant flooding in porous media. This is much worse when the porous media are made of sandstone such as those used in this study. The Boise sandstone was analyzed using X-ray diffraction (XRD), figure 20, to determine its clay content, which is one of the strongest contributors to adsorption during nonionic surfactant injection in sandstone formations. XRD measured a significant proportion of illite, about 13%, in these samples. This could cause a delay in foam generation due to high adsorption (Amirianshoja et al. 2013).

Evaluating the effects of adsorption is outside the scope of this work. Therefore, the important parameter to evaluate here is the pressure drop during steady state conditions. For surfactant alone, the steady state pressure drop was approximately 15 psi. Adding NPs to surfactant increased the steady state pressure drop to approximately 18.3 psi. This is significant since the permeability of these rocks, 3.47 Darcy, is relatively high. It also confirms the findings from the earlier bulk tests that NPs are able to produce stronger and more stable foams.

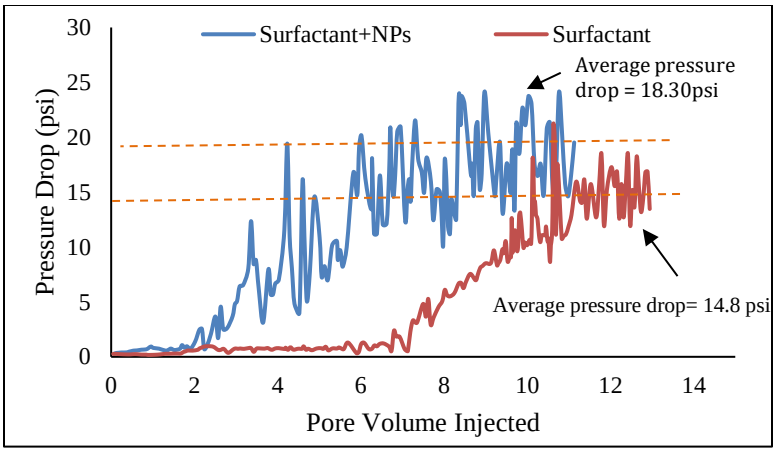

Figure 67: Pressure drop across the Boise sandstone for 0.30 wt% surfactant and a mixture of 0.30 wt% surfactant and 0.50 wt% NPs

However, the increase of surfactant or NPs concentrations might have a different effect on foam stability. This was confirmed by changing only the surfactant concentration, since the effect of NPs concentration is already addressed in the static foam section. The surfactant concentration was changed from 0.30 wt% to 1 wt%. The results, as appeared in **figure 68**, showed that both surfactant and NPs have almost the same pressure drop. This means the mixture in this case was not able to improve the foam stability. Instead, the mixture resulted in a weaker foam since the permeability of the rock used for surfactant is almost double that of NPs. More details about the role of surfactant and NPs concentrations on foam stability will be discussed in the next section.

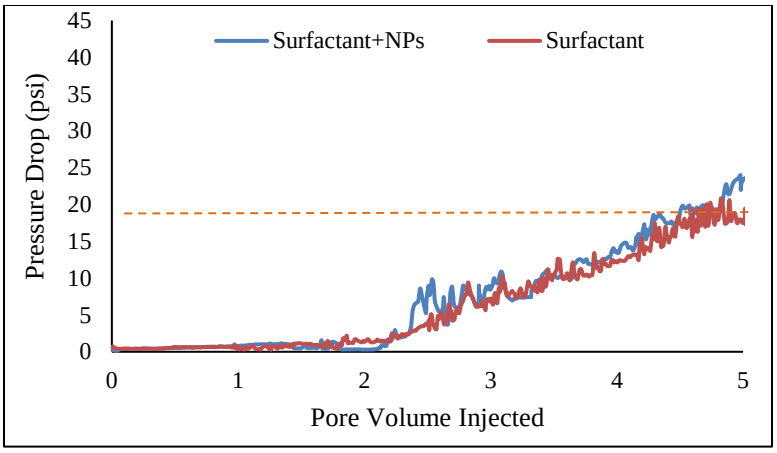

Figure 68: Pressure drop across the Boise sandstone for 1 wt% surfactant and a mixture of 1 wt% surfactant and 0.50 wt% NPs

4.2.1.4 Mechanism of Foam Stabilization

In this work, several analyses were conducted to assess the ability of solid NPs to improve foam strength. As mentioned earlier, a high concentration of surfactant and NPs might have a negative impact on foam stability. Thus, it is essential to understand the behavior of NPs when they mix with surfactant. To do so, the zeta potential was measured by altering the concentration of nonionic 1 surfactant while fixing NP concentration. **Figure 69** shows that there is an inverse relationship between the surfactant concentration and zeta potential values. As the concentration of surfactant increases, the zeta potential decreases. In the absence of surfactant, the zeta potential of 0.50 wt% NPs in deionized water was about -44.5 mV. This value dropped to around -33 mV when 0.10 wt% of surfactant was added.

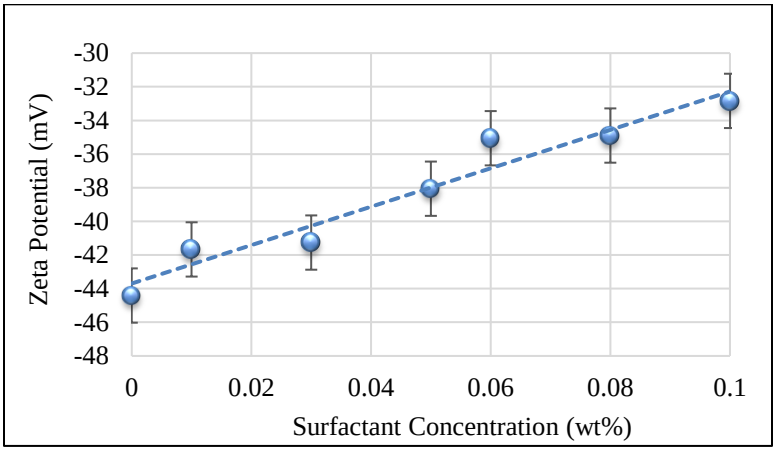

Figure 69: Zeta potential for NP with nonionic 1surfactant concentration

To proceed with analysis, the size of NPs was measured using DLS as a function of surfactant concentration. **Figure 70** shows that as the surfactant concentration increases, the size of NPs increases, too. The original size of nanoparticles was 22 nm. This changed to 23.3 nm and 26 nm, respectively, when 0.10 and 0.50 wt% of surfactant were added.

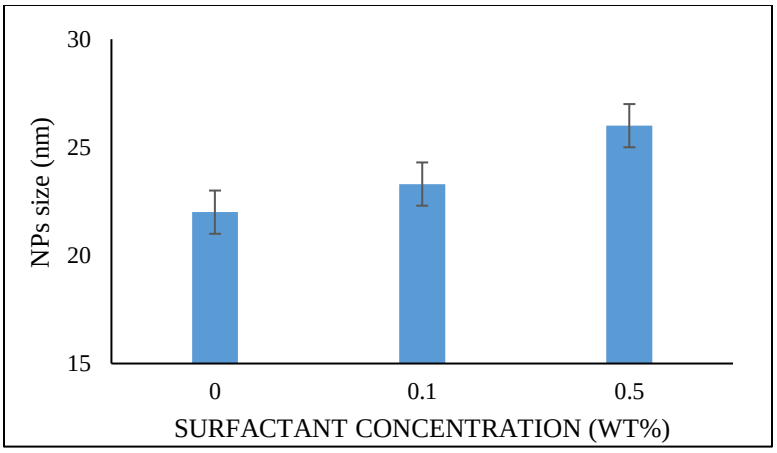

Figure 70: Silica particles size as a function of nonionic 1 surfactant concentration

More investigations are needed to understand this behavior. TEM was used to visualize NPs when they mixed with surfactant. **Figure 71** shows NPs diluted in deionized water, **figure 72** shows a mixture of surfactant and NPs, and **figure 73 shows** the same mixture, but at lower resolution. As can be seen in these images, some NP flocs were generated as a result of mixing the surfactant and NPs. These flocs may cause the zeta potential to get lower and the NP's size to get larger as surfactant concentration increases.

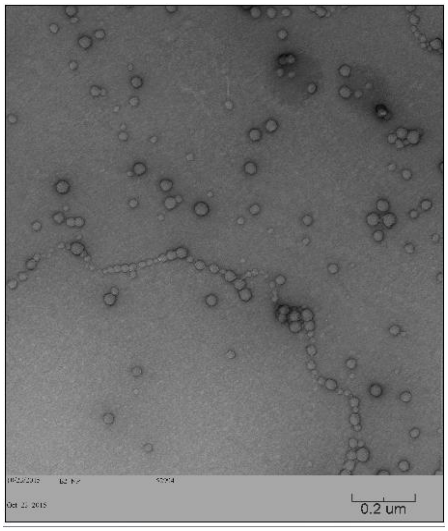

Figure 71: TEM images of diluted NPs

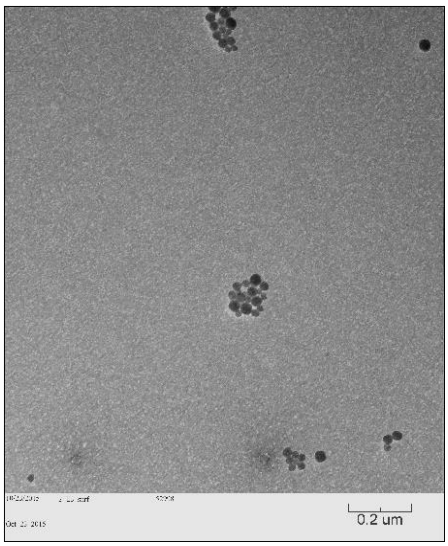

Figure 72: TEM images of high resolution of the mixture of surfactant 1 and NPs. (spot with high population flocs

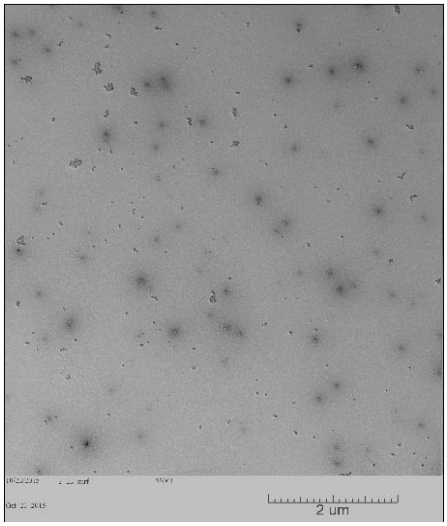

Figure 73: TEM images of lower resolution of the mixture of surfactant and NPs

If the concentration of the NPs gets much higher, as those shown in **figure 74**, then there will be more chances to generate more and larger flocs and aggregates.

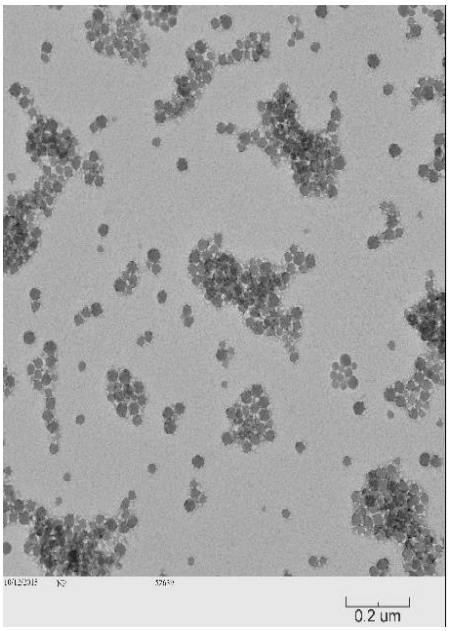

Figure 74: TEM image of the mixture of surfactant 1 and 1 wt% NPs

Taking these observations into account, the proposed explanation for the foam stability enhancement in this study is that, if suitable concentrations of surfactant and NPs are mixed, flocs might help to improve the stability of surfactant foams by increasing the solution viscosity and by increasing the maximum capillary pressure of coalescence as the packing number in the numerator of equation 2 increases. The increase in both viscosity and the maximum capillary pressure of coalescence will slow down drainage rate, thereby improving foam stability and strength. However, when the NP concentration is too high, the floc population and size will be larger. Moreover, the addition of surfactant will increase the flocs population and size. Thus, even though the viscosity might increase, the maximum capillary pressure of coalescence will decrease as the radius of the NPs increases. This leads to accelerate the rate of coalescence. This can explain the behavior when the concentrations of NPs were too high, as those with 1wt% presented in bulk tests and shown in TEM (**figure 74**). The aggregation of NPs at these concentrations formed intensive flocs with large diameters. These

reduced the maximum capillary pressure of coalescence and, hence, expedited film breakage. This also can explain the results reported in dynamic tests for the two conditions discussed earlier.

4.2.1.5 Summary

The combination of NPs and surfactant may offer a novel technique of generating stronger foams for gas mobility control. This study evaluates the potential of silica NPs to enhance the foam stability of three nonionic surfactants. Results showed that the concentration of surfactant and NPs is a crucial parameter for foam stability and that there is an optimum concentration for strong foam production. A balance in concentration between the nonionic surfactants and the NPs can enhance the foam stability as a result of forming flocs at the thin aqueous film. At fixed surfactant concentration, the addition of NPs at optimum concentration can produce a more stable foam compared to the surfactant. The production of small population of flocs as a result of mixing the surfactant and NPs can enhance the foam stability by providing a barrier between the gas bubbles and delaying the coalescence of bubbles. Moreover, these flocs can increase the solution viscosity and, therefore, slow the drainage of thin aqueous film (lamellae). The measurements of foam half-life, bubble size, and mobility tests confirmed this conclusion. However, the addition of more solid particles or surfactant might have a negative impact on foam stability and reduce the maximum capillary pressure of coalescence as a result of forming large and dense aggregates.

4.2.2 Surface Modified Silica NP and CNF Surfactant (N_2 Foam)

This section will cover the results of the CNF surfactant and the mixture of surface modified silica NPs and CNF surfactant. The synergistic effect of surfactant and NPs can help produce a stronger and more stable foam in reservoir porous media. The objective of this work was to assess the ability of surfactant and a mixture of surfactant and NPs to produce foam for gas mobility control and the enhancement of oil recovery. Anionic surfactant and a mixture of anionic surfactant and surface modified silica NPs were used in this study to assess the synergistic effect on foam stability.

4.2.2.1 Materials

The surfactant used in this study is anionic surfactant (CNF). The NPs used are surface modified silica received in aqueous form from Nyacol Chemicals. DLS was used to measure the size of the particles. The average size of particles was found to be 30 ±1 nm. Brine was prepared using deionized water (DI) (ASTM Type II, Lab Chem) and sodium chloride (99%, Cole-Parmer). Nitrogen gas (industrial grade) was used to conduct gas mobility tests and core flood experiments. The cores used in this study were Bentheimer sandstone from Kocurek Industries. **Table 24** summarizes the properties of these cores. North Burbank Unit (NBU) oil with an average viscosity of 8.1 cp at 25^{o}C and 3.2 cp at 50^{o}C was used to conduct bulk tests and core flood experiments.

Table 24: Properties of Bentheimer sandstone samples

Sample #	Length (in)	Diameter (in)	Porosity (%)	Pore Volume (cc)	Permeability (D)
1	12	1	22.08	34.11	1.61
2	12	1	20.79	32.09	1.47
3	12	1	21.84	33.74	1.55
4	12	1	20.55	31.74	1.69

4.2.2.2 Experimental Procedure and Conditions

This study consists mainly of two parts: static and dynamic tests. Static foams for surfactant and the mixture of surfactant and silica NPs were generated in test tubes. The half-life of captured foam columns with and without crude oil were measured using Image-J software. To understand the foam generation and stabilization processes, the IFT values of water/gas ($\sigma_{w/g}$), oil/gas ($\sigma_{o/g}$), and water/oil ($\sigma_{w/o}$) were measured using an OCA20 goniometer (Dataphysics, FDS). The dynamic foam was generated using a mobility test setup, figure 15, and the gas mobility was evaluated in rock samples at different conditions. The coreflood setup, figure 16, was used to conduct core flood experiments to assess the ability of generated foam to reduce gas mobility and enhance oil recovery.

4.2.2.2.1 Samples Preparation

The brine was first prepared using 1% NaCl in deionized water. The surfactant was then diluted in the solution and was stirred overnight to ensure homogeneity. The surface modified NPs were diluted in deionized water and were stirred overnight. The NPs were then added to the surfactant solution slowly, in stepwise fashion, to avoid aggregation of NPs. The size of NPs was measured before and after the mixing to verify there was no aggregation occurs during mixing.

4.2.2.2.2 Foam Static Tests

As a preliminary test to assess the foamability and stability of foam for both surfactant and a mixture of surfactant and NPs, a volume of 4 ml was taken from the samples prepared as explained above and put in 9 ml vials. This test was conducted with and without crude oil. Two conditions, effect of salinity and temperature, were tested to assess the ability to generate and stabilize foams. To evaluate the effect of salinity, bulk tests were conducted using DI water and 1% NaCl. The effect of temperature was tested by running the tests at 25ºC and 50ºC. To assess the foam behavior in the presence of crude oil, 10 wt% of NBU oil was used. All samples were shaken at least five times to generate the foam. Photos of foam columns were captured and uploaded to Image-J software to measure foam length at different times.

4.2.2.2.3 IFT Measurements

Two sets of IFT experiments were conducted to assess the effect of crude oil on foam stability. The first set was conducted using 0.50 wt% surfactant and a mixture of 0.50 wt% surfactant and 1 wt% NPs. The second set was similar to the first set but 1 wt% NaCl was added. The major parameters calculated here are spreading, entering, bridging coefficients and lamella number. The equations used to calculate these parameters were already discussed above.

4.2.2.2.4 Foam Dynamic Tests

The objective of this test is to examine the ability of the used materials to generate foam at reservoir conditions. The important measurement and observation here are the pressure drop across the core samples and foam generation in porous media. Bentheimer sandstone rock

samples #1 and #2 were used to perform these tests. The core samples were put in oven overnight to ensure they were dry. The samples were then set in the core holder and a vacuum was applied to remove all gases trapped inside pore spaces. At least five pore volume (PV) of brine were injected at 5 ft/day to ensure the sample was 100% saturated with brine. The BPR was set to be 200 psi. The samples were then pre-flushed with surfactant or a mixture of surfactant and NPs at 5 ft/day for 1 PV. Then, the co-injection of gas and surfactant/mixture was conducted at 90% quality and the drop in pressure was measured for each case. To make sure there was a flow of both gas and surfactant/mixture at the same time, the co-injection process was conducted first at a bypass line and then into the core sample. After finishing the test, the system was depressurized and at least 30 PV of brine were injected to clean the rock. The procedure of cleaning the rock consists of several cycles of pressurizing and depressurizing processes to ensure the removal of all trapped gases and surfactant. These tests were conducted at 25^{o}C and at 50^{o}C.

4.2.2.2.5 Coreflood Experiments

Coreflood experiments followed almost the same procedure for the mobility tests mentioned in the previous section. Bentheimer sandstone rock samples #3 and #4 were used to perform these tests. After the cores had been saturated with brine, two PVs of NBU oil were injected at 5 ft/day. The experiments were conducted at 1200 psi and 50^{o}C. The overburden pressure was set to be 1700 psi. After ensuring the rock reached the initial water saturation (S_{wi}), the water flooding test started. Once the maximum oil recovery with water flooding was achieved, the pre-flush process of surfactant or a mixture of surfactant/NPs was performed,

followed by a co-injection of immiscible gas and surfactant/mixture as a secondary mechanism for enhancing oil recovery.

4.2.2.3 Results and Discussion

4.2.2.3.1 Static Foam Test in the Absence of Crude Oil

The static foam test in the absence of crude oil showed that neither the samples at DI water nor at 1% NaCl at 25ºC had any improvement in foam generation or stability. There was no obvious changes in bubble size or foam column with time, as shown in **figure 75**. The foam half-life of 0.50 wt% surfactant and the mixture of surfactant and 0.50 wt% and 1 wt% of surface modified NPs was shown to be about 20 hours for both cases: DI water and 1% NaCl.

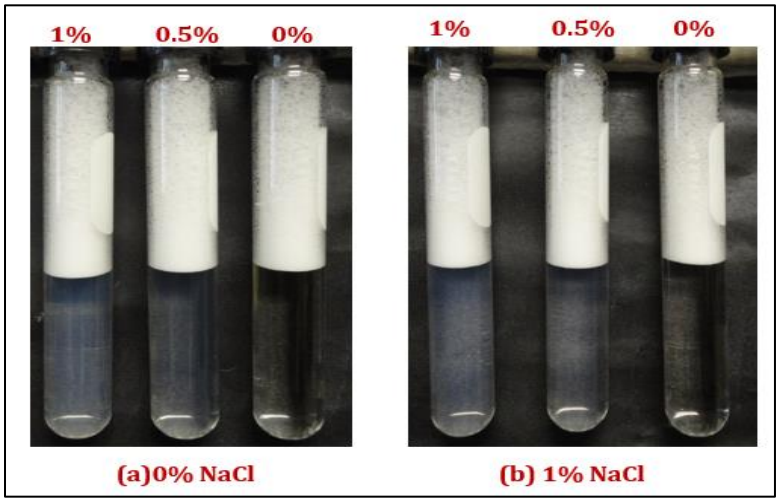

Figure 75: Initial foam generated using 0.50 wt% surfactant (0% NPs) and mixture of surfactant and 0.50 wt% and 1 wt% NPs at 25ºC. (a) Using only DI water (b) Brine,1 wt% NaCl

Figure 76 presents the results of static foam tests at 1% NaCl and 25ºC for the three tested cases. The change of temperature to 50ºC resulted in lower foam half-life compared to

25°C. The foam half-life at 1% NaCl is higher than that at DI water. This might be attributed to the increase in the viscosity of the solution in the presence of salt which might slowing down the drainage velocity and enhance the stability of the foam. Also, the mixture of NPs and surfactant showed a higher foam half-life (about 10% extra in time) compared to surfactant in the absence of salinity. **Figure 77** shows the foam half-lives of the surfactant and the mixtures at 50°C.

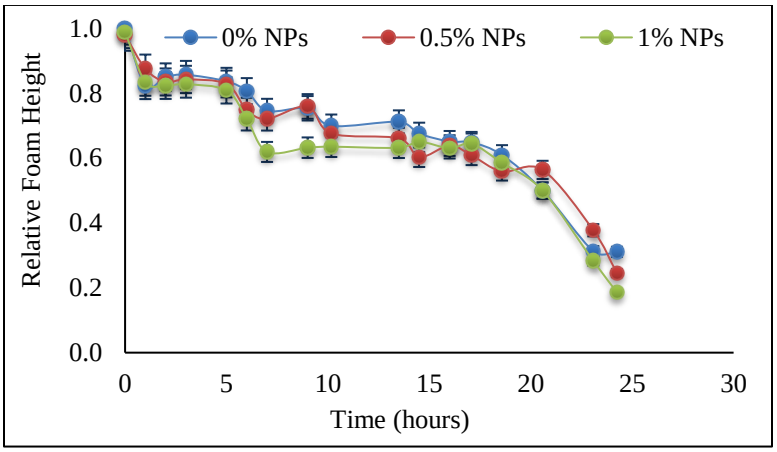

Figure 76: Foam life for 0.50 wt% surfactant and mixture of surfactant and 0.50 wt% and 1 wt% NPs at 25°C and 1% NaCl

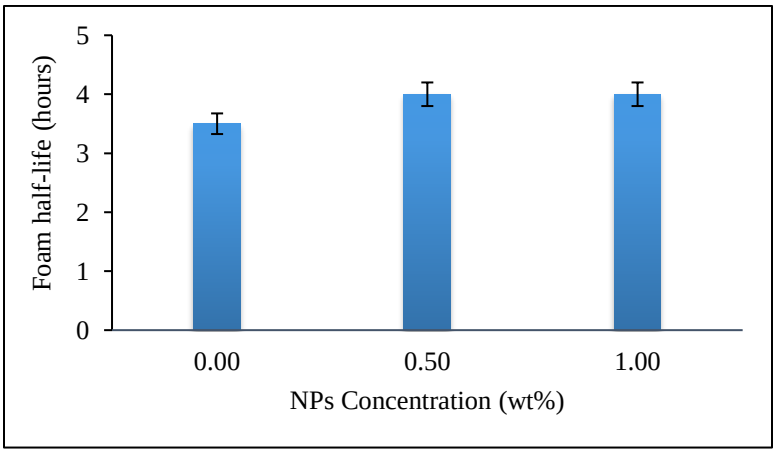

Figure 77: Foam half-lives of 0.50 wt% surfactant and mixture of surfactant and 0.50 wt% and 1 wt% NPs at 50°C using DI water

4.2.2.3.2 Static Foam Test in the Presence of Crude Oil

The static foam tests presented stronger evidence that the presence of surface modified silica NPs enhanced foam stability in the presence of crude oil. Relative to the cases where DI water was used, NPs clearly showed improved foam strength and, therefore, enhanced stability. **Figure 78** shows the foam at the DI water in the presence of crude oil at three different times: 0, 40 and 120 minutes. The foam decay with time for these cases are shown in **figure 79**. The foam half-lives of surfactant and 0.50 wt% and 1 wt% NPs were 5 and 8 times, respectively, greater than that of surfactant alone. The results showed that as the concentration of NPs increased, the foam half-life increased, too.

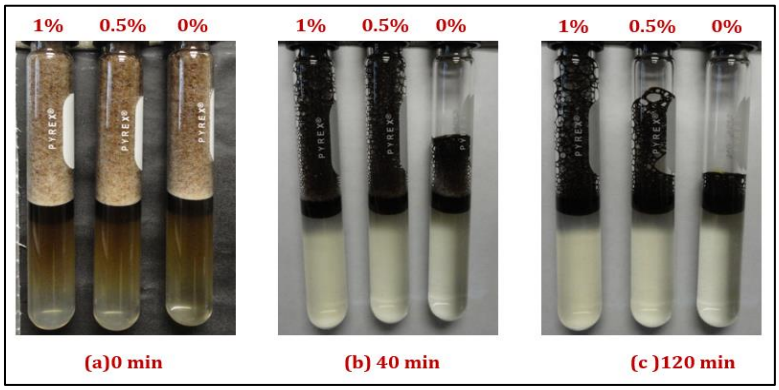

Figure 78: Foam decay with time for 0.50 wt% surfactant and mixture of surfactant and 0.50 wt% and 1 wt% NPs at 25^{o}C using DI water. (a) The initial foam generated at 0 minute (b) The foam after 40 minutes (c) The foam after 120 minutes

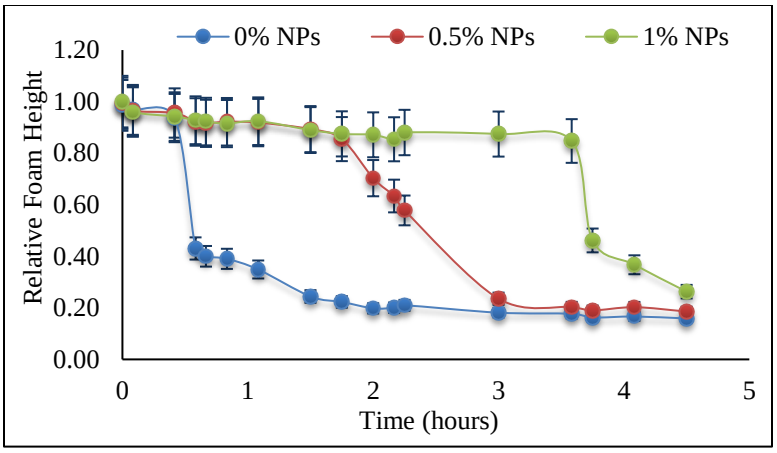

Figure 79: Foam life of 0.50 wt% surfactant and mixture of surfactant and 0.50 wt% and 1 wt% NPs at 25°C and DI in presence of crude oil

At 1 wt% NaCl, the foam is much stronger than in the DI water cases. **Figure 80** shows the foam column at 1 wt% NaCl at 0 and 470 minutes. It also shows that, in absence of NPs, the bubbles appear to be larger, which means they are expected to collapsing faster. The half-life of surfactant was around 13.5 hours while the half –lives of 0.50 wt% and 1wt% NPs were 15 hours. **Figure 81** summarizes the half-lives of all cases conducted in the presence of crude oil.

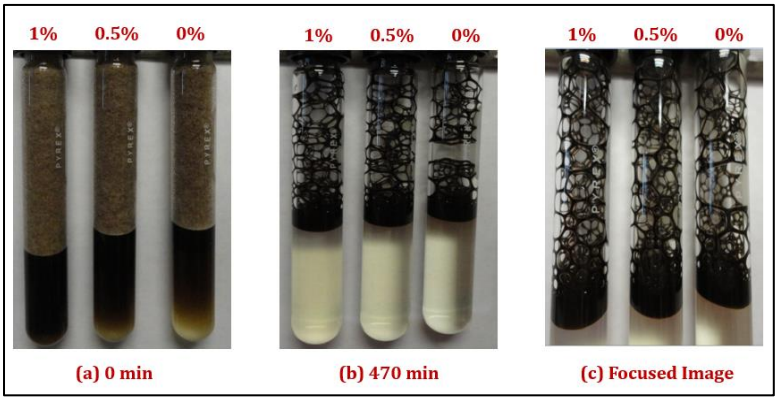

Figure 80: Foam decay with time for 0.50 wt% surfactant and mixture of surfactant and 0.50 wt% and 1 wt% NPs at 25°C using 1 wt% NaCl. (a) The initial foam generated at 0 minute (b) The foam after 470 minutes (c) Foam bubbles after 350 minutes showing smaller bubbles in presence of NPs

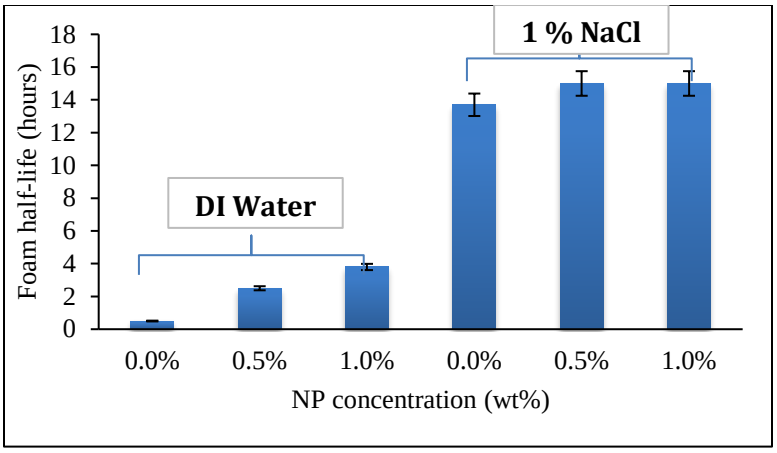

Figure 81: Foam half-lives of 0.50 wt% surfactant and mixture of surfactant and 0.50 wt% and 1 wt% NPs at 25°C and at DI water and 1% NaCl in presence of crude oil

4.2.2.3.3 IFT Measurements

Table 25 reports the IFT values for $\sigma_{w/g}$, $\sigma_{w/o}$, and $\sigma_{o/g}$. **Table 26** summarizes the results of the four parameters: spreading, entering, bridging, and lamella number, based on the measured IFT values. Two sets of experiments were conducted using DI water and 1 wt% NaCl. Each set consists of two cases, surfactant and a mixture of surfactant and NPs.

Table 25: IFT values at 25°C

	0% NaCl		1% NaCl	
	0% NPs	1% NPs	0% NPs	1% NPs
$\sigma_{w/g}$ (mN/m)	31.91	31.55	30.43	30.52
$\sigma_{w/o}$ (mN/m)	5.6	4.89	3.12	2.59
$\sigma_{o/g}$ (mN/m)	31.79			

Table 26: Spreading (S), entering (e), bridging (B), and lamella number (L) results based on IFT Measurements at 25°C

	0% NaCl		1% NaCl	
	0% NPs	1% NPs	0% NPs	1% NPs
S	-5.5	-5.1	-4.5	-3.9
e	5.7	4.7	1.8	1.3
B	39.0	8.7	-74.9	-72.4
L	0.9	1.0	1.5	1.8

Regardless of whether salts or NPs were added, the spreading coefficient gave negative values. This means that the oil will not spread at the foaming aqueous-gas interface. The entering coefficient resulted in positive values, which indicates that the oil will be drawn into the aqueous film and might affect foam stability and strength. As presented in **table 26**, the cases where NPs were added showed lower entering coefficients compared to the cases without the NPs. Also, the addition of NaCl resulted in smaller entering coefficient values compared to the cases with only DI water. This supports the results of static tests that showed the presence of NPs and NaCl improved the foam stability in the presence of crude oil. Based on these two parameters, where $S<0$ and $E>0$, if the amount of oil entering the lamella is significant, the oil will cause destabilization and destroy the film. The bridging coefficient showed two different behaviors: one in the absence of NaCl, and the other when 1 wt% NaCl was added. The bridging coefficient resulted in positive values in the absence of NaCl and negative values when NaCl was used. As mentioned earlier, oil can act as an active antifoaming agent if the bridging coefficient value is positive. This can help explain the better stability of foam found in the static tests in the presence of crude oil. The addition of NaCl resulted in a longer foam half-life in the presence of crude oil compared to the case where NaCl was not added. The oil can act as antifoaming, more quickly breaking the aqueous film in the latter case while slowing down the film breakage in the former case. Furthermore, the bridging coefficient was about 4 times smaller when NPs were added at the 0 wt% NaCl. This can also support the finding in bulk tests that NPs improved the foam stability and increased the foam half-life in the presence of crude oil. The lamella number showed values between 1 and 2, which means oil can be emulsified to smaller droplets, penetrate the thin film, and reside at the larger plateau borders. As such, the oil should not act as a strongly antifoaming agent in such cases. There is an

agreement between some of those parameters with the results of static foam tests. With some exceptions, the spreading, entering, and bridging coefficients, and lamella number support the findings in static foam tests.

4.2.2.3.4 Dynamic Tests

The foamability tests were conducted at two different temperatures: 25^{o}C and 50^{o}C. The comparison was made here based on the foam behavior and values of pressure drop across the core samples for both cases.

4.2.2.3.4.1 At 25^{o}C

The behavior of foam generation in porous media is totally different than that in the static foam test. The results in porous media are more reliable and representative of the process of foam generation in petroleum reservoirs. Rock sample #1 was used in these tests. The results showed that the presence of NPs resulted in higher steady state pressure drop compared to the surfactant case (**figure 82**). The steady state pressure drop for the mixture was about 100 psi, while for the surfactant was 88.5 psi. This is an indication of the ability of NPs to produce a more stable and stronger foam in porous media. The steady state pressure drop of the co-injection of gas and brine using the same rock was 0.35 psi. This means both the surfactant and the mixture were able to reduce the gas mobility with a higher reduction in the presence of NPs. The calculated mobility reduction factor (MRF) for the surfactant and the mixture were 253 and 286, respectively.

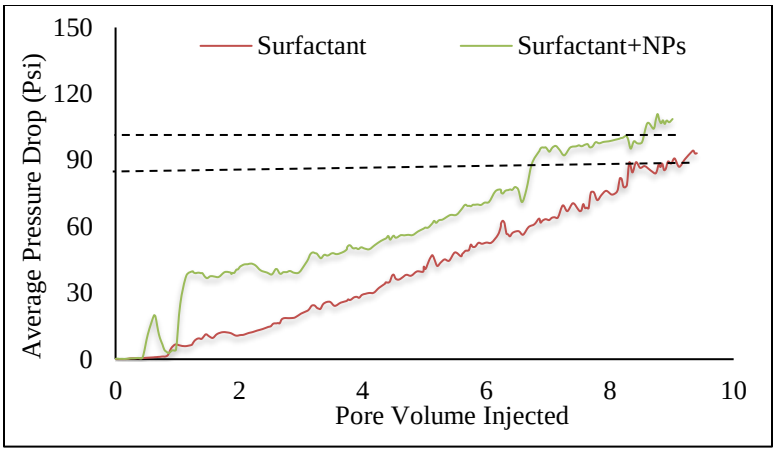

Figure 82: Average pressure drop across the Bentheimer sandstone for 0.50 wt% surfactant and a mixture of 0.50 wt% surfactant and 0.5 wt% NPs at 25°C

4.2.2.3.4.2 At Elevated Temperature 50°C

In these tests, rock sample# 2 was used. At 50°C, earlier foam generation was seen in the presence of nanoparticles (**figure 83**). The mixture resulted in a higher steady state pressure drop compared to surfactant. The steady state pressure drop for the mixture was around 45 psi. This was almost double the steady state pressure drop of surfactant, 21 psi. The steady state pressure drop of the co-injection of gas and brine using the same rock was 0.26 psi. This means both the surfactant and the mixture were able to reduce the gas mobility at elevated temperature with a higher reduction in the presence of NPs. The calculated mobility reduction factor (MRF) for the surfactant and the mixture were 81 and 173, respectively.

Based on the foamability test results, the presence of NPs strengthens the thin liquid film between bubbles and, therefore, reduces the rate of drainage, which can lead to the production of a stronger and more stable foam. This leads to the conclusion that the presence of NPs can resist the temperature effect on destroying foam bubbles and produces a more stable liquid film (lamella).

The increase in temperature from 25°C to 50°C for all tested cases, with/without NPs, resulted in a lower pressure drop. This was expected as temperature reduces foam viscosity and might affect negatively foam stability.

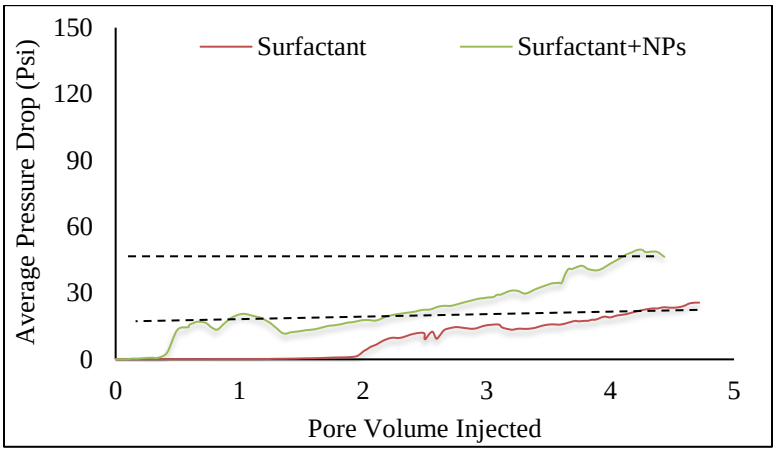

Figure 83: Average pressure drop across the Bentheimer sandstone for 0.50 wt% surfactant and a mixture of 0.50 wt% surfactant and 0.50 wt% NPs at 50°C

4.2.2.3.5 Coreflood Experiments

Two sets of experiments have been conducted to assess the ability of foam to enhance oil recovery, one in the absence of NPs and the other in the presence of NPs. The results of coreflood experiments showed that both experiments, with and without NPs, improved the oil recovery during foam injection processes, with higher recovery in the NPs case. **Figure 84** shows the results of coreflood experiments for the surfactant case. The oil recovery following the waterflooding process was about 34.95 % of the OOIP. At least 4 PVs of water were injected to ensure that no more oil could be recovered in this process and to diminish any capillary end effect that might exist. Then, 1 PV of surfactant was injected as a pre-flush step. The objective of this step was to minimize the adsorption that might occur during the co-

injection processes. There was no significant amount of oil produced during the pre-flush step. This is an indication that the surfactant is not an excellent oil-water IFT reducer. The surfactant foam was able to produce about 6.5% of the OOIP. This brought the total oil recovery to be around 41.45% of the OOIP. The pressure drop during the waterflooding processes was about 2 psi, and it reached about 6 psi during the co-injection processes.

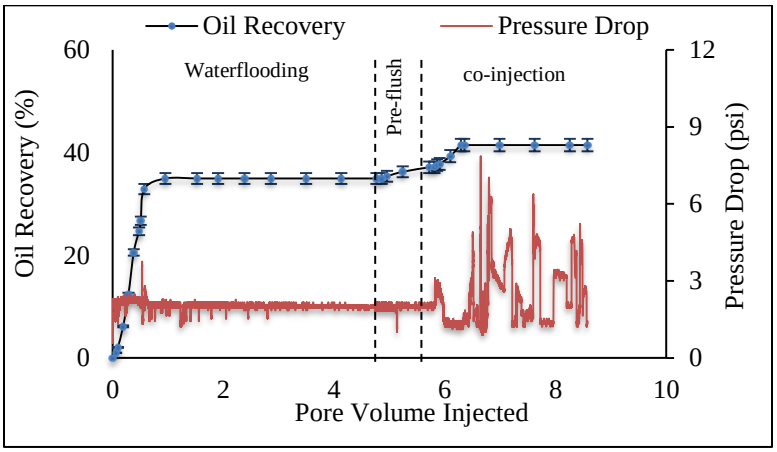

Figure 84: Oil recovery following waterflooding and foam injection for surfactant

The next experiment, as shown in **figure 85**, was for the case where the mixture of surfactant and NPs was used. The same procedure as in the previous experiment was used in this run. The oil recovery following the waterflooding process was about 39.29 % of the OOIP. The pre-flush with the mixture was not able to recover any additional oil. During the co-injection processes, the mixture was able to produce about 9.76% of the OOIP. This is 3.26% higher than injecting surfactant alone. The total oil recovery following the mixture foam process was around 49.05% of the OOIP. This is 7.6 % higher than the previous experiment where only surfactant was used. The pressure drop during the waterflooding processes was

about 1.75 psi and it reached 17 psi during the co-injection step. This is much higher than the surfactant foam. **Figure 86** shows a summary of the coreflood experiments.

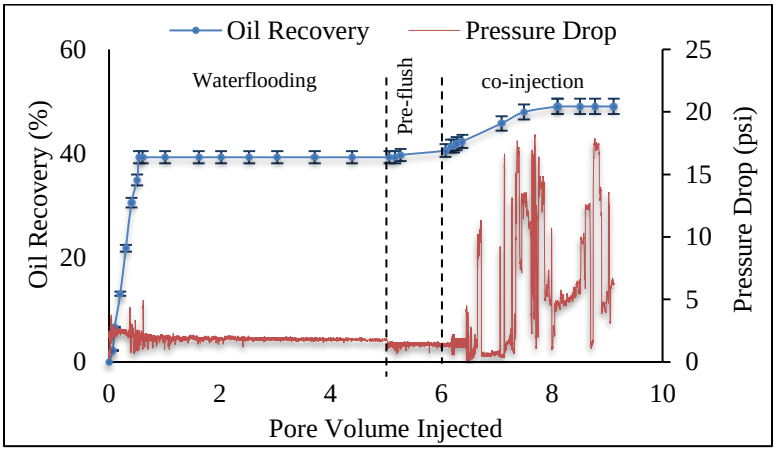

Figure 85: Oil recovery following waterflooding and foam injection for a mixture of surfactant and NPs

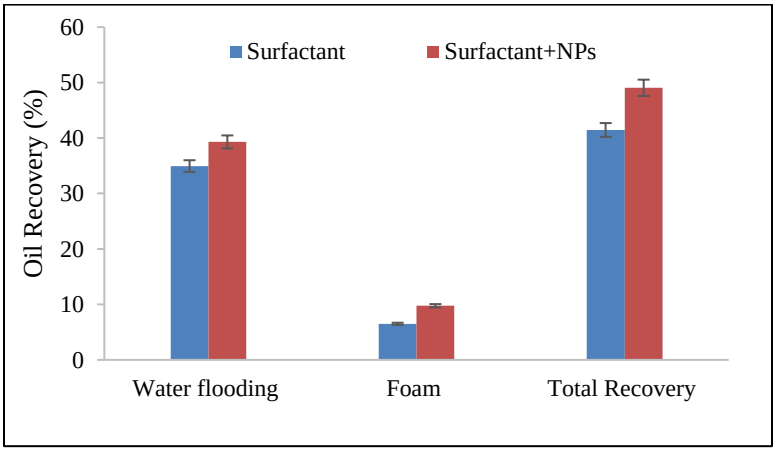

Figure 86: Summary of coreflood experiments

4.2.2.4 Mechanism of Foam Stabilization

The major mechanisms reported in the literature to explain the stability of foam for a mixture of surfactants and NPs are: particle attachment energy; particle arrangement during film drainage; maximum capillary pressure of coalescence; and growing aggregates.

The mixture used in this study consists of surfactant and NPs. The huge reduction of IFT due to the use of surfactant reduces the energy of attachment, thus resulting in poor stability of foam. As a result, particle attachment energy is not the appropriate mechanism to explain the enhancement of foam stability in the presence of NPs and surfactant. Also, growing aggregates mechanism is probably not the case in this study as the average particle size did not change as a result of mixing NPs and surfactant at different concentrations, so no aggregates or cork were formed. NPs used in this study seem to stabilize the liquid film by two mechanisms: particle arrangement during film drainage and increasing the capillary pressure of coalescence. The polydispersity index (PDI) of the silica particles used in this study was measured using the DLS and found to be around 0.11. This is within the range where monodispersity of particles is defined. The relatively low PDI value of those particles will help in producing the most efficient arrangements during film drainage processes which might help in slowing down the film thinning and, hence, resulting in a more stable film. The hydrophobicity of the solid particles is a crucial parameter on the stability of aqueous film, as it affects the contact angle the solid particle makes with the aqueous phase. (Aveyard et al. 1994) found that when particles are hydrophobic ($\theta > 90^{o}$), the aqueous film gets thinner when drainage occurs and, when the three phases (gas, liquid and solid) meet, holes form and the film ruptures. By contrast, if the particles are hydrophilic, the aqueous film starts thinning until it becomes flat. If the aqueous film thins further, capillary pressure will draw liquid toward the

particle and stabilize the aqueous film by bridging mechanisms. Accordingly, the mixture of hydrophilic particles, as those used in this study, and surfactant solution are expected to decrease the rate of film drainage using this mechanism.

In this work, we suggest both mechanisms: NPs arrangement during film drainage and the increase of maximum capillary pressure of coalescence, to help slowing down the film drainage and generate a more stable foam.

4.2.2.5 Summary

- Static foam tests in the absence of crude oil showed no obvious changes in foam height and bubble sizes.
- Static foam tests in the presence of crude oil showed a clear trend when solid NPs were added. With DI water, as the concentration of NPs increases, the foam half-life increases, too. The foam half-lives for 0.50 wt% and 1 wt% NPs were 5 and 8 times higher, respectively, than surfactant alone.
- Addition of NaCl improves the foam stability in the presence of crude oil. Static foam tests when 1 wt% NaCl was added showed higher foam half-lives than DI water tests. Also, the addition of NPs plus salt improves foam stability in the presence of crude oil. The foam half-life in the presence of nanoparticles and 1 wt% NaCl was 15 hours, while in the absence of nanoparticles it was 13.5 hours.
- The foamability tests using core samples showed higher pressure drop, more resistance to flow, when NPs were added to surfactant.
- The foamability tests also showed that the rise in temperature reduces the pressure drop which can be attributed to the reduction in foam viscosity and strength.

- Both surfactant and a mixture of surfactant and NPs were able to enhance oil recovery. The surfactant was able to bring the oil recovery to 41.45% of the OOIP. In contrast, the presence of NPs resulted in higher oil recovery, 49.05% of the OOIP.

4.2.3 Surface Modified Silica and CNF Surfactant (CO_2 Foam)

This part will discuss the results of foam generated using CO_2 rather than N_2. The materials used in the previous discussion, Surface Modified Silica NPs and CNF Surfactant, were used to conduct the experiments using CO_2. Mobility tests and coreflood experiments were conducted to assess the ability of surfactant and the mixture of surfactant and NPs to stabilize CO_2-water foam. Foam behavior in the presence and absence of crude oil were already discussed in the previous section.

4.2.3.1 Materials

The surfactant used in this study is anionic surfactant (CNF). The NPs are surface modified silica NPs described in the previous discussion. CO_2 gas (industrial grade) was used to conduct gas mobility tests and core flood experiments. The cores used in this study were Bentheimer sandstone from Kocurek Industries. For mobility tests, non-fractured rocks were used. However, for coreflood experiments fractured and non-fractured rocks were used. **Table 27** summarizes the properties of these cores. North Burbank Unit (NBU) oil with an average viscosity of 8.1 cp at 25^{o}C and 3.2 cp at 50^{o}C was used to conduct coreflood experiments.

Table 27: Properties of Bentheimer sandstone fractured and non-fractured samples

Sample #	Length (in)	Diameter (in)	Type of Rock	Porosity (%)	Pore Volume (ml)	Permeability (D)
5	12	1	Non-fractured	21.76	33.61	1.50
6	12	1	Non-fractured	21.44	33.11	1.55
7	12	1	Non-fractured	21.20	32.74	1.72
8	12	1	Non-fractured	21.20	32.74	1.76
9	12	1	Non-fractured	21.84	33.74	1.77
10	12	0.96	Fractured	20.68	29.74	-
11	12	0.95	Fractured	19.90	27.74	-
12	12	0.95	Fractured	19.90	27.74	-

4.2.3.2 Experimental Procedure and Conditions

This study consists mainly of dynamic foam tests and coreflood experiments. The dynamic foam was generated using a mobility test setup, figure 15, and the gas mobility was evaluated using rock samples. The coreflood experiments were conducted using coreflood setup, figure 16, to assess the ability of generated foam to reduce gas mobility and enhance oil recovery. Non-fractured rocks were used to run the mobility tests. While, fractured and non-fractured rocks were used to conduct the coreflood experiments.

4.2.3.2.1 Sample Preparation

Same as that presented in the previous section. Brine was made with 1 wt% NaCl.

4.2.3.2.2 Foam Dynamic Tests

The objective of this test is to examine the ability of the used materials to generate foam at reservoir conditions. The important measurement here is the pressure drop across the core samples. Bentheimer sandstone rock samples #5 and #6 were used to perform these tests. At least five pore volumes (PVs) of brine were injected at 5 ft/day to ensure the sample was 100% saturated with brine. The BPR was set to be 1550 psi. The baseline experiment was conducted through a co-injection of sc-CO_2 and brine at 90% quality. For other experiments, the samples were then pre-flushed with surfactant or a mixture of surfactant and NPs at 5 ft/day for 1 PV. Then, the co-injection of sc-CO_2 and surfactant/mixture was conducted at 90% quality and the drop in pressure was recorded for each case. After finishing the test, the system was depressurized and at least 30 PV of brine were injected to clean the rock. The procedure of cleaning the rock was already discussed previously. These tests were conducted at 50^{o}C.

4.2.3.2.3 Coreflood Experiments

Coreflood experiments followed almost the same procedure as the mobility tests discussed above. Bentheimer sandstone rock samples 7 through 12 were used to run coreflood experiments. Rocks 7 to 9 were non-fractured while 10 to 12 were fractured. For non-fractured rocks, once the cores had been saturated with brine, two PVs of NBU oil were injected at 5 ft/day. The experiments were conducted at 1550 psi and 50^{o}C. The overburden pressure was set to be 2000 psi. After ensuring the rock reached the initial water saturation (Swi), the waterflooding test started. Once the maximum oil recovery with water flooding was achieved, the pre-flush process of surfactant or a mixture of surfactant/NPs was performed, followed by a co-injection of miscible CO_2 and surfactant/mixture as a secondary mechanism for enhancing

oil recovery. For fractured rocks, same procedure was followed except that the rocks were 100% saturated with oil.

4.2.3.3 Results and Discussion

4.2.3.3.1 Foam Dynamic Tests

Comparisons here were based on recorded pressure drops across core samples and calculated MRF for the three cases: baseline, CNF, and mixture of CNF and NPs. Rock sample #5 was used to conduct the baseline experiment. The results, as shown in **figure 87**, showed that the steady state pressure drop for the baseline experiment was 0.29 psi. Bentheimer sample #6 was used to conduct the experiments in the absence and presence of NPs. In the absence of NPs, the foam behavior was excellent at the first PVs injected. After that, it had a sudden drop in the pressure values and it produced a foam with a steady state pressure drop of 0.88 psi, as shown in **figure 87**. These results reflect the stability rather than the foamability. Surfactants have the ability to reduce the CO_2-water IFT and generate foams, but the stability in the presence of CO_2 is challenging. In the presence of NPs, the behavior was similar to that in the absence of NPs. However, it had a lower foam generation ability in the first PVs injected. After 2 PVs of the co-injection process, the mixture resulted in a slightly higher steady state pressure drop, 1 psi. This is an indication of the ability of NPs to produce a more stable and stronger foam in porous media. The permeability of the rocks used here was about 1.5 Darcy, so these reported values are still acceptable. The MRF values calculated for both the surfactant and mixture were found to be 3.04 and 3.45, respectively. This means that both the surfactant and the mixture were able to reduce the CO_2 relative permeability and increase the gas apparent viscosity, thereby reducing gas mobility.

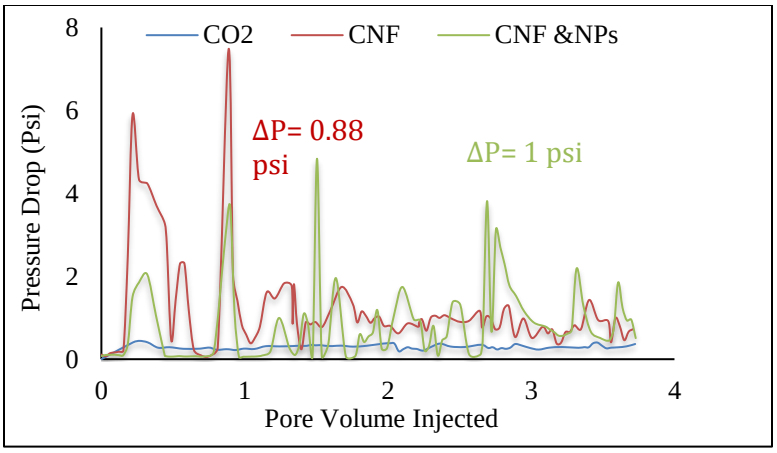

Figure 87: Average pressure drop across the Bentheimer for baseline, 0.50 wt% surfactant and a mixture of 0.50 wt% surfactant and 0.50 wt% NPs at 50°C using CO_2

4.2.3.3.2 Coreflood Experiments

Two sets of experiments were conducted to assess the ability of foam to enhance oil recovery, one in non-fractured rocks (7-9) and the other in fractured rocks (10-12).

4.2.3.3.2.1 Non-Fractured Rocks

Coreflood experiments showed that both conditions, with and without NPs, improved oil recovery during foam injection processes, with higher recovery in the presence of NPs. **Figure 88** shows the results of coreflood experiments using CO_2. Oil recovery following the waterflooding process was about 32.82% of the OOIP. At least 4 PVs of water were injected to ensure that no more oil could be recovered in this process and to diminish any capillary end effects that might exist. Then, CO_2 was injected at 5 ft/d and total oil recovery reached 71.50% of the OOIP. This means that CO_2 was able to produce about 38.68% of the OOIP.

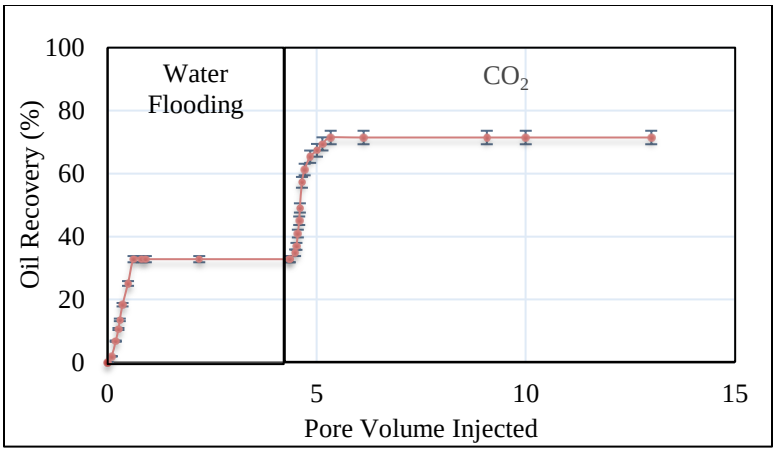

Figure 88: Oil recovery following waterflooding and CO_2 injection, Non-fractured rock

Figure 89 shows the results of coreflood experiments for surfactant. Oil recovery following the waterflooding process was about 36.15 % of the OOIP. As before, at least 4 PVs of water were injected to ensure that no more oil could be recovered in this process and to diminish any capillary end effects that might exist. Then, 1 PV of surfactant was injected as a pre-flush step. The objective of this step was to minimize the adsorption that might occur during the co-injection processes. There was no significant amount of oil produced during the pre-flush step. The surfactant foam was able to produce about 39.90% of the OOIP. This brought the total oil recovery to around 76.06% of the OOIP. This is 4.56% higher than injecting CO_2 alone.

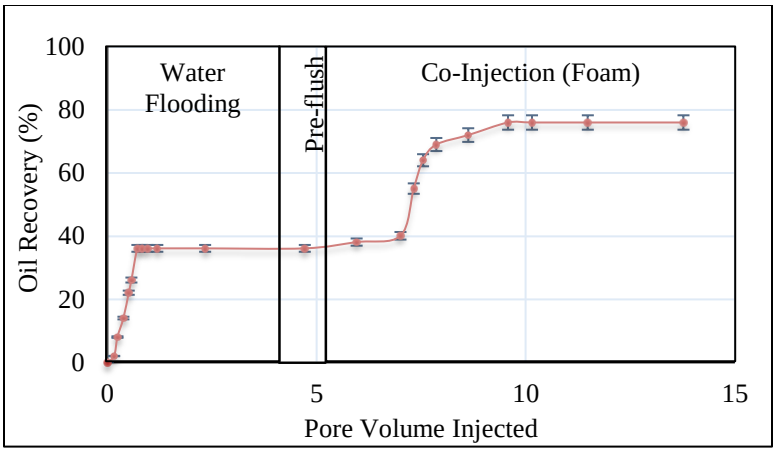

Figure 89: Oil recovery following waterflooding and foam injection for surfactant, Non-fractured rock

The next experiment, as shown in **figure 90**, was for the mixture of surfactant and NPs. The same procedures used in the previous experiment were used in this run. Oil recovery following the waterflooding process was about 35.73 % of the OOIP. The pre-flush with the mixture was not able to significantly recover any additional oil. During the co-injection processes, the mixture was able to produce about 44.33% of the OOIP. This is 4.43% higher than injecting surfactant alone. The total oil recovery following the mixture foam process was around 80.05% of the OOIP. This is around 4% higher than the previous experiment where only surfactant was used and 8.55% higher than CO_2.

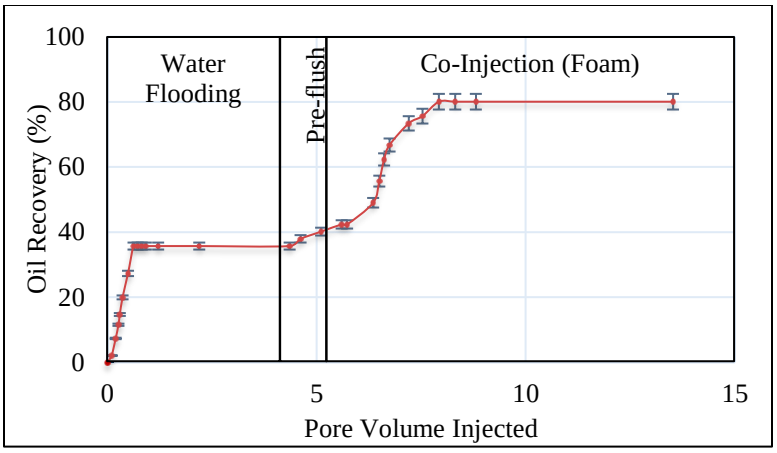

Figure 90: Oil recovery following waterflooding and foam injection for a mixture of surfactant and NPs, Non-fractured rock

A comparison between the three cases is presented in **figure 91**. The highest oil recovery was reported for the mixture while the lowest was for CO_2. The high oil recovery produced for CO_2 was because the experiment was conducted at or near the minimum miscibility pressure (MMP) of CO_2 in NBU oil. The higher oil recovery reported for surfactant compared to CO_2 demonstrates the ability of foam flooding to reduce gas mobility and enhance the sweep efficiency, hence, enhancing oil recovery. Also, the higher recovery of the mixture compared to that of surfactant demonstrates the ability of the presence of NP to further reduce gas mobility, improving the gas sweep efficiency and, therefore, recovering more oil.

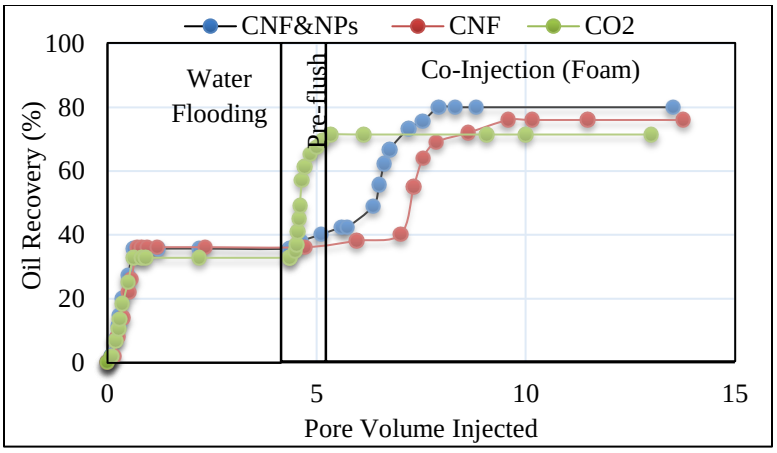

Figure 91: Oil recovery following waterflooding and CO_2 and foam injection, Non-fractured rock

4.2.3.3.2.2 Fractured Rocks

Similar to the previous experiments, the results of coreflood experiments here on non-fractured rocks showed improved oil recovery during the foam injection processes, with higher recovery when NPs were used. **Figure 92** shows the results of coreflood experiment for the baseline case, CO_2 injection. The oil recovery following the waterflooding process was about 59.71% of the OOIP. At least 3.5 PVs of water were injected at 3 ft/d to ensure that no more oil could be recovered in this process and to diminish any capillary end effects that might exist. Then, CO_2 was injected at 5 ft/d and the total oil recovery reached 66.92% of the OOIP. This means that the CO_2 was able to produce about 7.21% of OOIP.

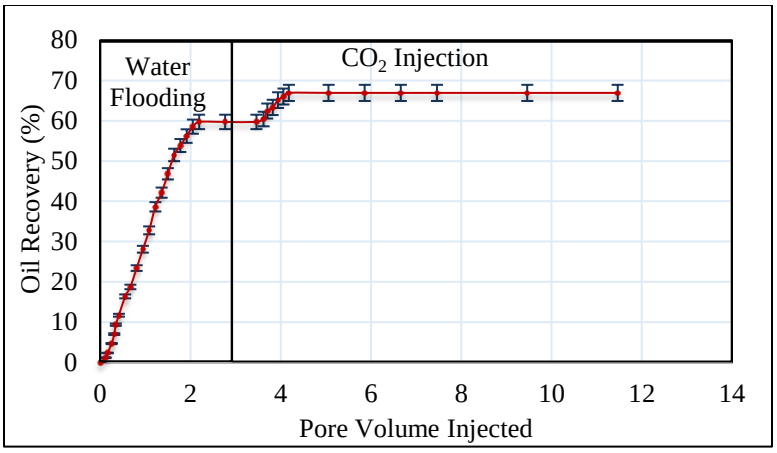

Figure 92: Oil recovery following waterflooding and CO_2 injection, fractured rock

Figure 93 presents the results of coreflood experiment for the surfactant case. The oil recovery following the waterflooding process was about 54.01% of the OOIP. At least 5.5 PVs of water were injected at 3 ft/d to ensure that no more oil could be recovered in this process and to diminish any capillary end effects that might exist. Then, 1 PV of surfactant was injected at 1.5 ft/d as a pre-flush step. There was no significant amount of oil produced during the pre-flush step. The co-injection process was conducted at 5 ft/d and 90% quality. The surfactant foam was able to produce about 8.41% of the OOIP. This brought the total oil recovery to be around 62.42% of the OOIP. Even though the total oil recovery of CO_2 was higher than surfactant, the recovery factor during foam injection was higher than the CO_2 case. The surfactant produced 8.41% following waterflooding, whereas the CO_2 recovered 7.21% of the OOIP. Also, the recovery factor during the waterflooding for the CO_2 case was higher than the surfactant case, 59.71% for CO_2 versus 54.01% for surfactant. This resulted in a higher total recovery for CO_2 compared to surfactant.

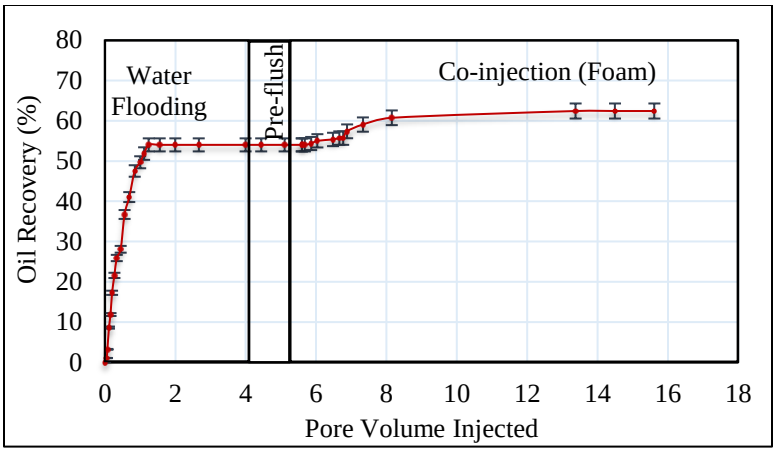

Figure 93: Oil recovery following waterflooding and foam injection for surfactant, fractured rock

The next run, as shown in **figure 94**, was for the case where the mixture of surfactant and NPs was used. The same procedure as in the previous experiment was used in this run. The oil recovery following the waterflooding process was about 57.90% of the OOIP. A small amount of oil was produced during the pre-flush process. During the pre-flush and co-injection processes, the mixture was able to produce about 12.62% of the OOIP. The total oil recovery following the mixture foam process was around 70.52% of the OOIP. This is around 8.10% higher than the previous experiment in which only surfactant was used and 3.60% higher than CO_2.

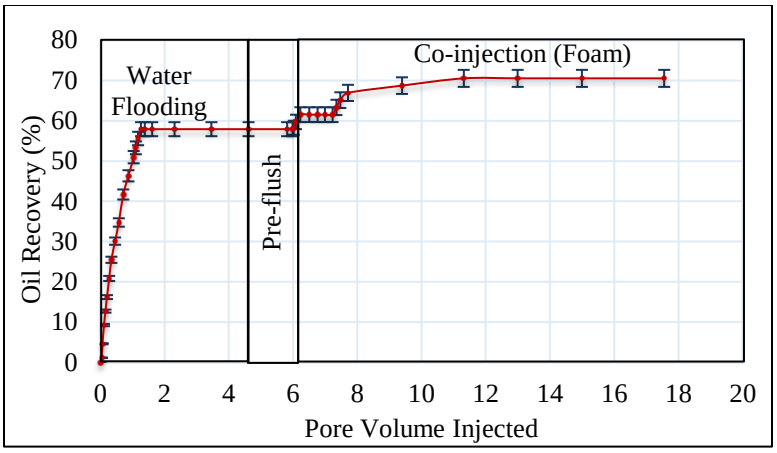

Figure 94: Oil recovery following waterflooding and foam injection for a mixture of surfactant and NPs, fractured rock

A comparison among the three cases is presented in **figure 95**. The highest oil recovery was reported for the mixture while the lowest was for surfactant. However, the results reported for surfactant compared to CO_2 are already discussed above. The high oil recovery reported for all cases was because the experiments were conducted at or near the minimum miscibility pressure (MMP) of CO_2 in NBU oil. Also, the rock samples were 100% saturated with oil. The higher oil recovery reported for surfactant compared to CO_2, at the secondary recovery scheme, demonstrates the ability of foam flooding to reduce gas mobility and to enhance the sweep efficiency, hence, improving oil recovery. Also, the higher recovery of the mixture compared to that of surfactant and CO_2 demonstrates the ability of NPs to further reduce gas mobility, improving the sweep efficiency and, therefore, recovering more oil. The summary of the performance of waterflooding and secondary recovery schemes can be found in **figure 96**.

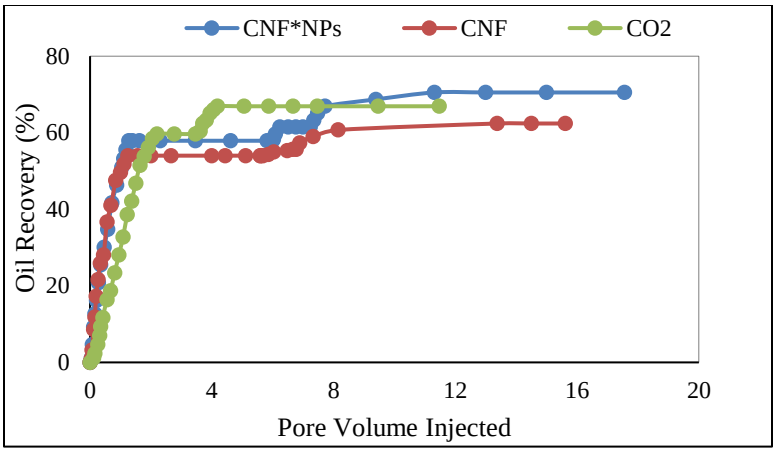

Figure 95: Oil recovery following waterflooding and CO_2 and foam injection, fractured rocks

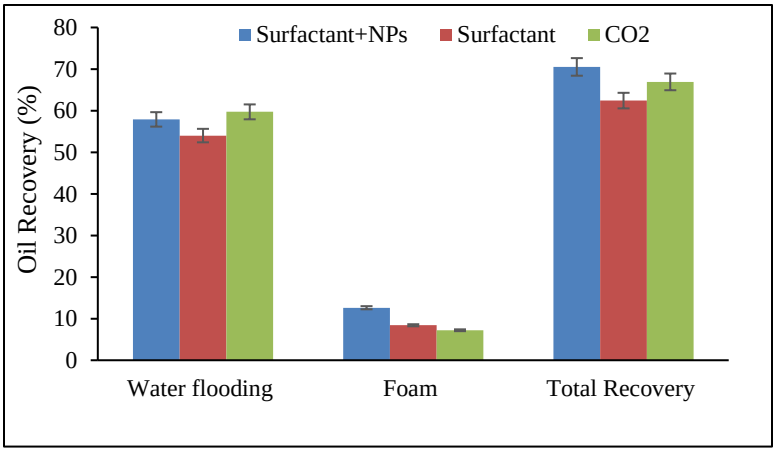

Figure 96: Summary of coreflood experiments, fractured rocks

4.2.3.4 Summary

Based on the results of foamability and coreflood experiments:

- At harsh reservoir conditions, surfactant was able to reduce the sc-CO_2 mobility about 3 times.
- In the presence of NPs, sc-CO_2 mobility was reduced about 3.4 times.
- Using non-fractured rocks, the mixture of surfactant and NPs recovered about 80.05% of the OOIP. This is around 4% higher than surfactant and 8.55% higher than CO_2.
- Using fractured rocks, the presence of NPs was able to improve the oil recovery compared to the surfactant and pure CO_2 injection cases. The oil recoveries during secondary production mechanisms for CO_2, surfactant, and mixture were 7.21, 8.41 and 12.62%, respectively.

4.2.4 Surface Modified Silica and ENORDET A031

The objective of this work was to assess the ability of NPs to improve the stability of foam generated by surfactant. ENORDET A031 surfactant and a mixture of the surfactant and surface modified silica NPs were used in this study to assess the synergistic effect on foam stability

4.2.4.1 Materials

The surfactant used in this study is ENORDET A031 surfactant. The properties of the surfactant were already presented in table 10. The NPs used are surface modified silica received in aqueous form from Nyacol Chemicals, same as those presented in previous mixture. Nitrogen gas (industrial grade) was used to conduct gas mobility tests. The cores used in this study were Bentheimer sandstone from Kocurek Industries. **Table 27** summarizes the properties of these cores.

Table 28: Properties of Bentheimer sandstone samples used for ENORDET surfactant and silica NPs

Sample #	Length (in)	Diameter (in)	Porosity (%)	Pore Volume (ml)	Permeability (D)
13	12	1	21.20	32.74	1.60
14	12	1	20.22	31.24	1.59
15	12	1	20.55	31.74	1.60

4.2.4.2 Experimental Procedure and Conditions

The dynamic foam experiments were conducted using the mobility tests apparatus (figure 15) and the gas mobility was evaluated in rock samples at different NP concentration.

These tests were performed to assess the ability of surfactant and mixtures to generate foam in porous media and to evaluate the foam strength. To test foam strength and stability, the pressure drop across rock samples was measured. Higher pressure drops indicate more viscous foam and, hence, more resistance to gas flow in porous media. Bentheimer sandstone rock samples 13, 14, and 15 were used to run these tests. Core samples were put in oven overnight to ensure they were dry. To remove any gases trapped inside pore spaces, the core samples were then set in a core holder and a vacuum was applied. Then at least five pore volumes (PV) of water were injected at 5 ft/day to ensure the samples were 100% saturated with water. The back pressure regulator (BPR) was set to 150 psi. Next, the samples were pre-flushed with surfactant or a mixture of surfactant and NPs at 5 ft/day for 1 PV. Finally, the co-injection of gas and surfactant/mixture was conducted at 70% quality and the drop in pressure was recorded for each case. Tests were conducted using 0.50 wt% surfactant, mixtures of 0.50 wt% surfactant and 0.50 wt% NPs, and 0.50 wt% surfactant and 1 wt% NPs. The experiments were conducted at 25 ^{o}C.

4.2.4.3 Results and Discussion

Rock sample #13 was used to run the mobility test using only surfactant. As shown in **figure 97**, the surfactant was able to produce foam and a steady state pressure drop of 25.4 psi was reported. The next experiment was conducted using rock sample #14 and at 0.50 wt% surfactant and 0.50 wt% NPs (mixture 1). Based on the pressure drop behavior (**figure 98)** the presence of NPs in solution was able to produce stronger foam with a steady state pressure drop of 26.4 psi.

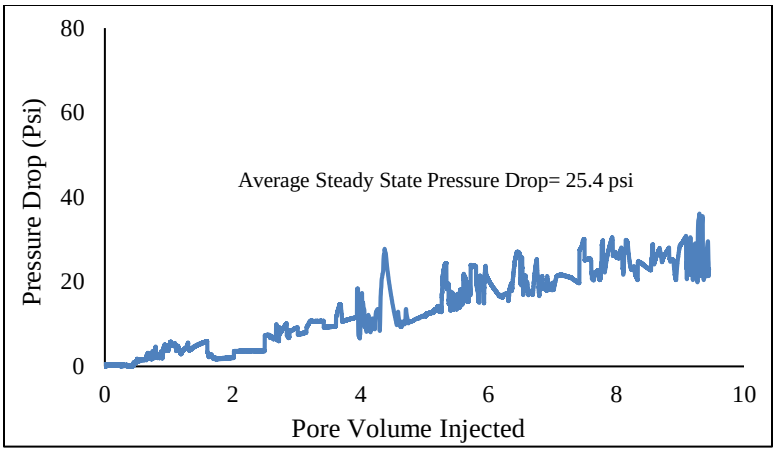

Figure 97: Pressure drop across rock sample#13, surfactant case

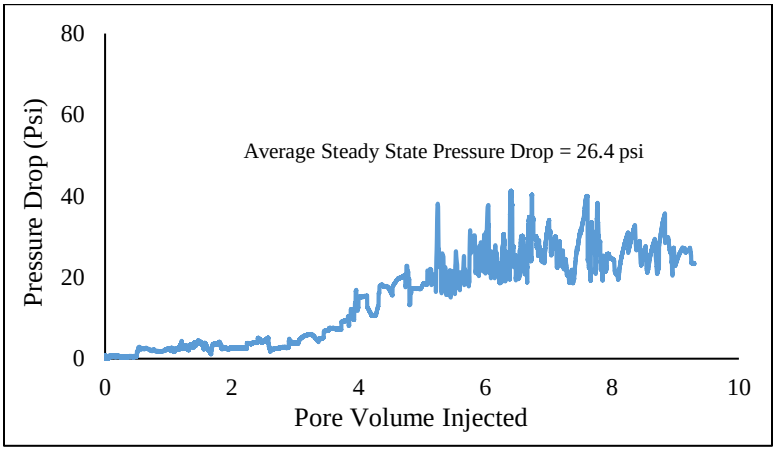

Figure 98: Pressure drop across rock sample#14, mixture 1

To evaluate the effect of NP concentration on foam stability and strength, a mobility test was conducted at 0.50 wt% surfactant and 1 wt% NPs (mixture 2) using rock sample #15. The results, as presented in **figure 99**, show that the addition of more solid particles resulted in a more stable foam with a higher steady state pressure drop, 29.6 psi. This is 3.2 psi higher than mixture 1 and 4.2 psi higher than the surfactant alone. The baseline experiment, injecting only N_2 and water, resulted in a 0.35 psi pressure drop.

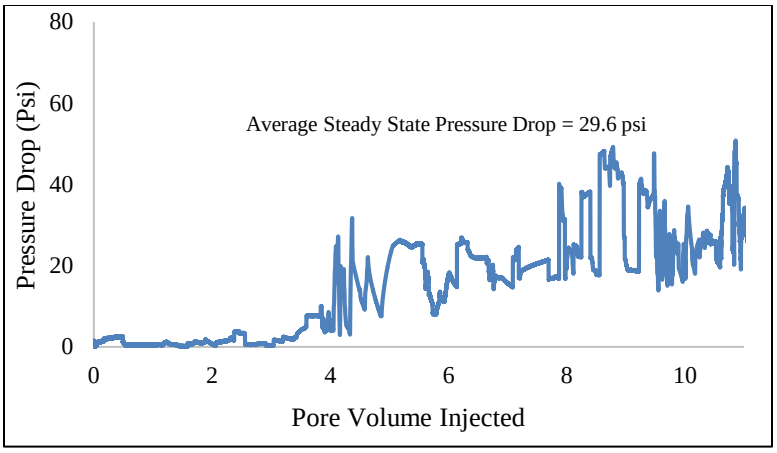

Figure 99: Pressure drop across rock sample#15, mixture 2

The MRF was calculated for the three cases. The values reported for the surfactant, mixture 1, and mixture 2 were 72.57, 75.43, and 84.57, respectively. The presence of NPs in solutions was able to enhance the foam stability and reduce gas mobility at least 75 times. The MRF values are reported in **figure 100**.

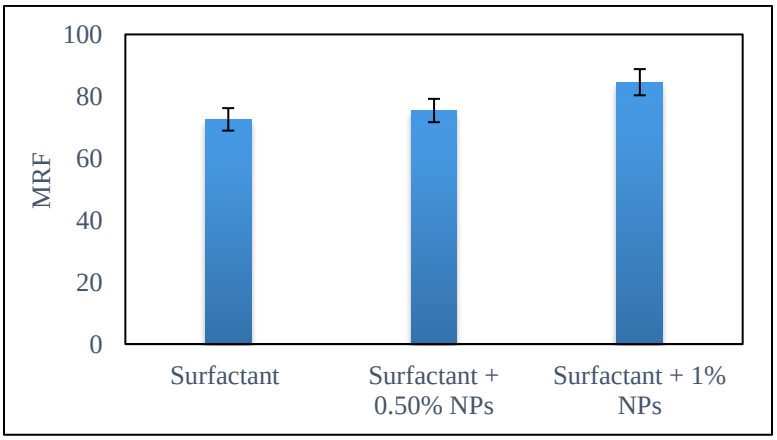

Figure 100: MRF for surfactant and mixture of surfactant and NPs

4.2.4.4 Mechanism of Foam Stabilization

The mechanisms presented for this mixture are similar to those presented for surface modified silica and CNF Surfactant (N_2 Foam) mixture. The mixture used in this study consists of surfactant and NPs. The huge reduction of interfacial tension due to the use of surfactant

reduces the energy of attachment, thus resulting in poor stability of foam. As a result, particle attachment energy is not the appropriate mechanism to explain the enhancement of foam stability in the presence of nanoparticles and surfactant. Also, growing aggregates mechanism is probably not the case in this study as the average particle size did not change, so no aggregates or cork were formed. NPs used in this study seem to stabilize the liquid film by two mechanisms: particle arrangement during film drainage and increasing the capillary pressure of coalescence. The polydispersity index (PDI) of the silica particles used in this study, was measured using the DLS and found to be around 0.11. This is within the range where monodispersity of particles is defined. The relatively low PDI value of those particles will help in producing the most efficient arrangements during film drainage processes which might help in slowing down the film thinning and, hence, resulting in a more stable film. As mentioned previously, if the particles used are hydrophilic, the aqueous film starts thinning until it becomes flat. If the aqueous film thins further, capillary pressure will draw liquid toward the particle and stabilize the aqueous film by bridging mechanisms. Accordingly, the mixture of hydrophilic particles, as these used in this study, and surfactant solution are expected to decrease the rate of film drainage using this mechanism.

In this work, we suggest both mechanisms: NPs arrangement during film drainage and the increase of maximum capillary pressure of coalescence to improve the gas -liquid foam stability and help slowing down the film drainage and generate a more stable foam.

4.2.4.5 Summary

Based on the experimental results:

- The presence of NPs in surfactant solution resulted in a more stable foam compared to surfactant alone.
- Higher pressure drops were reported for the mixtures compared to surfactant alone.
- The presence of NPs increased the MRF.
- As the NP concentration increases, MRF increases, too.
- The MRF reported for surfactant, mixture 1, and mixture 2 were 72.57, 75.43 and 84.57, respectively.

CHAPTER V

CONCLUSIONS AND RECOMMENDATIONS

5.1 Conclusions

This work uses NPs to stabilize gas-liquid foams/emulsions for gas mobility control and to improve the gas sweep efficiency in petroleum reservoirs. This work uses surface modified silica NPs and the synergistic effect of surfactants and NPs to stabilize gas-liquid foams/emulsions as alternatives to the use of surfactants alone to stabilize foams and control gas mobility. Static foam tests were conducted to evaluate the potential of tested materials to stabilize or improve foam strength at ambient conditions. These tests consisted primarily of foam half-life, foam bubble size, and IFT measurements. Dynamic foam tests, by contrast, were used to assess the ability of tested materials to generate and stabilize foam at reservoir conditions: high pressure, high temperature, high salinity, and in porous media. These tests consisted primarily of viscosity measurements, gas mobility tests, and coreflood experiments. NPs were used to stabilize gas-liquid foam/emulsion in two different ways. First, NPs were used alone to stabilize gas-liquid foam/emulsions. Second, NPs and surfactants were used synergistically to improve the stability of foam that had been initially generated using surfactants.

Surface modified silica NPs with DCDMS, hidden chemical, and PEG were used to assess the ability of NPs to stabilize gas-liquid emulsions at reservoir conditions. The effects of quality, salinity, shear rates, NPs size, NPs concentration, pressure, and different gases on emulsion strength were evaluated. Based on emulsion stability and viscosity measurements:

- All three surface modified NPs were able to stabilize gas-liquid emulsion and produce viscous emulsions compared to CO_2 and N_2 at harsh reservoir conditions.

- Silica modified partially with DCDMS was able to increase the CO_2 viscosity 26-60 fold.
- Silica modified with hidden chemical was able to increase the CO_2 viscosity 25-53 fold and N_2 viscosity 22-54 fold.
- Silica modified with PEG was able to increase the CO_2 viscosity 24-49 fold.
- All tested materials showed an inverse relationship between the emulsion quality and viscosity.
- In most cases, salinity was found to have a significant impact on emulsion strength. As salinity increased, the emulsion viscosity increased, too.
- The concentration of NPs showed similar behavior, with NPs concentration and viscosity being directly proportional.
- Shear rate was found to be a crucial parameter for foam/emulsion stability and viscosity, with a threshold shear rate being necessary to stabilize gas-liquid emulsions.
- NP's size had no significant effect on emulsion stability and strength.
- Increased pressure can improve emulsion stability to produce a more viscous emulsion.

Five mixtures consisting of surfactants and NPs were used to enhance foam stability and viscosity. These mixtures consisted of silica NPs and three nonionic surfactants (NEODOL91-8, 25-7 and 25-9), surface modified silica NPs and CNF surfactant (two cases, N_2 foam and CO_2 foam), and surface modified silica NPs and ENORDET A031 surfactant. Based on the experimental results:

- The presence of NPs in all surfactant solutions enhanced foam stability and produced more viscous foams in porous media, thereby further reducing gas mobility and improving gas sweep efficiency compared to surfactant alone.

- The presence of NPs with ENORDET A031 was able to increase the gas MRF up to 84.57 compared to 72.57 for surfactant. As the NP concentration increases, MRF increases, too.
- For the mixtures of silica NPs and nonionic surfactants, results showed that the concentration of surfactant and NPs is a crucial parameter for foam stability and that there is an optimum concentration for strong foam production. A balance in concentration between the nonionic surfactants and the NPs can enhance the foam stability by forming flocs at the gas-liquid interface.
- For sc-CO_2 and N_2 foams, the coreflood experiments showed remarkable improvements when NPs were added to surfactant solutions. For N_2 foam, the mixture of surface modified silica NPs and CNF surfactant resulted in a total recovery of 49.05% compared to 41.45% for surfactant alone.
- The total oil recovery for the same mixture (the mixture of surface modified silica NPs and CNF surfactant) with sc-CO_2 was 80.05% of the OOIP. This is around 4% higher than the surfactant case and 8.55% higher than sc-CO_2.
- In fractured rocks, the presence of NPs was able to improve oil recovery compared to the surfactant and sc-CO_2 injection cases. Oil recoveries during secondary production mechanisms for the mixture of surface modified silica NPs and CNF surfactant, the surfactant alone, and sc-CO_2 alone were 12.62, 8.41 and 7.21% of the OOIP, respectively.

5.2 Recommendations

- In an effort to simulate actual reservoir conditions, it is recommended that foam/emulsion stability and viscosity measurements for NPs be taken in rock samples instead of glass beads porous media.
- Tests conducted were either at room temperature or 50^{o}C. It is recommended to evaluate the potential of tested materials on foam/emulsion behavior at higher temperatures.
- The effect of salinity was mainly conducted using NaCl. It is recommended to add other salts to study the effect of salinity on foam stability and strength and to simulate the actual reservoir salinity in which the formation brine has other salts in addition to NaCl.
- Rock samples used in this study were mostly homogeneous sandstone with high permeability. Heterogeneity was only introduced during the coreflood experiments by creating smooth fractures along the core samples. It is recommended to study foam behavior using actual heterogeneous reservoir rocks with lithology different from sandstone.
- For coreflood experiments, it is recommended to use cores with diameters larger than those used here. Due to the technical and operational issues, cores used in this study had 1 in diameter.
- It is also recommended to ensure the transportation of NPs in porous media by conduction dynamic adsorption tests. This will enable better understanding of the NPs-rock interactions and to ensure that NPs can pass through the pore spaces without causing any issues.

- This study only shows experimental results. It would be of great value for the results presented here to be simulated using commercial software.
- Coreflood experiments were conducted only for one mixture. Other mixtures still have to be evaluated by running coreflood experiments at different conditions.
- All tests were conducted using the co-injection scheme of gas and liquid. It is recommended to conduct other tests to compare the results of this scheme with a surfactant alternating gas (SAG) scheme, which has been reported in the literature and has produced encouraging results.

REFERENCES

Ahmed, T. 2000. Minimum Miscibility Pressure from EOS. Canadian International Petroleum Conference, Calgary, Alberta. PETSOC 2000-001.

Al-Hashim, H. S., M. S. Celik, M. M. Oskay et al. 1988. Adsorption and Precipitation Behaviour of Petroleum Sulfonates from Saudi Arabian Limestone. *Journal of Petroleum Science and Engineering* **1** (4): 335-344.

Al Otaibi, Fawaz Mohammed, Sunil Lalchand Kokal, Yun Chang et al. 2013. Gelled Emulsion of CO_2-Water-Nanoparticles. SPE Annual Technical Conference and Exhibition, New Orleans, Louisiana, USA. SPE 166072.

Alvarado, Vladimir, Eduardo Manrique. 2010. Enhanced Oil Recovery: An Update Review. *Energies* **3**:1529-1575.

Amanullah, Md, Ashraf M. Al-Tahini. 2009. Nano-Technology - Its Significance in Smart Fluid Development for Oil and Gas Field Application. SPE Saudi Arabia Section Technical Symposium, Al-Khobar, Saudi Arabia SPE-126102-MS.

Amanullah, Md, Mohammed K. AlArfaj, Ziad Abdullrahman Al-abdullatif. 2011. Preliminary Test Results of Nano-based Drilling Fluids for Oil and Gas Field Application. SPE/IADC Drilling Conference and Exhibition, Amsterdam, The Netherlands. SPE-139534-MS.

Amirianshoja, Tahmineh, Radzuan Junin, Ahmad Kamal Idris et al. 2013. A Comparative Study of Surfactant Adsorption by Clay Minerals. *Journal of Petroleum Science and Engineering* **101**: 21-27.

Aroonsri, Archawin, Andrew J. Worthen, Tarek Hariz et al. 2013. Conditions for Generating Nanoparticle-Stabilized CO_2 Foams in Fracture and Matrix Flow. SPE Annual Technical Conference and Exhibition, New Orleans, Louisiana, USA SPE-166319-MS.

Aveyard, R., B. P. Binks, P. D. I. Fletcher et al. 1994. Aspects of Aqueous Foam Stability in the Presence of Hydrocarbon Oils and Solid Particles. *Advances in Colloid and Interface Science* **48**: 93-120.

Bae, J.H., C.A. Irani. 1993. A Laboratory Investigation of Viscosified CO_2 Process. *SPE Advanced Technology Series* **1** (1):166-171.

Bank, Gregory Charles, David Edward Riestenberg, George Jonathan Koperna. 2007. CO_2-Enhanced Oil Recovery Potential of the Appalachian Basin. Eastern Regional Meeting, Lexington, Kentucky USA. SPE-111282-MS.

Bartscherer, K. A., M. Minier, H. Renon. 1995. Microemulsions in Compressible Fluids — A Review. *Fluid Phase Equilibria* **107** (1): 93-150.

Bayraktar, Zeynep, Erdogan Kiran. 2000. Miscibility, Phase Separation, and Volumetric Properties in Solutions of Poly(Dimethylsiloxane) in Supercritical Carbon Dioxide. *Journal of Applied Polymer Science* **75** (11): 1397-1403.

Bhatia, Kutbuddin Hakimuddin, Levin Plakottu Chacko. 2011. A Novel Approach to Recover Hydrates Using Ni-Fe Nanoparticles. SPE EUROPEC/EAGE Annual Conference and Exhibition, Vienna, Austria. SPE-143088-MS.

Binks, B. P., S. O. Lumsdon. 2000. Influence of Particle Wettability on the Type and Stability of Surfactant-Free Emulsions. *Langmuir* **16** (23): 8622-8631.

Caldelas, Federico Manuel, Michael Murphy, Chun Huh et al. 2011. Factors Governing Distance of Nanoparticle Propagation in Porous Media. SPE Production and Operations Symposium, Oklahoma City, Oklahoma, USA. SPE-142305-MS.

Campbell, Bruce T., Franklin M. Orr, Jr. 1985. Flow Visualization for CO_2/Crude-Oil Displacements. *Society of Petroleum Engineers Journal* **25** (5): 665-678.

Carn, Florent, Annie Colin, Olivier Pitois et al. 2009. Foam Drainage in the Presence of Nanoparticle−Surfactant Mixtures. *Langmuir* **25** (14): 7847-7856.

Chakravarthy, D., V. Muralidharan, E. Putra et al. 2004. Application of X-Ray CT for Investigation of CO_2 and WAG Injection in Fractured Reservoirs. Canadian International Petroleum Conference, Calgary, Alberta. PETSOC-2004-232.

Christensen, J. R., E. H. Stenby, A. Skauge. 1998. Review of WAG Field Experience. International Petroleum Conference and Exhibition of Mexico, Villahermosa, Mexico. SPE-39883-MS.

Crews, James B., Tianping Huang. 2008. Performance Enhancements of Viscoelastic Surfactant Stimulation Fluids With Nanoparticles. Europec/EAGE Conference and Exhibition, Rome, Italy. SPE-113533-MS.

Cui, Z. G., Y. Z. Cui, C. F. Cui et al. 2010. Aqueous Foams Stabilized by in Situ Surface Activation of $CaCO_3$ Nanoparticles via Adsorption of Anionic Surfactant. *Langmuir* **26** (15): 12567-12574.

Dalland, Mariann, Jan Erik Hanssen. 1997. Enhanced Foams for Efficient Gas Influx Control. International Symposium on Oilfield Chemistry, Houston, Texas. SPE-37217-MS.

Dandge, D. K., J. P. Heller. 1987. Polymers for Mobility Control in CO_2 Floods. SPE International Symposium on Oilfield Chemistry, San Antonio, Texas. SPE-16271-MS.

Denkov, N. D., I. B. Ivanov, P. A. Kralchevsky et al. 1992. A Possible Mechanism of Stabilization of Emulsions by Solid Particles. *Journal of Colloid and Interface Science* **150** (2): 589-593.

Denkov, Nikolai D. 2004. Mechanisms of Foam Destruction by Oil-Based Antifoams. *Langmuir* **20** (22): 9463-9505.

Dickson, Jasper L., Bernard P. Binks, Keith P. Johnston. 2004. Stabilization of Carbon Dioxide-in-Water Emulsions with Silica Nanoparticles. *Langmuir* **20** (19): 7976-7983.

DOE/NETL. 2008. Storing CO_2 with Enhanced Oil Recovery. (402/1312/02-07-08).

Dong, M., S. Huang, R. Srivastava. 2000. Effect of Solution Gas in Oil on CO_2 Minimum Miscibility Pressure. *Journal of Canadian Petroleum Technology* **39** (11): 53-61.

Eastoe, J., A. Dupont, A. Paul et al. 2003. Design and Performance of Surfactants for Carbon Dioxide. *ACS Symposium Series* **860 (Supercritical Carbon Dioxide)**: 285-308.

EIA. 2011. Annual Energy Outlook 2011 with Projections to 2035. *US Department of Energy.*

Enick, Robert M. 1998. A Literature Review of Attempts to Increase the Viscosity of Dense Carbon Dioxide. University of Pittsburgh, Pittsburgh, Pennsylvania.

Enick, Robert M., Eric J. Beckman, J. Karl Johnson. 2010. Synthesis and Evaluation of CO_2 Thickeners Designed with Molecular Modeling. *National Energy Technology Laboratory.*

Enick, Robert M., Gerald D. Holder, Badie I. Morsi. 1988. A Thermodynamic Correlation for the Minimum Miscibility Pressure in CO_2 Flooding of Petroleum Reservoirs. *SPE Reservoir Engineering* 3 (1): 81-92.

Enick, Robert Michael, David Kenneth Olsen, James Robert Ammer et al. 2012. Mobility and Conformance Control for CO_2 EOR via Thickeners, Foams, and Gels -- A Literature Review of 40 Years of Research and Pilot Tests. SPE Improved Oil Recovery Symposium, Tulsa, Oklahoma, USA. SPE-154122-MS.

Espinoza, David Alejandro, Federico Manuel Caldelas, Keith P. Johnston et al. 2010. Nanoparticle-Stabilized Supercritical CO_2 Foams for Potential Mobility Control Applications. SPE Improved Oil Recovery Symposium, Tulsa, Oklahoma, USA. SPE-129925-MS.

Falls, A. H., G. J. Hirasaki, T. W. Patzek et al. 1988. Development of a Mechanistic Foam Simulator: The Population Balance and Generation by Snap-Off. *SPE Reservoir Engineering* **3** (3): 884-892.

Farhadi, Hamed, Siavash Riahi, Shahab Ayatollahi et al. 2016. Experimental Study of Nanoparticle-Surfactant-Stabilized CO_2 foam: Stability and Mobility Control. *Chemical Engineering Research and Design* **111**: 449-460.

Feynman, Richard P. 1960. There's Plenty of Room at the Bottom. *Engineering and Science magazine* 13.

Figdore, Phillip Eugene. 1982. Adsorption of Surfactants on Kaolinite: NaCl versus $CaCl_2$ Salt Effects. *Journal of Colloid and Interface Science* **87** (2): 500-517.

Gharbi, R.B., E.J. Peters, A. Elkamel et al. 1997. The Effect of Heterogeneity on the Performance of EOR Processes with Horizontal Wells. SPE Western Regional Meeting, Long Beach, California, USA. SPE-38320-MS.

Grigg, R. B., B. Bai. 2005. Sorption of Surfactant Used in CO_2 Flooding onto Five Minerals and Three Porous Media. SPE International Symposium on Oilfield Chemistry, The Woodlands, Texas. SPE-93100-MS.

Grigg, Reid B., David S. Schechter. 1997. State of the Industry in CO_2 Floods. SPE Annual Technical Conference and Exhibition, San Antonio, Texas. SPE-38849-MS.

Gullapalli, Pratap, Jyun-Syung Tsau, John P. Heller. 1995. Gelling Behavior of 12-Hydroxystearic Acid in Organic Fluids and Dense CO_2. SPE International Symposium on Oilfield Chemistry, San Antonio, Texas. SPE 28979-MS.

Hamilton, Robert M. Enick ; Eric J. Beckman ; Andrew. 2004. Inexpensive CO_2 Thickening Agents for Improved Mobility Control of CO_2 Floods. University of Pittsburgh (US). DOI: 10.2172/968338.

Harkins, William D. 1941. A General Thermodynamic Theory of the Spreading of Liquids to Form Duplex Films and of Liquids or Solids to Form Monolayers. *The Journal of Chemical Physics* **9** (7): 552-568.

Heller, J.P. 1994. Foams: Fundamentals and Applications in the Petroleum Industry. CO_2 Foams in Enhanced Oil Recovery, *ACS Advances in Chemistry* (Reprint) **242**: 201–234 . Washington DC.

Heller, J.P., D.K. Dandge, R.J. Card et al. 1985. Direct Thickeners for Mobility Control of CO_2 Floods. *SPE Journal* **25** (5): 679-686.

Hendraningrat, Luky, Shidong Li, Ole Torsaeter. 2013. Enhancing Oil Recovery of Low-Permeability Berea Sandstone through Optimised Nanofluids Concentration. SPE Enhanced Oil Recovery Conference, Kuala Lumpur, Malaysia. SPE-165283-MS.

Hendraningrat, Luky, Shidong Li, Ole Torsater. 2013. Effect of Some Parameters Influencing Enhanced Oil Recovery Process using Silica Nanoparticles: An Experimental Investigation. SPE Reservoir Characterization and Simulation Conference and Exhibition, Abu Dhabi, UAE. SPE-165955-MS.

Hirasaki, George, Clarence A. Miller, Maura Puerto. 2011. Recent Advances in Surfactant EOR. *SPE Journal* **16** (4): 889-907.

Hite, J. Roger, S. M. Avasthi, Paul L. Bondor. 2005. Planning Successful EOR Projects. *Journal of Petroleum Technology* **57** (3): 28-29.

Hoelscher, Katherine Price, Guido De Stefano, Meghan Riley et al. 2012. Application of Nanotechnology in Drilling Fluids. SPE International Oilfield Nanotechnology Conference and Exhibition, Noordwijk, The Netherlands. SPE-157031-MS.

Horozov, Tommy S. 2008. Foams and Foam Films Stabilised by Solid Particles. *Current Opinion in Colloid & Interface Science* **13** (3): 134-140.

Huang, Tianping, James B. Crews. 2008. Nanotechnology Applications in Viscoelastic Surfactant Stimulation Fluids. *SPE Production & Operations* **23** (4): 512-517.

Huang, Zhihua, Chunmei Shi, Jianhang Xu et al. 2000. Enhancement of the Viscosity of Carbon Dioxide Using Styrene/Fluoroacrylate Copolymers. *Macromolecules* **33** (15): 5437-5442.

Kanj, Mazen Y., Jim J. Funk, Zuhair Al-Yousif. 2009. Nanofluid Coreflood Experiments in the ARAB-D. SPE Saudi Arabia Section Technical Symposium, Al-Khobar, Saudi Arabia. SPE-126161-MS.

Kaptay, G. 2006. On the Equation of the Maximum Capillary Pressure Induced by Solid Particles to Stabilize Emulsions and Foams and on the Emulsion Stability Diagrams. *Colloids and Surfaces A: Physicochemical and Engineering Aspects* **282–283**: 387-401.

Kovscek, A. R., C. J. Radke. 1994. Fundamentals of Foam Transport in Porous Media. In *Foams: Fundamentals and Applications in the Petroleum Industry*, Chap. 3, 115-163. *Advances in Chemistry*, American Chemical Society.

Kumar, Deepak, Sadaf Shoukatali Chishti, Abhishek Rai et al. 2012. Scale Inhibition Using Nano-Silica Particles. SPE Middle East Health, Safety, Security, and Environment Conference and Exhibition, Abu Dhabi, UAE. SPE-149321-MS.

Li, Shidong, Luky Hendraningrat, Ole Torsaeter. 2013. Improved Oil Recovery by Hydrophilic Silica Nanoparticles Suspension: 2-Phase Flow Experimental Studies. International Petroleum Technology Conference, Beijing, China. IPTC-16707-MS.

Liave, Feliciano M., Frank T-H. Chung, Thomas E. Burchfield. 1990. Use of Entrainers in Improving Mobility Control of Supercritical CO_2. *SPE Reservoir Engineering* **5** (1): 47-51.

Liu, Wen-Tso. 2006. Nanoparticles and their Biological and Environmental Applications. *Journal of Bioscience and Bioengineering* **102** (1): 1-7.

Mannhardt, Karin, L. L. Schramm, J. J. Novosad. 1993. Effect of Rock Type and Brine Composition on Adsorption of Two Foam-Forming Surfactants. *SPE Advanced Technology Series* 1 (1): 212-218.

Manrique, Eduardo Jose, Charles Philip Thomas, Ravi Ravikiran et al. 2010. EOR: Current Status and Opportunities. SPE Improved Oil Recovery Symposium, Tulsa, Oklahoma, USA. SPE-130113-MS.

Masalmeh, Shehadeh K., Heiko Hillgartner, Rifaat Abdul-Munim Al-Mjeni et al. 2010. Simultaneous Injection of Miscible Gas and Polymer (SIMGAP) to Improve Oil Recovery and Sweep Efficiency from Layered Carbonate Reservoirs. SPE EOR Conference at Oil & Gas West Asia, Muscat, Oman. SPE-129645-MS.

Mazumder, Saikat, Amit A. Karnik, Karl-Heinz A. A. Wolf. 2006. Swelling of Coal in Response to CO_2 Sequestration for ECBM and Its Effect on Fracture Permeability. *SPE Journal* **11** (3): 390-398.

McElfresh, Paul M., David Lee Holcomb, Daniel Ector. 2012. Application of Nanofluid Technology to Improve Recovery in Oil and Gas Wells. SPE International Oilfield Nanotechnology Conference and Exhibition, Noordwijk, The Netherlands. SPE-154827-MS.

NNI. 2017. What's So Special about the Nanoscale, http://www.nano.gov/nanotech-101/special (downloaded May 1 2017).

Ogolo, N. A., O. A. Olafuyi, M. O. Onyekonwu. 2012. Enhanced Oil Recovery Using Nanoparticles. SPE Saudi Arabia Section Technical Symposium and Exhibition, Al-Khobar, Saudi Arabia. SPE-160847-MS.

Oil and Gas Journal. 2010. Special Report:EOR/Heavy Oil Survey: CO_2 Miscible, Steam Dominate Enhanced Oil Recovery Processes.

Rindfleisch, Frank, Todd P. DiNoia, Mark A. McHugh. 1996. Solubility of Polymers and Copolymers in Supercritical CO_2. *The Journal of Physical Chemistry* **100** (38): 15581-15587.

Robinson, J. V., W. W. Woods. 1948. A Method of Selecting Foam Inhibitors. *Journal of the Society of Chemical Industry* **67** (9): 361-365.

Ryoo, Seungyup, Amir Reza Rahmani, Ki Youl Yoon et al. 2012. Theoretical and Experimental Investigation of the Motion of Multiphase Fluids Containing Paramagnetic Nanoparticles in Porous Media. *Journal of Petroleum Science and Engineering* **81**: 129-144.

Sandrea, Ivan, Rafael Sandrea. 2007. Global Oil Reserves - Recovery Factors Leaves Vast Target for EOR Technologies. *Oil & Gas Journal* **105**(41): 1-8.

Schmidt, Gudrun, Matthew M. Malwitz. 2003. Properties of Polymer–Nanoparticle Composites. *Current Opinion in Colloid & Interface Science* **8** (1): 103-108.

Schramm, Laurier L., Jerry J. Novosad. 1990. Micro-Visualization of Foam Interactions with a Crude Oil. *Colloids and Surfaces* **46** (1): 21-43.

Singh, Robin, Abhay Gupta, Kishore K. Mohanty et al. 2015. Fly Ash Nanoparticle-Stabilized CO_2-in-Water Foams for Gas Mobility Control Applications. SPE Annual Technical Conference and Exhibition, Houston, Texas, USA. SPE-175057-MS.

Singh, Robin, Kishore K. Mohanty. 2014. Synergistic Stabilization of Foams by a Mixture of Nanoparticles and Surfactants. SPE Improved Oil Recovery Symposium, Tulsa, Oklahoma, USA. SPE-169126-MS.

Singh, Robin, Kishore K. Mohanty. 2015. Foams Stabilized by In-Situ Surface-Activated Nanoparticles in Bulk and Porous Media. *SPE Journal* **21** (1): 121-130.

Slobod, R. L., H. A. Koch, Jr. 1953. High-Pressure Gas Injection- Mechanism of Recovery Increase. Drilling and Production Practice, New York, USA. API-53-082.

Terry, R.E., A. Zaid, C. Angelos et al. 1987. Polymerization in Supercritical CO_2 To Improve CO_2/Oil Mobility Ratios. SPE International Symposium on Oilfield Chemistry, San Antonio, Texas. SPE-16270-MS.

Whorton, L. P., W. F. Kieschnick. 1950. A Preliminary Report on Oil Recovery by High-Pressure Gas Injection. Drilling and Production Practice, New York, USA. API-50-247.

Worthen, Andrew J., Hitesh G. Bagaria, Yunshen Chen et al. 2013. Nanoparticle-Stabilized Carbon Dioxide-in-Water Foams with Fine Texture. *Journal of Colloid and Interface Science* **391**: 142-151.

Worthen, Andrew J., Steven L. Bryant, Chun Huh et al. 2013. Carbon Dioxide-in-Water Foams Stabilized with Nanoparticles and Surfactant Acting in Synergy. *AIChE Journal* **59** (9): 3490-3501.

Xue, Zheng, Andrew Worthen, Ali Qajar et al. 2016. Viscosity and Stability of Ultra-High Internal Phase CO_2-in-Water Foams Stabilized with Surfactants and Nanoparticles with or without Polyelectrolytes. *Journal of Colloid and Interface Science* **461**: 383-395.

Yongmao, Hao, Wu Zenggui, Ju Binshan et al. 2004. Laboratory Investigation of CO_2 Flooding. Nigeria Annual International Conference and Exhibition, Abuja, Nigeria. SPE-88883-MS

Yu, Jianjia, Sai Wang, Ning Liu et al. 2014. Study of Particle Structure and Hydrophobicity Effects on the Flow Behavior of Nanoparticle-Stabilized CO_2 Foam in Porous Media. SPE Improved Oil Recovery Symposium, Tulsa, Oklahoma, USA. SPE-169047-MS.

Yu, Jie, Jacob M. Berlin, Wei Lu et al. 2010. Transport Study of Nanoparticles for Oilfield Application. SPE International Conference on Oilfield Scale, Aberdeen, UK. SPE-131158-MS.

Zhang, Shiyang, Yuehui She, Yongan Gu. 2011. Evaluation of Polymers as Direct Thickeners for CO_2 Enhanced Oil Recovery. *Journal of Chemical & Engineering Data* **56** (4): 1069-1079.

Zhang, Shuiyan, Dejun Sun, Xiaoqiang Dong et al. 2008. Aqueous Foams Stabilized with Particles and Nonionic Surfactants. *Colloids and Surfaces A: Physicochemical and Engineering Aspects* **324** (1–3): 1-8.